Probing the Substrate Specificity of 3-Deoxy-D-*arabino*-Heptulosonate 7-Phosphate Synthase and 3-Deoxy-D-*manno*-Octulosonate 8-Phosphate Synthase using Analogues of Phosphoenolpyruvate

---

A thesis submitted in partial fulfilment of the requirements for the degree of

Master of Science

in

Chemistry

at the

University of Canterbury

by

Hemi Adam Cumming

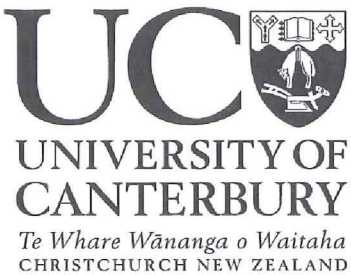

December 2007

for grandad (John Hugh Moffatt)

May you rest in peace

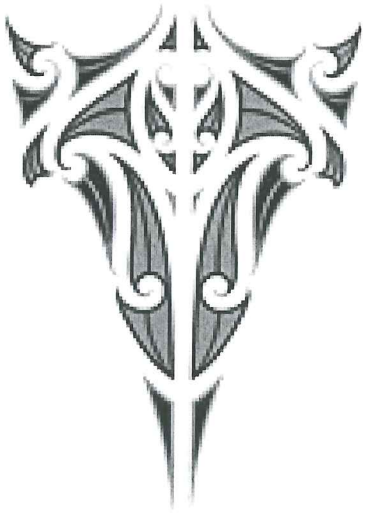

Preface

The work described in this thesis was carried out by the author under the supervision of Dr Emily Parker. The study was initiated at Massey University (Palmerston North), and completed at the University of Canterbury (Christchurch).

Acknowledgements

Thank you to my supervisor Emily Parker for the all the help and support you have given me over the years. It has been great to have been apart of your project.

Thank you to the other members of the Parker lab group, both those of the originals from Palmerston North and the newer members that joined in Christchurch, for all the help I have received and for the munches at group meetings. In particular, I'd like to thank Scott Walker and Aidan Harrison, who migrated with me from Palmerston North for your helpful discussions.

Thank you to Fiona Cochrane and Tim Alison for allowing me to steal some of your nicely purified enzymes.

Thank you to the members of the chemistry departments from Massey University and Canterbury University for all the help I have received. In particular, Steve McNabb, who performed the molecular docking models, and to Sarah Lundy for the use of your keen eye in proof reading my writing.

Thank you to the Foundation of Science, Research and Technology (FoRST) for the financial support (Tuapapa Putai-ao Maori Fellowship).

Last but not least, I'd like to thank my family, especially mum and dad, who are always there if I need anything, and to nana for your concerns, but no more need to worry, one masters thesis as promised!

"Ehara taku toa, i te toa taki tahi, engari he toa taki tini."

"My strength is not that of one, but that of many."

Abstract

3-Deoxy-D-*arabino*-heptulosonate 7-phosphate (DAH7P) synthase and 3-deoxy-D-*manno*-octulosonate 8-phosphate (KDO8P) synthase are two bacterial enzymes that are vital for host virulence. DAH7P synthase catalyses the first commited step of the shikimate pathway that results in the biosynthesis of aromatic metabolites. KDO8P synthase catalyses the formation of the sugar KDO, which is an essential component of the cell wall of Gram-negative bacteria. The enzymes that catalyse these reactions are not present in animals, and therefore they are attractive targets for anti-bacterial agents.

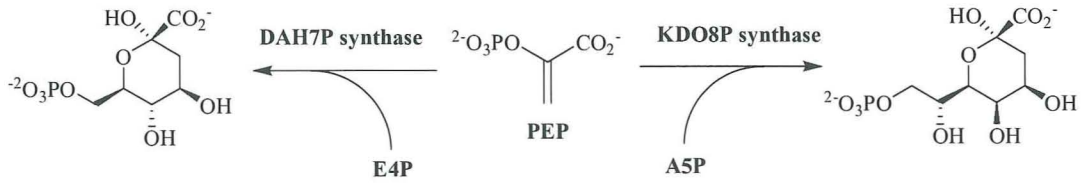

Interestingly, these two enzymes catalyse very similar aldol-like reactions and share a common substrate, phosphoenolpyruvate (PEP). In this thesis, the synthesis of various analogues to the shared substrate, PEP, has been described. Alterations to PEP include; substitution of a vinylic proton for either a fluorine, a bromine, a chlorine, a methyl group or deuterium; substitution of the carboxylic acid group for a methylchloride or a phosphonate; reduction of the double bond, and substituting the phosphate bridging oxygen for a methylene group. These analogues were tested as competitive inhibitors, and some as substrates and irreversible inhibitors against DAH7P synthase (from *E. coli*) and KDO8P synthase (from *N. meningitidis*).

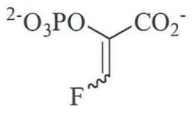

3-FluoroPEP was observed to act as a substrate for both DAH7P synthase and KDO8P synthase. However, following the reaction progress *via* ^{19}F NMR spectroscopy showed that in the KDO8P synthase reaction the (*Z*)-isomer was processed much slower than the (*E*)-isomer, whereas in the DAH7P synthase reaction both isomers were processed at a similar rate.

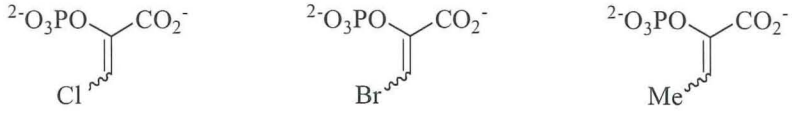

Chloro, bromo and methyl 3-substituted PEP analogues were found to be reasonable competitive inhibitors of DAH7P synthase and KDO8P synthase. DAH7P synthase was

shown to have better inhibition with the (*E*)-isomers of these 3-substituted PEP analogues, whereas in KDO8P synthase this varied.

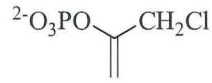

1-(Chloromethyl)vinyl phosphate was shown to be a poor competitive inhibitor of both DAH7P synthase and KDO8P synthase. However, this compound showed time-dependent covalent inactivation of both DAH7P synthase and KDO8P synthase.

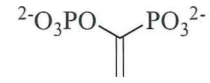

DiphosphoPEP was shown to be a reasonable competitive inhibitor towards DAH7P synthase, and was a poor competitive inhibitor of KDO8P synthase (at pH 6.5). Lowering the pH to 5.3 resulted in significantly greater inhibition of KDO8P synthase. DiphosphoPEP was shown not to act as a substrate to both enzymes.

(*R*) (*S*)

The (*R*)-isomer of 2-phospholactic acid was found to be the best competitive inhibitor of DAH7P synthase, from the PEP analogues tested, and the (*S*)-isomer had approximately 6-fold weaker inhibition. Inhibition of KDO8P synthase with 2-phospholactic acid was poor, with slightly better inhibition with the (*R*)-isomer.

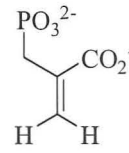

The phosphonate of PEP was shown to be a reasonable competitive inhibitor towards DAH7P synthase and close to no inhibition was observed of KDO8P synthase (at pH 6.5). Lowering the pH to 5.3 resulted in some inhibition of KDO8P synthase.

Table of Contents

Preface / Acknowledgements iii

Abstract iv

Abbreviations ix

Chapter One: Introduction

1.1 Introduction 2

1.2 The Shikimate Pathway 2

1.2.1 Introduction 2

1.2.2 Mechanism of DAH7P Synthase 4

1.3 The Lipopolysaccharide Pathway 11

1.3.1 Introduction 11

1.3.2 Mechanism of KDO8P Synthase 14

1.3.3 Metal Dependency in KDO8P Synthase 22

1.4 Mechanistic Comparison of DAH7P and KDO8P Synthases 25

1.5 Phylogenetic Relationship between DAH7P and KDO8P Synthases 27

1.6 Comparison of Enzyme Structure 28

1.7 Enzyme Interactions with Substrates 32

1.7.1 Interaction with PEP 32

1.7.2 Interaction with E4P and A5P 34

1.7.3 Source of the Water Reactant in the Enzyme Catalysed Reactions 35

1.8 Phosphoenolpyruvate (PEP) 38

1.9 Work Described in This Thesis 40

Chapter Two: Synthesis

2.1 Introduction 43

2.2 Perkow Reaction 43

2.2.1 Mechanism of the Perkow Reaction 44

2.2.1.1 Mechanism A: *Attack at the carbonyl oxygen* 44
2.2.1.2 Mechanism B: *Attack at the halogen* 45
2.2.1.3 Mechanism C: *Attack at the carbonyl carbon* 46
2.2.1.4 Mechanism D: *Attack at the halogenated α-carbon* 48
2.2.1.5 Summary 50
2.2.2 The Use of Triethylphosphite in the Perkow Reaction 50
2.3 3-Substituted Analogues of Phosphoenolpyruvate 52
2.3.1 Preparation of 3-FluoroPEP 52
2.3.2 Preparation of 3-ChloroPEP 55
2.3.3 Preparation of 3-BromoPEP 56
2.3.4 Preparation of 3-MethylPEP 58
2.3.5 Preparation of 3,3-DideuteriumPEP 59
2.4 Carboxyl Substituted Analogues of Phosphoenolpyruvate 61
2.4.1 Preparation of 1-(Chloromethyl)vinyl Phosphate 61
2.4.2 Preparation of 1-(Dihydroxyphosphinyl)vinyl Phosphate 62
2.5 2-Phospholactic Acid 64
2.5.1 Preparation of 2-Phospholactic Acid 64
2.6 2-(Phosphonomethyl)acrylic Acid 65
2.6.1 Preparation of 2-(Phosphonomethyl)acrylic Acid 66

Chapter Three: Testing of PEP Analogues with DAH7P and KDO8P Synthases

3.1 Introduction 69
3.2 Testing 3-Substituted Analogues Against DAH7P and KDO8P Synthases 70
3.2.1 3-FluoroPEP 70
3.2.2 Chloro-, Bromo- and Methyl-PEP 74
3.3 Testing Carboxyl Substituted Analogues against DAH7P and KDO8P synthases 81
3.3.1 1-(Chloromethyl)vinyl Phosphate 81
3.3.2 1-(Dihydroxyphosphinyl)vinyl Phosphate 86
3.4 Testing 2-Phospholactic Acid Against DAH7P and KDO8P synthases 88

3.5 Testing PEP Phosphonate Against DAH7P and KDO8P synthases 90
3.6 Implication of Results to Inhibitor Design 92
3.7 Future Work 93

Chapter Four: Experimental

4.1 General Procedures 97
4.2 General Biochemical Methods 98
4.3 Experimental for Chapter Two 100
4.4 Experimental for Chapter Three 114

Appendices 120

References 130

Abbreviations

A5P	D-arabinose-5-phosphate
BTP	Bis Tris propane
CHA	cyclohexylamine
$CHCl_3$	chloroform
CH_2Cl_2	dichloromethane
Da	daltons
g	relative centrifugal force
HCl	hydrochloric acid
d	doublet
DAH7P	3-deoxy-D-*arabino*-heptulosonate 7-phosphate
δ	chemical shift in parts per million
E4P	D-erythrose-4-phosphate
EDTA	ethylene diamine tetraacetic acid disodium salt
ES-MS	electrospray mass spectrometry
EtOAc	ethyl acetate
g	grams
Hz	herts
J	coupling constant
KDO8P	3-deoxy-D-*manno*-octulosonate 8-phosphate
K_i	inhibition constant
K_M	Michaelis constant
KOH	potassium hydroxide
L	litres
LPS	lipopolysaccharide
m	milli-
M	molar (or moles per litre)
M_r	relative molecular weight
min	minutes
μ	micro-
NMR	nuclear magnetic resonance
PEP	phosphoenolpyruvate
pet ether	petroleum ether
ppm	parts per million
P_i	inorganic phosphate
q	quartet
RT	room temperature
s	singlet
t	triplet
THF	tetrahydrofuran
TLC	thin layer chromatography
TMSBr	bromotrimethylsilane
UV	ultra-violet
V_{max}	maximum verlocity

Chapter One

Introduction

1.1 Introduction

The aim of this thesis is to compare the reactions catalysed by two similar bacterial enzymes that operate in distinctly different biosynthetic pathways. The two enzymes are 3-deoxy-D-*manno*-octulosonate 8-phosphate (KDO8P) synthase; a key enzyme in the biosynthesis of lipopolysaccharides in Gram-negative bacteria, and 3-deoxy-D-*arabino*-heptulosonate 7-phosphate (DAH7P) synthase; the first enzyme of the shikimate pathway (**Figure 1.1**). Finding key differences in the way these two enzymes process analogues of the common substrate, phosphoenolpyruvate (PEP) **1**, would provide information and clarifying aspects of the mechanism to their respective reactions. Because neither of these enzymes is present in mammals, this information may aid in the synthesis of specific inhibitors, and ultimately target specific antibiotics.

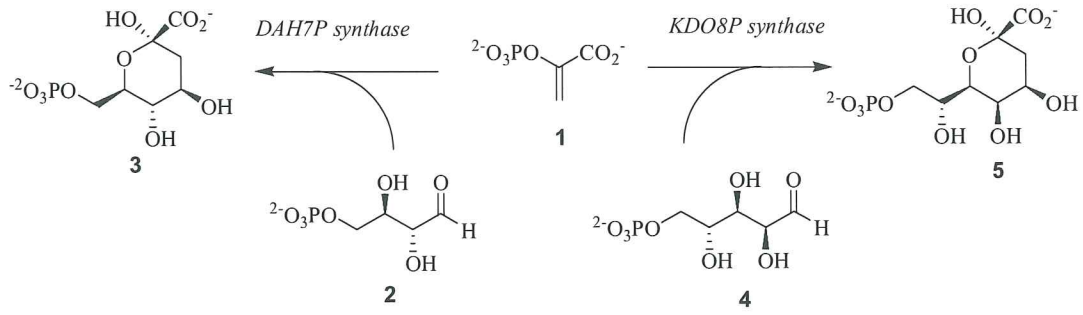

Figure 1.1 Reactions catalysed by DAH7P synthase and KDO8P synthase.

1.2 The Shikimate Pathway

1.2.1 Introduction

The shikimate pathway (**Figure 1.2**) is present in plants, fungi and bacteria and is responsible for the biosynthesis of chorismate **6**, a precursor to aromatic metabolites. These metabolites include: the three aromatic amino acids, L-phenylalanine, L-tyrosine and L-tryptophan, biologically important metabolites such as folic acid, vitamin K and vitamin E, and the structural polymer, lignin, found in higher plants.[1,2]

The shikimate pathway is not present in mammals, and therefore essential aromatic metabolites must be included in our diet.[3] It is not known why this important pathway does

not occur in mammals, but is proposed to have been an evolutionary strategy, due to its high energy cost (ATP equivalence).

An estimated 20% of carbon fixed by plants is channelled through this pathway. The combination of this high carbon flux, and the pathway being non-existent in mammals, makes it an attractive target for herbicides, fungicides and microbial agents. A good example is *N*-phosphonomethylglycine (glyphosate), an inhibitor of the sixth enzyme of the shikimate pathway that has had huge success as the active ingredient in herbicides.[4]

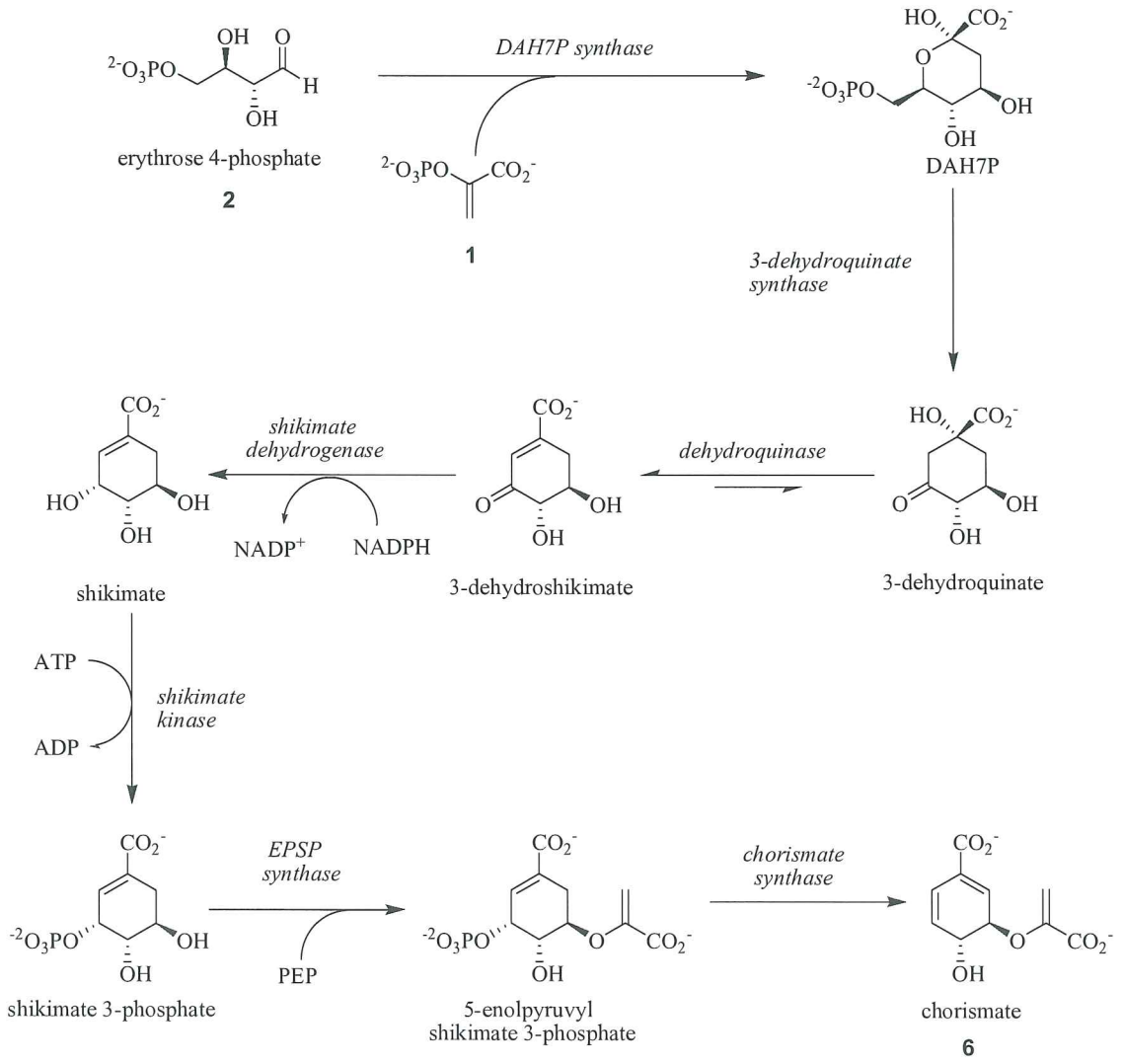

Figure 1.2 The shikimate pathway.

1.2.2 Mechanism of DAH7P Synthase

DAH7P synthase catalyses the first committed step of the shikimate pathway. It condenses phosphoenolpyruvate (PEP) **1** with the four-carbon sugar, erythrose 4-phosphate (E4P) **2** to give the eight-carbon sugar 3-deoxy-D-*arabino*-heptulosonate 7-phosphate (DAH7P) **3** and inorganic phosphate (P_i) (**Figure 1.3**).[2, 5]

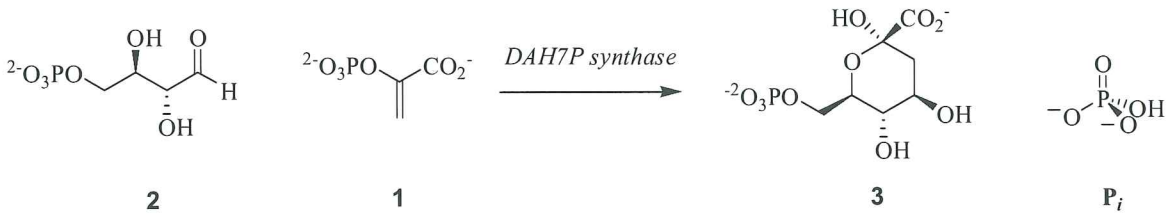

Figure 1.3 The catalysed reaction of DAH7P synthase.

All DAH7P synthases characterised to date have been found to require a divalent metal ion for activity. The metal is coordinated to four residues that are conserved in all DAH7P synthases. These include, from the phenylalanine sensitive (Phe) isozyme of *E. coli*, cystine 61^{Ec}, histidine 268^{Ec}, glutamic acid 302^{Ec} and aspartic acid 326^{Ec} (**Figure 1.4**).[6]

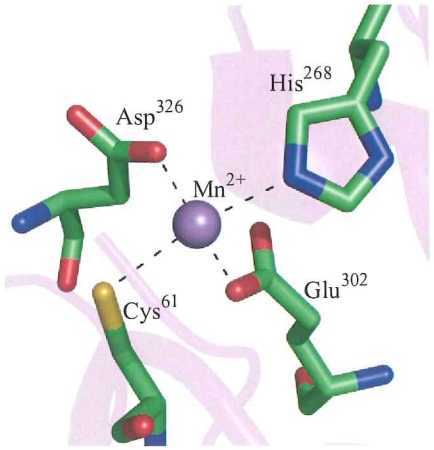

Figure 1.4 Metal coordination in (Phe) DAH7P synthase (*E. coli*) (PDB code 1KFL).

Enzymes treated with the metal chelator ethylenediaminetetraacetic acid (EDTA), then reactivated by treatment with a variety of divalent metal ions showed that the metal ion present in the active site influences the activity of the catalysed reaction. The specific activity of (Phe) DAH7P synthase from *E. coli*, with a variety of metal ions is as follows: $Mn^{2+} > Cd^{2+}$, $Fe^{2+} > Co^{2+} > Ni^{2+}$, Cu^{2+}, $Zn^{2+} >> Ca^{2+}$.[7]

Steady state kinetic analysis of DAH7P synthase from *E. coli* (Phe) using a variety of metal ions revealed that metal variation significantly affected the apparent affinity for the substrate, E4P, but not for the second substrate, PEP. The metal ion that is likely to be preferred *in vivo* is either Zn^{2+} or Fe^{2+}. This conclusion is based on the presence of these two metals in purified enzymes, on the high apparent affinity found in DAH7P synthase (from *E. coli* (Phe)) for these ions *in vitro*, and on their relatively high bioavailability.[7]

The reaction begins with the binding of PEP **1** to the active site, and is followed by the binding of E4P **2**. Structural and biochemical studies have provided much information on the enzyme reaction, but the exact mechanism is still not fully understood. Early studies with reactions performed in radio-labelled $H_2{}^{18}O$ showed that the P_i released did not contain ^{18}O, and that the labelled oxygen was found in the sugar product, DAH7P **3**.[8] This indicated that the release of P_i involved the cleavage of the C-O bond of PEP and not the more common O-P cleavage found in other PEP-utilising enzyme reactions. Consequently, the anomeric oxygen of DAH7P comes from the bulk solvent (**Figure 1.5**).

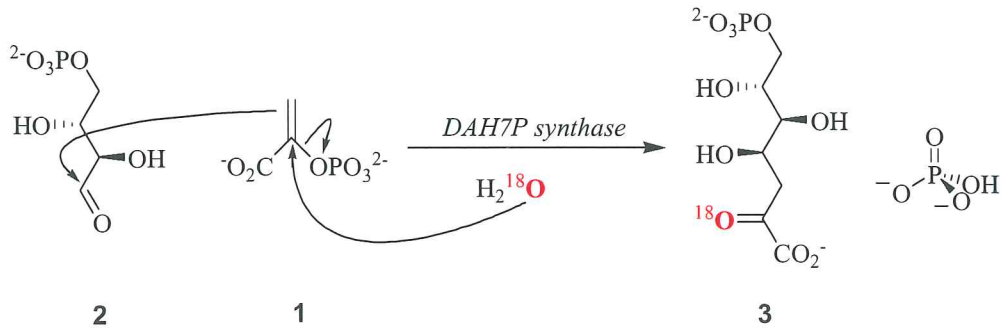

Figure 1.5 DAH7P synthase catalysed reaction performed in radio-labelled water, demonstrating that the water oxygen is incorporated in the sugar product and that inorganic phosphate must be cleaved *via* the C-O bond.

The reaction was shown to be stereospecific with the *si* face of PEPs C3 reacting with the *re* face of E4P. This was determined by enzymatically synthesising (*Z*)- and (*E*)-[3-^{3}H]PEP and observing the stereochemistry at C3 of the product (DAH7P) after reaction with E4P, catalysed by DAH7P synthase. It was observed that the ^{3}H in the (*E*) position of PEP gave [3-^{3}H]DAH7P predominantly in the (*R*) configuration (**Figure 1.6**), and ^{3}H in the (*Z*) position of PEP gave [3-^{3}H]DAH7P predominantly in the (*S*) configuration.[9]

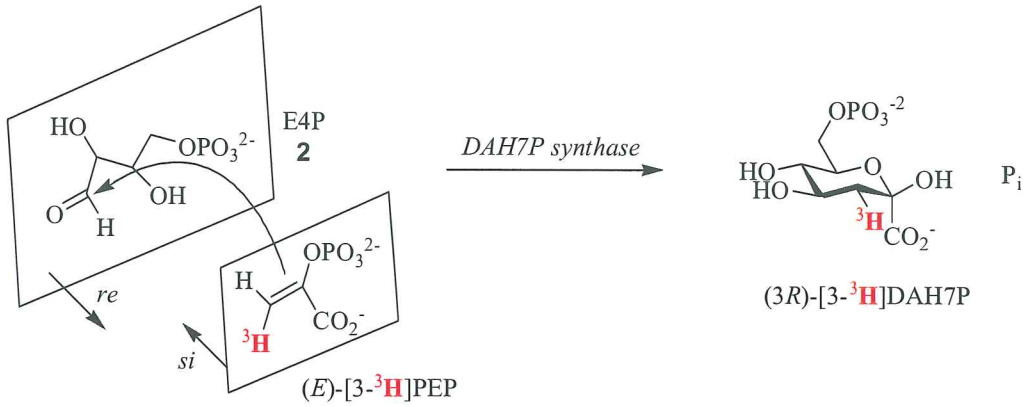

Figure 1.6 Radio-labelling experiment showing the stereochemistry of the DAH7P synthase catalysed reaction.

The basic reaction mechanism requires two steps; condensation of C3 of PEP with C1 of E4P, and attack of C2 of PEP by a water molecule. The two possible reaction mechanisms (**Figure 1.7, Path A and Path B**) differ in the order of these two steps.

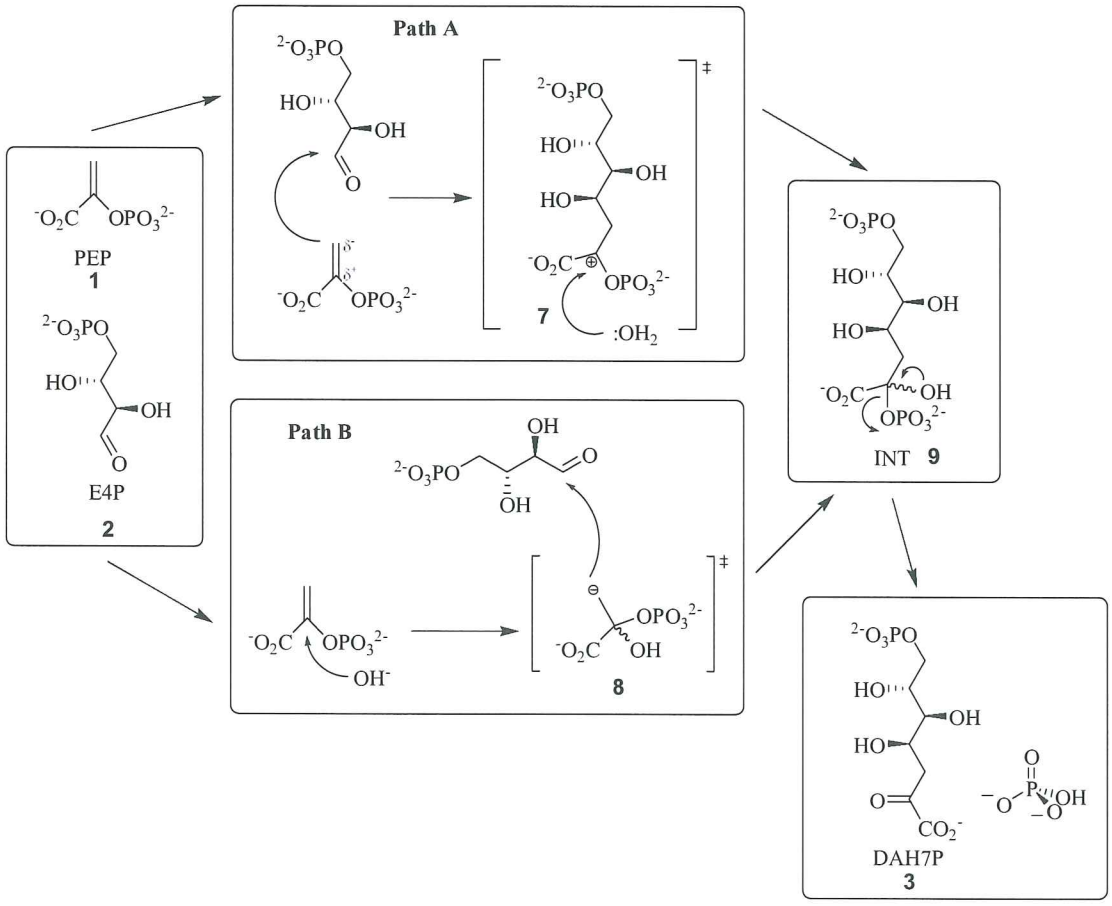

Figure 1.7 Proposed mechanism of DAH7P synthase.

Path A commences with the nucleophilic attack of the carbonyl of E4P by the C3 of PEP, resulting in the formation of a linear oxocarbenium ion **7**. The positively charged C2 is then attacked by a water molecule present in the active site, with subsequent loss of P_i.

In contrast, Path B begins with the production of a hydroxide ion by the deprotonation of a water molecule in the active site. This hydroxide ion attacks C2 of PEP, leading to the formation of a tetrahedral carbanion intermediate **8**, on the C3 of PEP. The carbanion then attacks the carbonyl carbon of E4P to produce the intermediate **9**.

Two key aspects are required for Path B to be a plausible mechanism, there cannot be free rotation about the C2-3 bond of the carbanion, and there must be a general base present in the active site to produce the hydroxide ion. The carbanion **8** formed, due to hydroxide attack at the C2 of PEP **1**, may freely rotate at the C2-3 bond (**Figure 1.8**). This could result in undefined stereochemistry at C2 of the product, DAH7P **3**. As mentioned previously, the reaction catalysed by DAH7P synthase proceeds in a stereospecific manner with regard to the protons at C3 of PEP, making it unlikely that this species is formed. The transient C3 carbanionic species of PEP (**Figure 1.7, Path B**) also seems less plausible since such a species is highly basic ($pK_a > 30$), has no resonance stabilisation, and as such, can rapidly decompose by abstracting a proton from water or surrounding residues. These two arguments suggest that if the reaction was initiated by an activated water molecule, as depicted in Path B, the two reaction steps occur simultaneous and not in a stepwise manner. This solves the problem of free rotation, causing epimerisation at C3, and rapid decomposition of the carbanion.

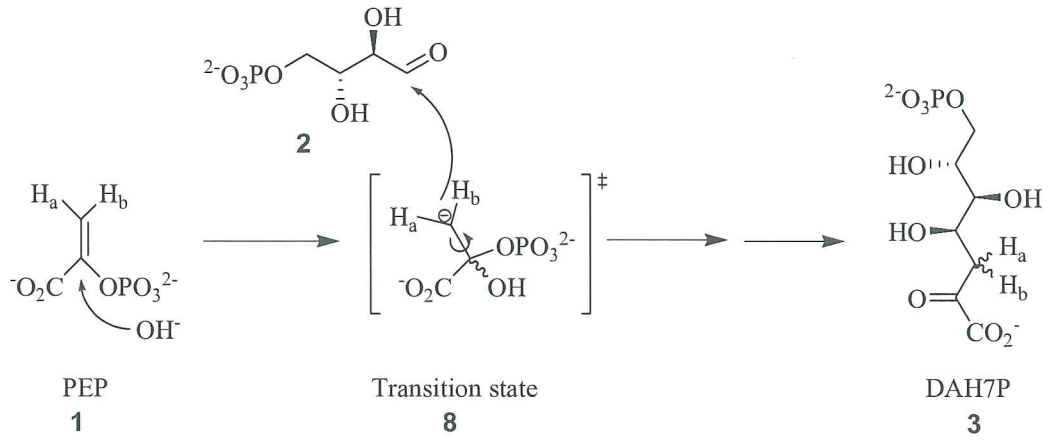

Figure 1.8 From Path B, free rotation of carbanion **8** resulting in undefined stereo chemistry at C3 of DAH7P.

It has been proposed that the hydroxide ion required for Path B could be generated from a histidine that coordinates the metal ion in the active site acting as a base to deprotonate a water molecule.[10] The hydroxide ion produced would be in a good location for nucleophilic attack of the C2 of PEP. However, the protonated histidine would disengage from the divalent metal, involving the movement of a considerable number of atoms. This would likely lead to steric problems for the approach of E4P to PEP.[11]

Another candidate proposed to be capable of producing the hydroxide ion to support the mechanism from Path B, is the divalent metal located in the active site. Crystal structures of DAH7P synthase have shown a water molecule either coordinating or in close proximity to the divalent metal. The interaction of the water molecule with the metal ion is expected to lower the pK_a, facilitating its ionisation.[12] The water molecule is positioned on the same side as the aldehyde of E4P to the enol of PEP, and therefore the reaction would represent an unusual *syn* addition of water and E4P to the *si* side of PEP.

Path A on the other hand requires that the environment of the active site is able to facilitate nucleophilic attack on the carbonyl of E4P by C3 of PEP. Before 3-dimensional crystal structures of DAH7P synthase were available, a theoretical analysis of PEP was carried out, and it was predicted that the reactivity of PEP is controlled by the relative rotation of its carboxylate and enol groups.[13]

A high resolution structure of DAH7P synthase (E24Q mutant) from *E. coli* showed a twist in the plane of the carboxylate by 30° (**Figure 1.9**), usually approximately 0° in solution due to conjugation of its π-orbitals.[14] The twist in the carboxylate is thought to lower the activation energy of the nucleophilic attack of E4P by PEP.

It appears that the extensive interactions of PEP in the active site causes this deviation from planarity and suggest that PEP is completely ionized carrying three negative charges.

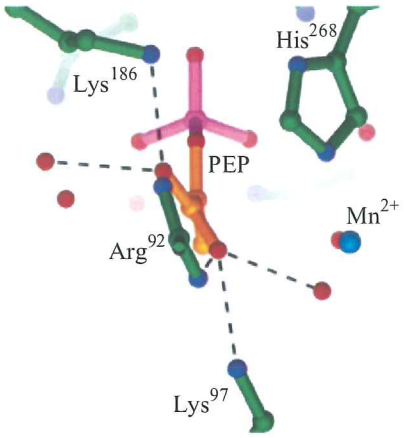

Figure 1.9 Rotation of the carboxyl group of PEP in the crystal structure of DAH7P synthase from E24Q mutant of DAH7P synthase (PDB code 1N8F).[14]

PEP, in its trianionic form, is predicted to lower the energy for the rotation of the carboxylate. Also, having PEP in its fully ionized state would make the C2 of PEP less susceptible to nucleophilic attack from water in Path B compared to PEP in its dianionic form. This observation supports the mechanism of Path A.

Taking advantage of the negligible activity of DAH7P synthase, at low temperatures, from the thermophilic bacterium, *T. maritima*, Shumilin and co-workers[15] were able to obtain crystal structures containing both substrates (PEP and E4P) and the metal co-factor in the active site. The position of E4P was not highly defined, as two independent crystal structures showed different conformations for the bound E4P, neither giving indication of the carbonyl oxygen coordinating with the metal. Konig and co-workers[16] solved the crystal structure of DAH7P synthase from *S. cerevisiae* and E4P was modelled in the active site using the bound glycerol 3-phosphate (an E4P analogue lacking its aldehyde group) as a tethering point. Their model demonstrated that the carbonyl oxygen of E4P could be coordinated to the divalent metal. Under these conditions, the metal ion would act as a Lewis acid removing electron density from the carbonyl carbon, activating it for nucleophilic attack by C3 of PEP. Such an attack is consistent with the observed stereochemistry of the product.[16]

A water molecule and two residues in the active site of DAH7P synthases (from *T. maritima*), lysine 131^{Tm} and glutamic acid 164^{Tm}, are proposed to be involved in catalysis to facilitate the movement of protons (**Figure 1.10**), following Path A.

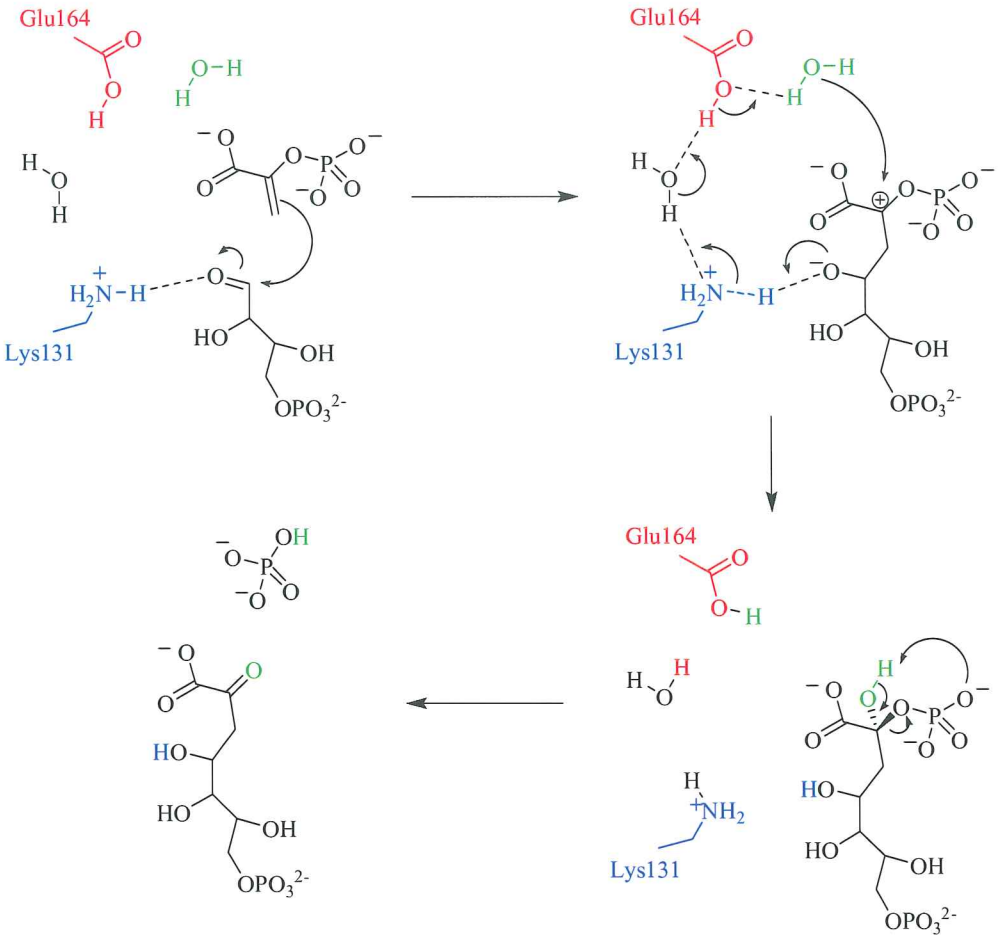

Figure 1.10 Proposed movement of protons in the DAH7P synthase catalysed reaction.

Lysine 131^{Tm} is positioned in the active site to hydrogen bond with the carbonyl oxygen of E4P, and after nucleophilic attack of the carbonyl of E4P, may provide a proton to produce the hydroxyl group. A water molecule hydrogen bonded to lysine 131^{Tm}, donates a proton and accepts a proton from a glutamic acid 164^{Tm}. This generates a hydroxide ion to attack the C2 carbocation transition state. The intermediate interacts less strongly in the active site allowing greater manuverability. The short-lived intermediate reacts through cleavage of the C-O bond of the phosphate, which accepts the proton from the C2 hydroxyl group to form the carbonyl functionality. The ex-PEP phosphate is released, completing the reaction.[15]

1.3 The Lipopolysaccharide Biosynthetic Pathway

1.3.1 Introduction

Gram-negative bacteria possess two membranes that separate the cytoplasmic compartment from the extracellular environment. While the inner layer is composed mostly of phospholipids, the outer monolayer contains a unique molecule known as the lipopolysaccaride (LPS) that covers approximately three quarters of the cells outer surface. LPS determines the surface recognition of bacteria, and varies between species and between different strains of the same species. LPS also acts as an endotoxin, causing a strong immune response in animals when the bacteria are lysed.[17]

LPS is composed of four main regions: **(Figure 1.11)**

1. Lipid A; the hydrophobic component that anchors LPS to the outer surface of the cell. It is a phosphorylated disaccharide containing six fatty acids.
2. The inner core region; composed of two or three molecules of 3-deoxy-D-*manno*-octulosonate and two or three heptose residues. This region is fairly constant among species.
3. The outer core region; a pentasaccharide whose covalent structure is more variable than that of the inner core. The outer core provides the attachment site for the O antigen.
4. The *O*-polysaccharide; extends into the extracellular environment. It is composed of up to 40 repeating units, which may contain up to seven different or identical sugars, each of which is interlinked by glycosidic linkages. This determines the antigenic specificity of the strain.

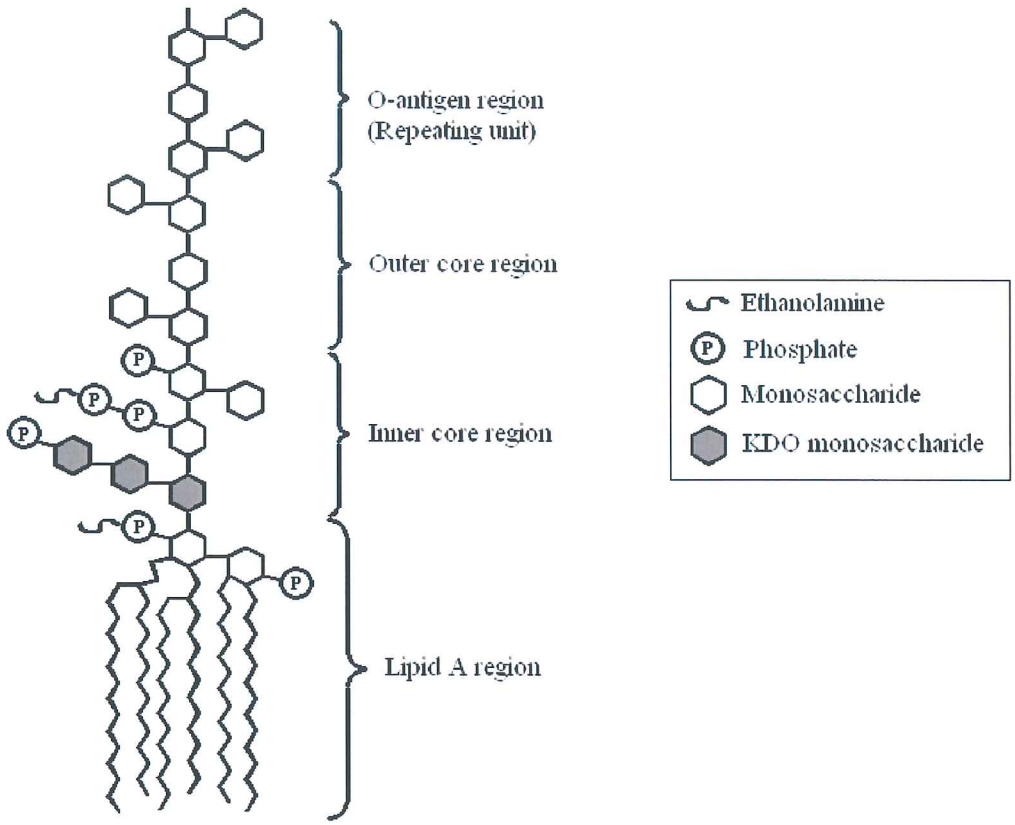

Figure 1.11 Schematic diagram of the general structure of LPS from *Salmonella*.[18]

LPS is first assembled in the inner membrane, by the sequential addition of sugars to lipid A, and then transported to the outer membrane by an unknown mechanism.[18] Synthesis of lipid A proceeds in two steps; first is the acylation of glucosamine molecules, which adds four acyl chains, followed by the addition of two 2-keto-3-deoxy-D-*manno*-octulosonate (KDO) molecules, coupled *via* the activated sugar nucleotide cyclomonophosphate-KDO (CMP-KDO) (**Figure 1.12**).

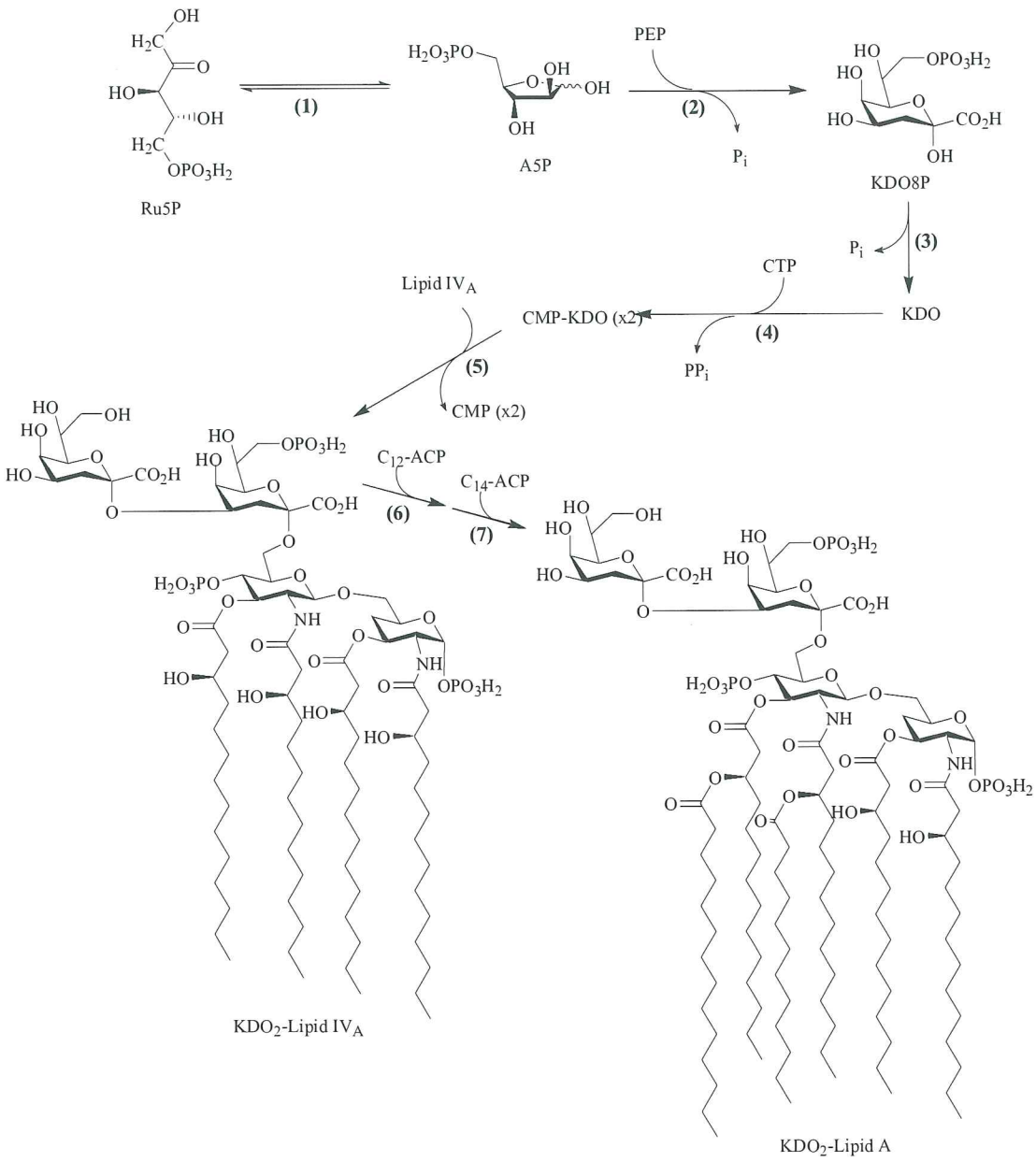

Figure 1.12 Biosynthesis and incorporation of KDO into LPS. **(1)** D-Arabinose 5-phosphate isomerase, **(2)** KDO8P synthase , **(3)** KDO8P phosphatase, and **(4)** CMP-KDO synthetase. In *E. coli*, two molecules of activated KDO are then sequentially transferred to lipid IVA by KDO transferase **(5)** before the stepwise addition of the secondary acyl chains laurate **(6)** and myristate **(7)**.

Rick and co-workers isolated a mutant of *S. typhimurium* that had a defective KDO8P synthase.[19] This was caused by a single mutation that gave rise to a temperature-sensitive enzyme. The mutant enzyme was shown to have an increased K_M, and thus a decreased affinity for A5P at increased temperatures. Mutant bacterial cells had relatively normal growth and synthesis of LPS at temperatures below 30°C, however, above this temperature an increasing dependence on exogenous A5P was observed. When a temperature of 42°C was reached, exogenous A5P was no longer taken up, and this was followed by a halt in

the synthesis of protein, DNA, RNA, peptidoglycan and ultimately cell death.[20] These results indicate that KDO8P synthase is required for cell growth and makes it an attractive target for Gram-negative specific antibiotics.

1.3.2 Mechanism of KDO8P Synthase

KDO8P synthase catalyses the first committed step in the biosynthesis of LPS. It catalyses the aldol-like condensation of PEP **1** and *arabinose* 5-phosphate (A5P) **4** to give the 8-carbon sugar 3-deoxy-D-*manno*-octulosonate 8-phosphate (KDO8P) **5** and P_i (**Figure 1.13**).[21]

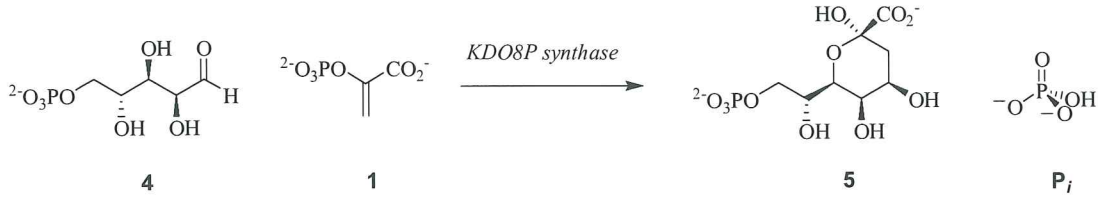

Figure 1.13 Reaction catalysed by KDO8P synthase.

Like DAH7P synthase, KDO8P synthase was found to have a preferred order of substrate binding, with PEP preceding the binding of A5P.[22] Radio-labelled PEP studies indicate that the loss of inorganic phosphate occurred *via* C-O bond cleavage, and that the reaction requires a water molecule to form the C2 hydroxyl group of the product, KDO8P.[23] The reaction is stereospecific with the *si* face of PEP (C3) attacking the *re* face of the carbonyl group of A5P (**Figure 1.14**).[24]

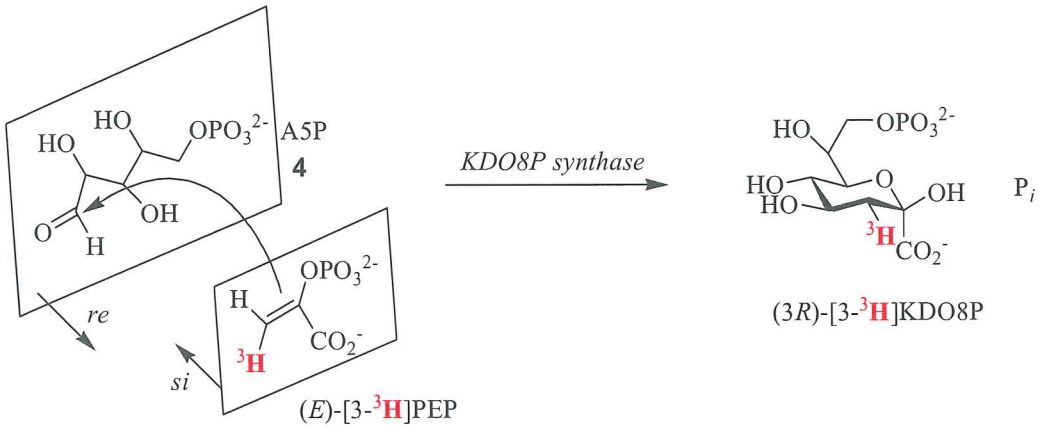

Figure 1.14 Radio-labelling experiment showing the stereochemistry of the KDO8P synthase catalysed reaction, with (*E*)-[3-^{3}H]PEP producing [3-^{3}H]KDO8P as the (*R*) form.

Interestingly, KDO8P synthases from different species have been observed to either have a metallo or non-metallo requirement for activity. Whereas all DAH7P synthases require a divalent metal for activity.

The first proposed mechanism of KDO8P synthase involved a linear bisphosphate intermediate **10** (**Figure 1.15**),[23] however, there was no evidence to support this.

The 2-hydroxyl analogue of KDO8P **11** (**Figure 1.15**) was synthesised by the reduction of KDO8P and mimicked the proposed linear intermediate **10**.[25] This analogue did not inhibit the *E. coli* enzyme catalysed reaction, suggesting the structure of the proposed intermediate **10** may not be plausible. In the same study, analogues of A5P were tested and it was demonstrated that 3-deoxyA5P **12** was not a substrate for KDO8P synthase (from *E. coli*).[25] This was interesting, as the 3-hydroxyl group of A5P would be required to form a cyclic intermediate **13**. Therefore, these results supported an enzyme reaction involving a cyclic intermediate.

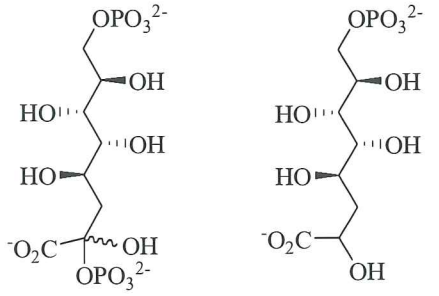

Fig. 1.15 Proposed linear intermediate **10** and its proposed mimic 2-hydroxy KDO8P **11**.

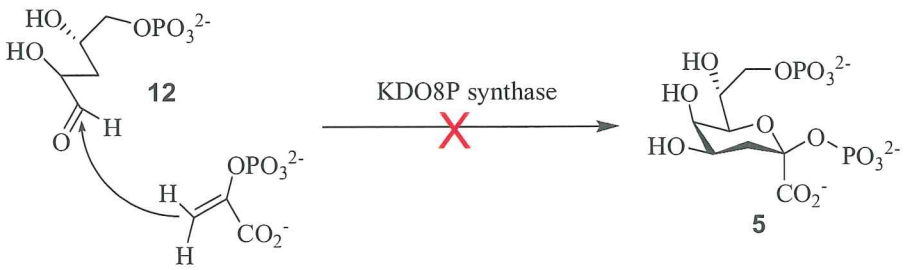

Figure 1.16 3-Deoxy A5P **12** is not a substrate for KDO8P synthase.

Baasov and co-workers proposed a reaction mechanism that proceeded *via* a cyclic intermediate **13** (**Figure 1.17**).[26] To support their mechanism they synthesised analogues of the proposed cyclic intermediate and observed weak competitive inhibition with respect to PEP binding. The best of these analogues being a phosphonate analogue of the proposed cyclic intermediate having a K_i value of 5 μM **14** (**Figure 1.17**).

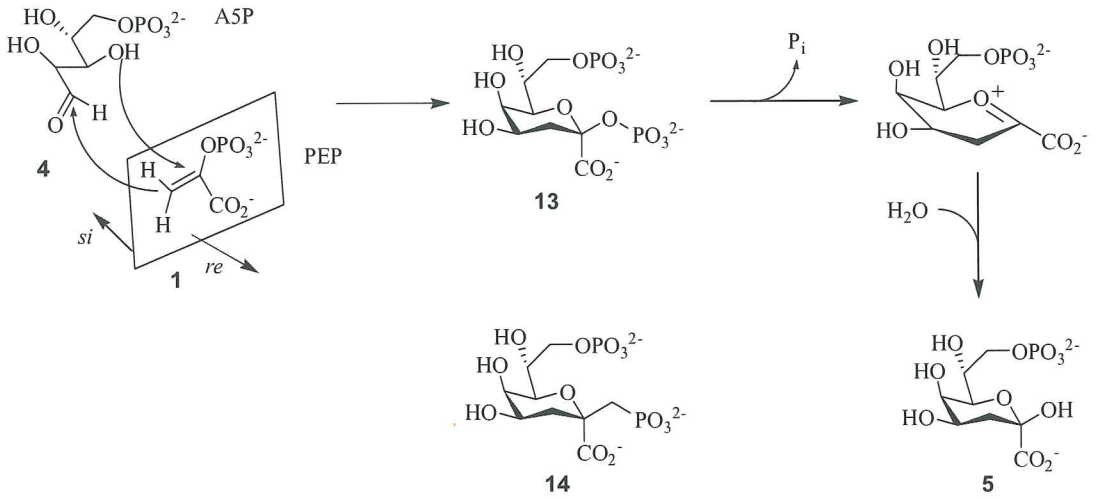

Figure 1.17 Proposed reaction of KDO8P synthase *via* cyclic intermediate **13,** and the phosphonate analogue of the cyclic intermediate **14.**

The proposed cyclic intermediate **13** was synthesised to examine its ability to act as an alternative substrate for KDO8P synthase.[27] Its failure to act as an alternative substrate or as a potent inhibitor suggested that the enzyme catalysed reaction did not involve the formation of **13** as a reaction intermediate.[28]

The determination of the crystal structure of KDO8P synthase from *E. coli* provided significant information about the mechanism.[29] Two sulphate ions from the crystallising medium bound in the active site indicated the binding position of the phosphate moieties of PEP and A5P. Their distance apart (13 Å) was consistent with an end on linear approach in the condensation reaction, and was too far apart to support a reaction mechanism involving a cyclic intermediate. This evidence ruled out the mechanism involving a cyclic intermediate **13**, and demonstrated that the reaction proceeded with a linear intermediate **10**, as initially proposed.

The reaction of KDO8P synthase involves two steps; condensation of C3 of PEP with the carbonyl carbon of A5P and the attack of C2 of PEP by a water molecule.

Like DAH7P synthase, KDO8P synthase has two possible reaction pathways that proceed *via* a linear intermediate, and differ by the order of the two steps (**Figure 1.18**).

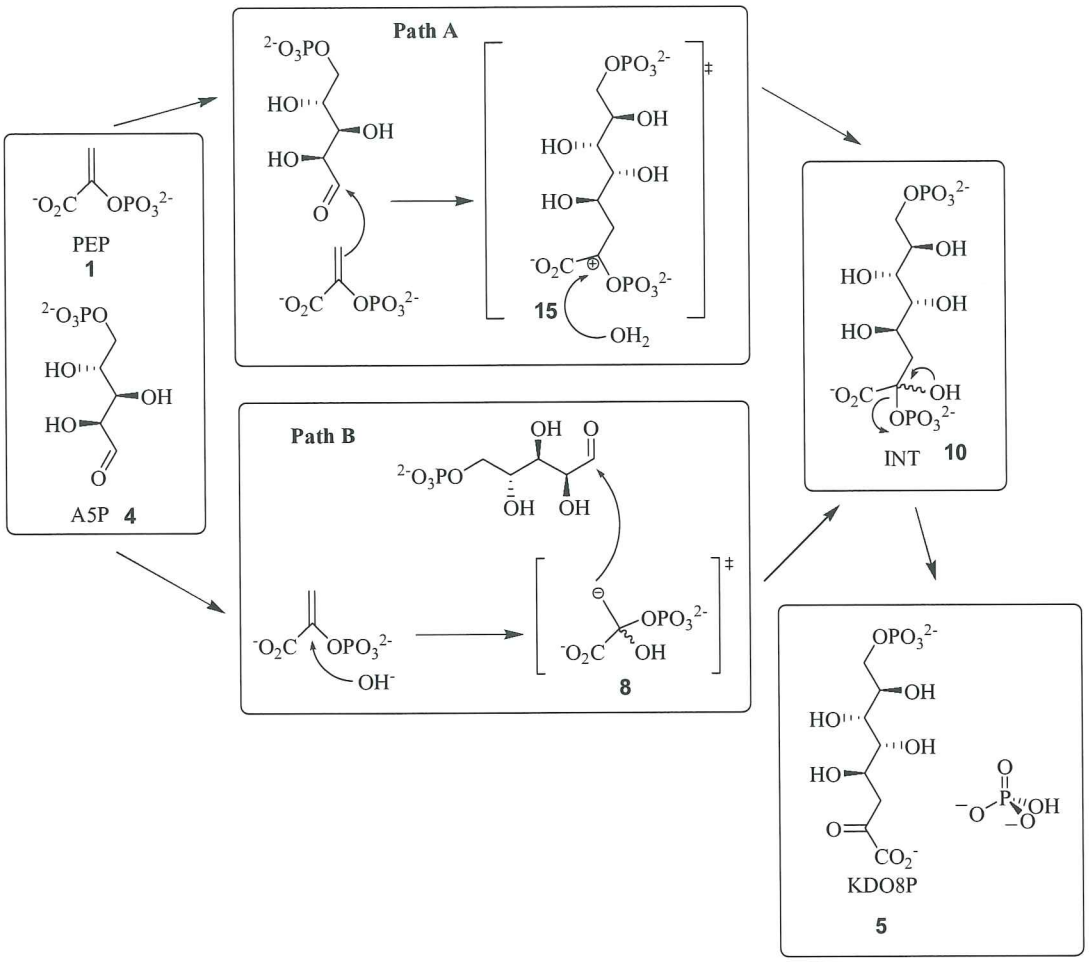

Figure 1.18 The two proposed mechanisms of KDO8P synthase.

Similar to DAH7P synthase, Path A of the KDO8P synthase mechanism commences with nucleophilic attack of the carbonyl of A5P by C3 of PEP. This forms an oxocarbenium ion transition state **15**. A water molecule then attacks the positively charged C2 to form the linear bisphosphate intermediate **10**.

Reaction *via* Path B requires deprotonation of a water molecule, to form a hydroxide ion, to initiate catalysis. The nucleophilic attack of C2 of PEP by the hydroxide ion produces a carbanion transition state **8**, with the negative charge on the C3. This carbanion **8** nucleophilically attacks the carbonyl of A5P to give the intermediate **10**. The putative linear intermediate **10** (**Figure 1.18**) involved in both pathways, decomposes generating the products, KDO8P **5** and inorganic phosphate.

The proposed stepwise reaction sequence in Path B for KDO8P synthase (**Figure 1.18**) is problematic, as mentioned for Path B of DAH7P synthase. The carbanion formed is very reactive, and would rapidly decompose. In addition, free rotation at the C2-3 bond of the carbanion species could lead to epimerisation at C3 of the final product, KDO8P, when it has previously been shown to be stereospecific at this position.[24]

Catalysis *via* Path B also appears unlikely as there is no suitable candidate in the active site for production of the hydroxide ion. In the crystal structure of the metal-dependent KDO8P synthase from *A. aeolicus*,[10] a water molecule is found to coordinate to the divalent metal, which could possibly facilitate deprotonation. Using their crystal structure of KDO8P synthase from *A. aeolicus*, Wang and co-workers[10] envisioned a sequence mechanism that involved a metal activated water molecule, by holding the phosphate moiety of A5P and only altering substrate torsional angles (**Figure 1.19**).

In their proposed mechanism the divalent metal would lower the pK_a of the coordinated water molecule favouring deprotonation to a hydroxide ion and subsequent attack of C2 of PEP (**Figure 1.19, A**). The C2 hydroxyl of A5P is thought to replace the coordinated water molecule and position the carbonyl of A5P in the correct orientation for nucleophilic attack (**Figure 1.19, B**). The consequent negative charge on C3 of PEP drives the condensation reaction to form the putative intermediate (**Figure 1.19, C**). This mechanism would imply that the metallo and non-metallo forms of KDO8P synthase catalyse the reaction differently.

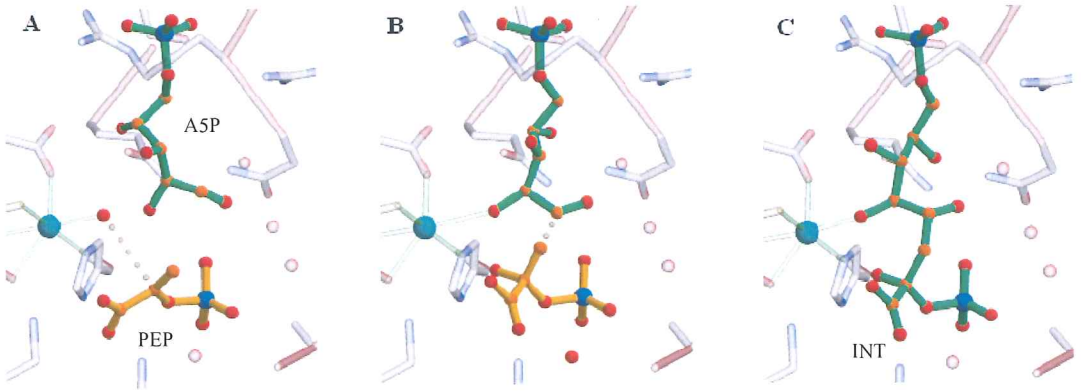

Figure 1.19 A proposed snap shot sequence of the reaction mechanism of metallo KDO8P synthase. Substrates are modelled to the crystal structure of KDO8P synthase from *A. aeolicus* (PDB code 1FWW).[10]

The reaction mechanism depicted by pathway A for both DAH7P synthase and KDO8P synthase, is dependent on the ability of C3 of PEP to act as a nucleophile. As mentioned, this is predicted to be possible through the relative rotation of functional groups on PEP, which was observed in the crystal structure of DAH7P synthase (E24Q mutant from *E. coli*, **Figure 1.9**). The crystal structure of KDO8P synthase from *A. aeolicus* showed a distortion in the planarity of PEP. **Figure 1.20** shows the structure of PEP when bound to the active site of KDO8P synthase, and the plane defined by C1, C3 and O2 deviates by approximately 12°.[12] These deviations from the stable planar conformation of PEP caused by interactions in the active site are not consistent amongst the solved crystal structures of DAH7P synthase or KDO8P synthase. However, this could be due to the effects different enzymes have on crystallisation and the different resolutions achieved for the structures.

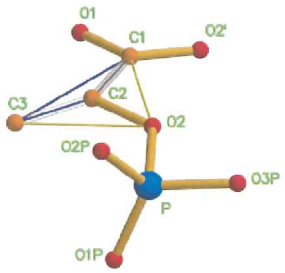

Figure 1.20 Deviation of planarity of PEP in the active site of KDO8P synthase from *A. aeolicus* (PDB code 1FWS).[12]

The most potent inhibitor of KDO8P synthase synthesised to date **15** (**Figure 1. 21**) further supports a reaction mechanism *via* Path A (**Figure 1.18**). This inhibitor is a slow binding competitive inhibitor with respect to PEP binding (K_i value of 0.4 μM against *E. coli* KDO8P synthase) and mimics features of the transition state found only in Path A **14** (**Figure 1.21**). The positive charge of the carbocation in the transition state is replaced by an ammonium functionality and one of the phosphate groups is replaced by a phosphonate moiety.[30,31] Despite it's strong inhibition, **15** lacked antibacterial activity. The phosphonate of **15** was synthesised, **16** (**Figure 1.21**), to test whether lack of antibacterial activity was due to the hydrolysis of the crucial C6 phosphate.[32] Compound **16** was found to be a competitive inhibitor of KDO8P synthase (*E. coli*), however it was 15-fold weaker than inhibitor **15**. Inhibitor **16** also displayed no antibacterial activity. It was proposed that the lack of antibacterial activity of **15** and **16** was due to their reduced ability to penetrate the bacterial cell membrane.

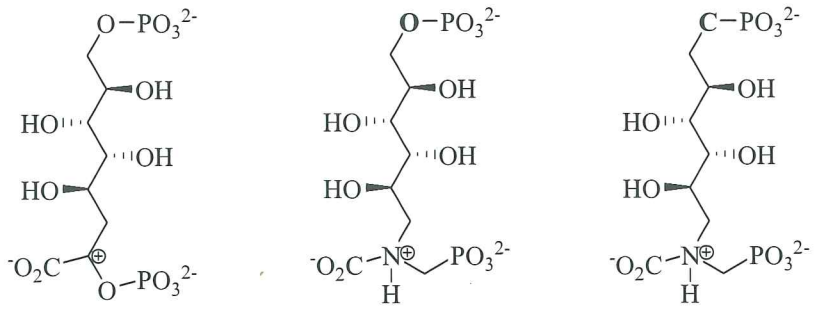

14 Transition state **15** **16**

Figure 1.21 Comparison of the transition state **14** from Path A, the structure of inhibitory mimic **15** and the mimic phosphonate **16**.

When PEP is bound in the active site of KDO8P synthase it is thought to be in its dianionic form. This prediction is based on the substitution of a conserved arginine (Arg165 from *E. coli*) in DAH7P synthase that interacts with the phosphate of PEP, for a conserved hydrophobic residue, phenylalanine (Phe103 from *A. aeolicus*) in KDO8P synthases. This conserved substitution results in the loss of an ionic contact in KDO8P synthase in comparison to DAH7P synthase and the hydrophobic phenylalanine in KDO8P synthase is predicted to lower the pK_a of the phosphate, therefore promoting its protonation. This protonated phosphate of PEP when in the active site of KDO8P synthase may hydrogen bond to the carbonyl oxygen of A5P. This would aid in the activation of the condensation reaction and could provide the proton to form the C4 hydroxyl of the product KDO8P (**Figure 1.22**).

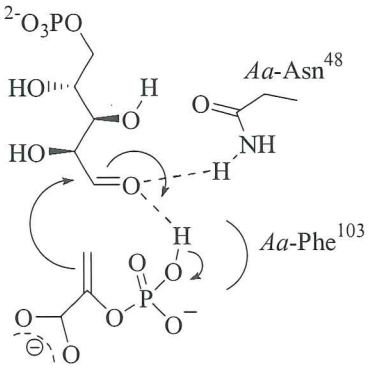

Figure 1.22 Possible movement of protons, based on the proposed dianionic nature of PEP in KDO8P synthase.

A conserved motif in KDO8P synthases, LysAlaAsnArgSer, forms a pocket for the binding of A5P in the active site. This is proposed to be a key feature of KDO8P synthase, in its

recognition and specificity for its substrate, A5P.[33] The crystal structure of KDO8P synthase from *A. aeolicus* shows the asparagine residue from the motif, Asn48 in **Figure 1.22**, hydrogen bonded with the carbonyl oxygen of A5P. This hydrogen bond would contribute to its activation and correctly orientate A5P for nucleophilic attack by PEP, supporting the mechanism from Path A.

The C2 hydroxyl of A5P is critical for the enzyme catalysed reaction, as removal[33] or alteration of its stereochemistry (i.e. D-ribulose 5-phosphate)[10,34,35] results in loss of activity in KDO8P synthase. Currently, the only crystal structure available of KDO8P synthase containing both substrates (A5P and PEP) is from *A. aeolicus* (wild-type and mutants).[12,36,37] Crystal structures of the wild type KDO8P synthase (*A. aeolicus*) show the C2 hydroxyl of A5P coordinated to the metal ion, positioning the carbonyl correctly for nucleophilic attack. This illustrates the possible role of the metal ion in metallo KDO8P synthases and explains the necessity of the C2 hydroxyl of A5P (**Figure 1.23**).

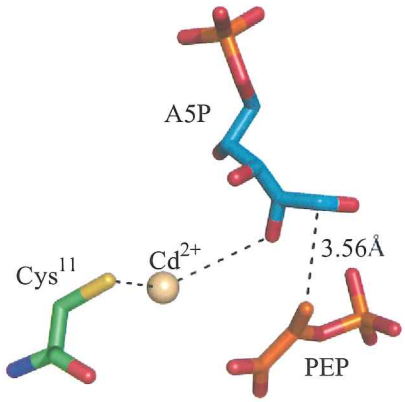

Figure 1.23 Interaction of metal with the C2 hydroxyl of A5P in wild-type KDO8P synthase from *A. aeolicus* (PDB code 1FWW).

However, a crystal structure of a triple mutant of KDO8P synthase (*A. aeolicus*) (C11N/S235P/Q237A- mutations of "naturally" substituted residues from metallo and non-metallo KDO8P synthases) shows a different conformation of A5P with a 180° twist, orientating the carbonyl oxygen towards asparagine Asn11 (**Figure 1.24, A**).

Kona and co-workers[37] propose that this orientation represents the catalytically competent conformation of A5P. As the carbonyl oxygen and all of the hydroxyl groups of A5P are in the same position that they assume in a crystal structure containing the reaction

intermediate (**Figure 1.24, B**). Furthermore, the distance between C3 of PEP and C1 of A5P is shorter (2.98 Å) in this conformation than in the other conformation (3.56 Å in wild-type, **Figure 1.23**), which would favour the formation of a bond between these atoms.[37] However, the crystal structure of the linear intermediate is not well defined, and its visualisation is somewhat debateable, as both chemical and experimental studies suggest that this chemical species is highly unstable.[38]

However, this proposed 'competent' conformation of A5P does not explain the absolute stereochemistry required at the C2 hydroxyl of A5P, placing it at hydrogen bond distance to the phosphate of PEP.

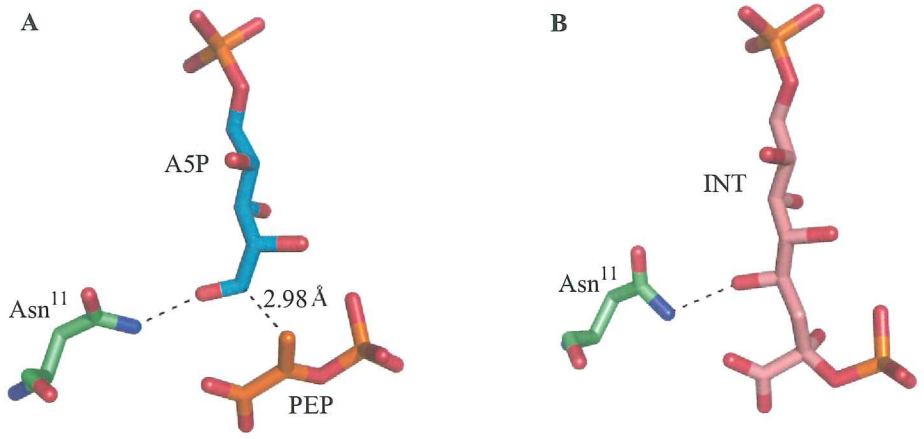

Figure 1.24 Crystal structures of the interaction of Asn11 from the triple mutant (C11N/S235P/Q237A) from *A. aeolicus*, showing similar conformations between, **A**, the proposed orientation of the substrates at the moment before condensation reaction, and **B**, the linear intermediate (PDB code 2NX3).[37]

1.3.3 Metal Dependency in KDO8P Synthase

KDO8P synthase from different Gram-negative species are found to be either metal or non-metal dependent for activity. The metal dependent KDO8P synthases, and DAH7P synthases, share four conserved residues that coordinate the metal ion.[39] These are aspartic acid, histidine, glutamic acid and cysteine. In non-metal dependent KDO8P synthases, three of these residues are conserved but cysteine is "naturally" substituted to an asparagine (**Figure 1.25**).

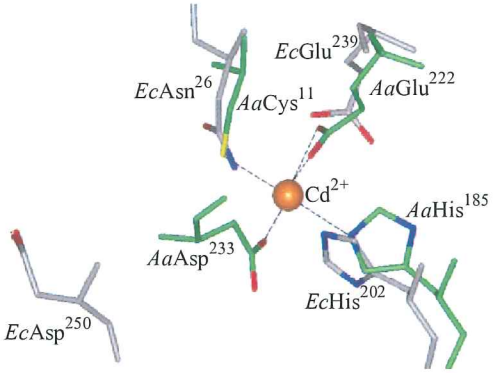

Figure 1.25 Superimposed metal binding residues from a metallo enzyme, *A. aeolicus* (in green – PDB code 1FWS), and the equivalent residues of a non-metallo enzyme, *E. coli* (in grey – PDB code 1G7U).[40]

Interestingly, metallo KDO8P synthases have been mutated to allow catalysis in the absence of a metal ion (from *A. pyrophilis*[40] and *A. aeolicus*[41]). This was achieved by substituting the metal binding cysteine for an asparagine, the residue universally conserved at the same position in non-metallo KDO8P synthases.

The crystal structure of the C11N mutant (Cys-M^{2+} moiety is replaced with an asparagine) has been solved for KDO8P synthase from *A. aeolicus*.[37] This shows a similar A5P conformation in its active site to the wild-type, with the C2 hydroxyl of A5P coordinating to the same position, but to the asparagine (Asn11) (**Figure 1.26**).[37] This illustrates the ability of the cysteine to asparagine substitution in metallo KDO8P synthase to remove metal dependency.

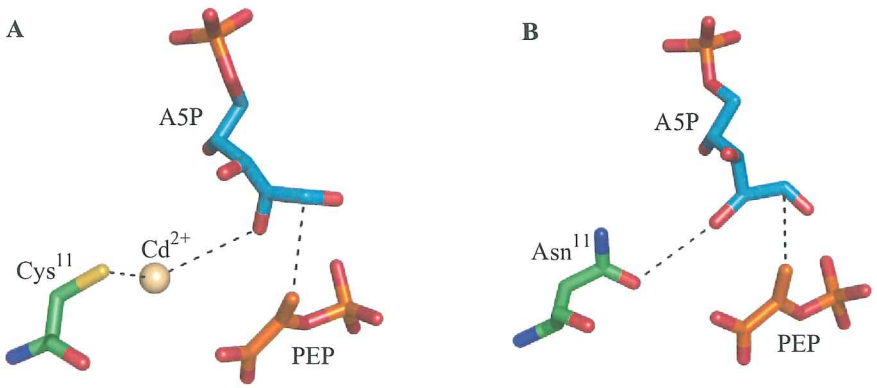

Figure 1.26 Crystal structure comparison of the C2 hydroxyl interaction of A5P in *A. aeolicus*, **A**, wild-type (PDB code 1FWW) and, **B**, C11N mutant (PDB code 2NWS).

Inversely, the non-metallo KDO8P synthase (from *E. coli*) has had its asparagine residue (Asn26) replaced by a cysteine residue.[40,42] The *Ec*N26C mutant displayed characteristics similar to metallo KDO8P synthases. For instance, the purified mutant enzyme gave an absorbance peak in the visible spectrum around 575 nm which is characteristic of a protein bound ferrous ion (Fe^{2+}), and is absent in the wild-type enzyme (*E. coli).*[40] It was found that addition of Mn^{2+} or Fe^{2+} increased the activity of the *Ec*N26C mutant, suggesting that the engineered Cys26 residue fulfils the role of the native, metal-ligated cysteine in metal dependent KDO8P synthases. However, unlike wild-type metallo KDO8P synthases, the *Ec*N26C mutant maintained some activity after treatment with the metal chelator EDTA, and interestingly, addition of divalent metal ions other than Mn^{2+} and Fe^{2+} were found to inhibit the *Ec*N26C mutant.[42]

Naturally occurring non-metallo KDO8P synthases are as active as their metallo counterparts, and non-metallo enzymes engineered *via* cysteine to asparagine substitution still maintain considerable activity. Thus, it implies that the metal ion is not necessary for catalysis or that at best it serves an auxiliary role in assuring the proper orientation of the substrates. These results support the notion that metallo and non-metallo KDO8P synthase catalyse with the same mechanism.

The reason for the existence of the two forms (metallo and non-metallo) of KDO8P synthase remains elusive. It has been argued that the metal only has a structural role in KDO8P synthase. However, the free energy of unfolding in water of wild-type KDO8P synthase deprived of the active site metal ion, or of engineered forms of KDO8P synthase lacking the metal binding Cys11, is actually larger than that of the metallo-enzyme. Whether the metal is directly involved in catalysis in metallo KDO8P synthases, its presence or absence affects the binding properties of both substrates (A5P and PEP).[37] Very little is known about the actual concentrations of metabolites such as PEP, A5P, R5P or even P_i *in vivo* in different bacteria. Significant variations in the concentrations of these compounds across different Gram-negative bacteria may make use of the metal ion (or lack thereof) as an adaptation of the enzymes to different cellular environments, without having to modify the core catalytic mechanism in a more drastic way.[37]

1.4 Mechanistic Comparison of DAH7P and KDO8P Synthases

DAH7P synthase and KDO8P synthase are involved in very different biosynthetic pathways but catalyse almost identical reactions, differing in one carbon and the altered stereochemistry on the C2 of the sugar substrate (**Figure 1.27**).

Figure 1.27 Differences in the molecular structure of E4P and A5P.

Both enzymes catalyse their reactions with the same overall stereospecificity, with the *si* face of PEP condensing with the *re* face of the carbonyl from the sugar substrate, and the reaction of both enzymes results in the dissociation of P_i *via* the cleavage of the C-O bond of PEP. Both enzymes show low sequence identity, but despite this, the enzymes have almost superimposable TIM barrel structures. These similarities have led to the hypothesis that these enzymes diverged from a common broad specificity ancestor.

X-ray crystal structures have shown that although the two enzymes take up different length sugar substrates the distance between PEP and the phosphate moieties of the sugar substrates, E4P (in DAH7P synthase) and A5P (in KDO8P synthase) are very similar. This is interesting, as it appears that in the divergence of the ancestor enzyme to give the two substrate specific enzymes, two different catalytic mechanisms evolved instead of just forming active sites that specifically accommodate the different sugar lengths.

A striking difference between the two enzymes is that KDO8P synthases can either be metal or non-metal dependent, whereas, all DAH7P synthases require a divalent metal ion for activity. A single point mutation has been observed to define the metal dependence in KDO8P synthase, the conserved metal coordinating cysteine (*Aa*-Cys^{11}) in the metallo form is "naturally" replaced by a conserved asparagine (*Ec*-Asn^{26}) residue in the non-metallo form. A cysteine to asparagine mutation in metal dependent KDO8P synthase restored some activity in the absence of a divalent metal ion.[40] When the same mutation

was made in DAH7P synthase all activity was lost.[33] This supports the hypothesis that the two enzymes differ mechanistically, requiring different roles for the metal ion.

It has been proposed that the role of the metal ion in DAH7P synthase is to activate the carbonyl of E4P to nucleophilic attack. However, the metal ion in KDO8P synthase is too far from the carbonyl oxygen of A5P for any interaction, and instead coordinates with the C2 hydroxyl. This interaction orientates the carbonyl correctly for nucleophilic attack on C1 of E4P by C3 of PEP.[16]

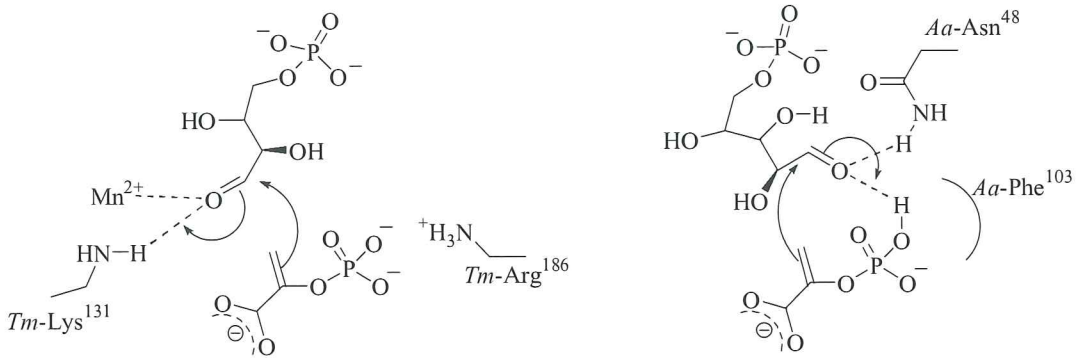

DAH7P synthase KDO8P synthase

Figure 1.28 Comparison of the proposed activation of the carbonyl in the first step of the condensation reaction of DAH7P synthase and KDO8P synthase.

It has been proposed that an absolute conserved substitution in the active site of the two enzymes is responsible for the different ionisation states of PEP when bound. The substitution of a positively charged arginine in DAH7P synthase to a hydrophobic phenylalanine in KDO8P synthase eliminates a salt bridge to the PEP phosphate. This increase in hydrophobicity in the vicinity of the PEP phosphate group in KDO8P synthase causes the PEP to be bound in its dianionic rather than the trianionic form. The proton on the phosphate of PEP in KDO8P synthase is proposed to aid in activation of the carbonyl in the condensation reaction and is a candidate for providing its proton in the formation of the hydroxyl at C4 of the product, KDO8P. This evidence suggests that DAH7P synthase and KDO8P synthase bind and process PEP differently. Thus, this thesis aims to test this hypothesis by comparing the effect changes made to PEP have on its ability to act as a substrate or as an inhibitor in both DAH7P synthase and KDO8P synthase.

1.5 Phylogenetic Relationship between DAH7P and KDO8P Synthases

There are two distinct types of DAH7P synthases that have little sequence homology; type I DAH7P synthases, defined as "*E. coli*-like" homologs having a subunit molecular mass of approximately 39,000 Da; and type II DAH7P synthases, defined as "plant-like" homologs having a larger subunit molecular mass of approximately 54,000 Da.[43]

Type I DAH7P synthases are further separated into two subfamilies.[44] Subfamily Iα which consists entirely of DAH7P synthases, and subfamily Iβ, which contains one group of DAH7P synthase proteins (class Iβ_D) and one group of KDO8P synthase proteins (class Iβ_K). The Iβ subfamily is therefore, more appropriately labelled as a 3-deoxy-ald-2-ulosonate phosphate synthase subfamily, to accommodate the different substrate specificities.[44]

Even though members of type Iβ_D are functionally equivalent to members of type Iα in that they catalyze the DAH7P synthase reaction, they exhibit greater overall similarity to members of type Iβ_K, which catalyse the closely related KDO8P synthase reaction. The class Iβ_D DAH7P synthases possess 17 residues that are conserved within subfamily Iα DAH7P synthases, but not within type Iβ_K KDO8P synthases. Some of these residues may therefore, be important for the specific utilisation of E4P. The type Iβ_D DAH7P synthases possess an additional 19 residues which are conserved within the KDO8P synthases of class Iβ_K, but not within the subfamily Iα DAH7P synthases.[45]

It is thought that the ancestral enzyme was closer to the Iβ subfamily, and had fundamental broad substrate specificity. This ancestral enzyme could have duplicated to produce the initial ancestors of subfamily Iα and subfamily Iβ.[46]

Sequence identity between the type I and type II DAH7P synthases is less than 10%, raising the possibility that they represent distinct protein families, but the high structural similarity and conserved active site residues indicate that they are indeed related by evolution.[47]

Organisms that have subfamily Iα DAH7P synthases often possess more than one DAH7P synthase isozyme. For example, in *E. coli* there are three isozymes of DAH7P synthase, each allosterically inhibited by one of the three aromatic amino acids, tryptophan, tyrosine or phenylalanine. This feed back inhibition is the major quantitative mechanism present in *E. coli* to control carbon introduction into the shikimate pathway.[1,48]

1.6 Comparison of Enzyme Structure

Although there is low sequence identity, DAH7P synthase shows high structural homology with KDO8P synthase. Structures from the same subfamilies show structural similarities, and interestingly, subfamily Iβ DAH7P synthases are more structurally similar to KDO8P synthases than to subfamily Iα DAH7P synthases.

Currently from the type I enzymes, crystal structures are known for two subfamily Iα DAH7P synthase enzymes from *E. coli* (phenylalanine sensitive),[14, 49] and *S. cerevisiae* (tyrosine sensitive),[16, 50] for two class $I\beta_D$ DAH7P synthase enzymes from *T. maritima*[15] and *P. furiosus*[51], and two subfamily $I\beta_K$ KDO8P synthase enzymes from *E. coli*[11,52] and *A. aeolicus*[10,12,36].

In their crystal structures all six of these enzymes form a dimer of a tight binding dimer, a homotetramer. However, in solution DAH7P synthase from *P. furiosus* is in its dimeric form.[51] The structures share a common $(\beta/\alpha)_8$ barrel domain containing the active site and the divalent metal ion at the C-terminal end of the barrel. KDO8P synthases characteristically lack allosteric inhibition, whereas DAH7P synthases are commonly inhibited by one or more pathway intermediates or products.

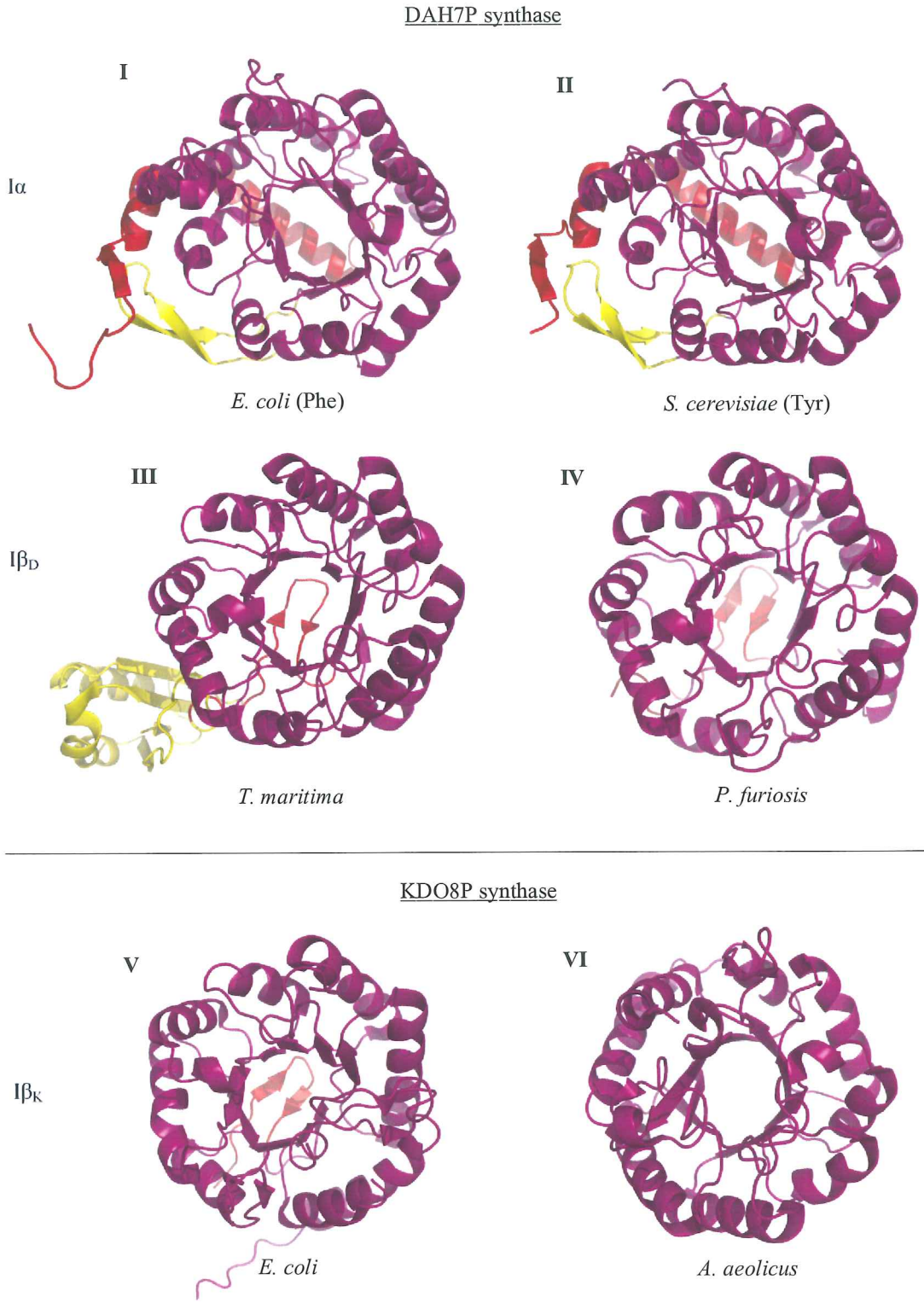

Figure 1.29 Crystal structures of the monomer from the type I enzymes (PDB codes from **I** to **VI**, are 1KFL, 1OAB, 1RZM, 1ZCO, 1X6U and 2NWR).

Aa-KDO8P synthase is the minimalist structure (**Figure 1.29, VI**), relative to this other structures of KDO8P synthase and DAH7P synthase have additional features. The Iα DAH7P synthases *Ec*(Phe)-DAH7P synthase (**Figure 1.29, I**) and *Sc*(Tyr)-DAH7P synthase (**Figure 1.29, II**) contain two extra features, an N-terminal extension (comprising a β-strand and a helix-turn-helix motif) and a two stranded β-hair pin extension located between α5 and β6. The latter, together with β0, complete a three-stranded sheet involved in binding the feedback inhibitor phenylalanine (*Ec*-DAH7P synthase) or tyrosine (*Sc*-DAH7P synthase).

The Iβ_D enzymes, *Pf*-DAH7P synthase (**Figure 1.29, IV**) and *Tm*-DAH7P synthase (**Figure 1.29, III**), and the Iβ_K enzyme *Ec*-KDO8P synthase (**Figure 1.29, V**) contain a similar N-terminal extension of a two stranded β-hair pin that blocks the N-terminal end of the barrel. *Tm*-DAH7P synthase also has an additional ferredoxin-like domain on its N-terminus, which is implicated in feedback regulation.[15]

The Iα DAH7P synthases have a twist in the rotation (**Figure 1.30**) between the dimers (ϕ approximately 28° and 76°, for DAH7P synthase from *E. coli* and *S. cerevisiae*, respectively) which is nearly flat in Iβ_D and Iβ_K enzymes.[16]

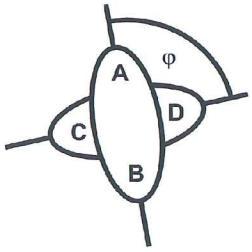

Figure 1.30 Rotation vector of dimers.[16]

The dimers of the six structures associate in a similar orientation, with interactions between the $(\beta/\alpha)_8$ barrels that approach each other from the sides of helices α4 and α5. The barrels are in a tilted orientation and contacts are formed at the C-terminal end of the barrel, near the active site. The inter-subunit contacts of Iβ_D and Iβ_K enzymes are limited to interactions between the barrels. In the Iα enzymes the interactions are significantly enhanced by the inter-subunit β-sheet formed by the extra barrel segments that form the inhibitor binding pocket.

The crystal structure of type II DAH7P synthase from *M. tuberculosis* has also been solved (**Figure 1.31**),[47] and despite the low sequence identity to the type I homologs (less than 10%), the enzyme also contains the common $(\beta/\alpha)_8$ barrel domain containing the active site and a divalent metal at the C-terminal end of the barrel.

Like the type I enzymes, this type II DAH7P synthase exists in the tetrameric form in both solution and in its crystal structure.[53] However, the interactions between its monomers show no commonality with any subunit interface found in any type I enzyme structure.

The extensions of the type II DAH7P synthase also differ from the type I enzymes with a major extension at the N-terminus, comprising a β-strand and two helices (α0a and α0b), and an insertion of two helices (α2a and α2b) into the α2–β3 connecting loop (**Figure 1.31**). These enhanced features are separate to each other and have been proposed to act as two distinct inhibitory binding sites, giving rise to the synergistic inhibition displayed with tryptophan and phenylalanine.[47]

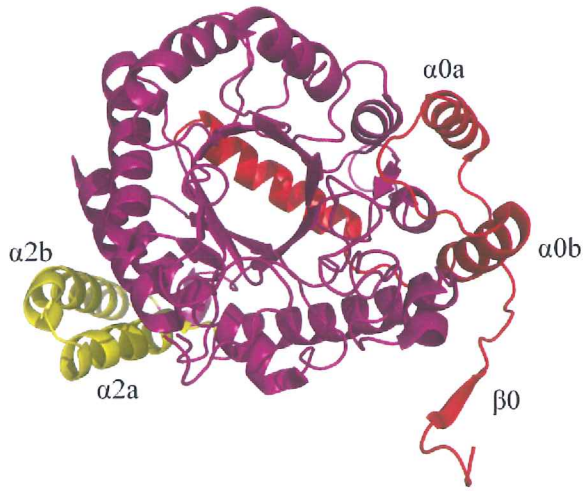

Figure 1.31 Crystal structure of the monomer of a type II DAH7P synthase from *M. tuberculosis* (PDB code 2B7O).

1.7 Enzyme Interactions with Substrates

1.7.1 Interaction with PEP

In all structures of DAH7P synthase and KDO8P synthase PEP binds at the bottom of the active site cavity, with its phosphate and carboxylate moieties stabilised by a network of hydrogen bonds and salt bridges.

In type I DAH7P synthases (Iα and Iβ_D) PEP is held in the active site by three arginine residues, two lysine residues, a main chain nitrogen atom from alanine and a histidine that is in close proximity to PEP, which may also have π-π interactions. The class Iβ_D enzymes have an additional glutamine that interacts with the carboxylate of PEP (**Figure 1.32**).

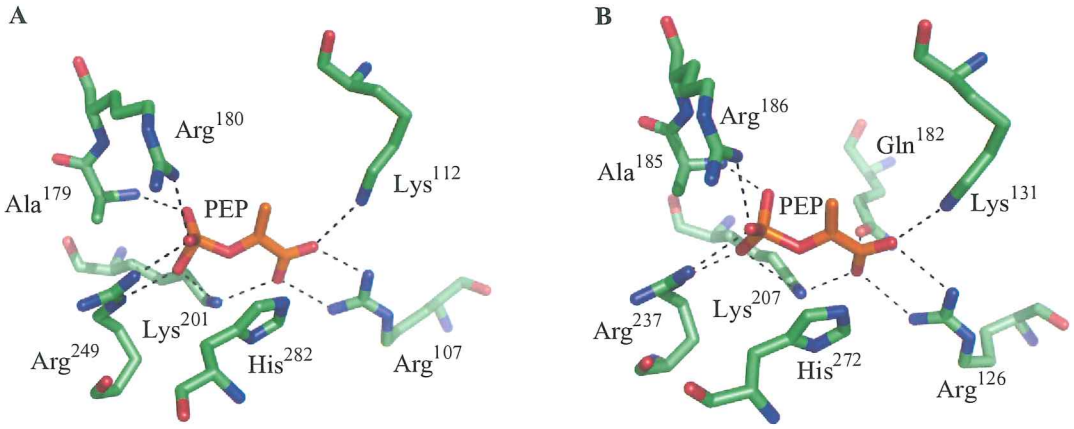

Figure 1.32 Residues that interact with PEP from, **A**, subfamily Iα DAH7P synthase (*S. cerevisiae*) (PDB code 1OAB) and, **B**, subfamily Iβ DAH7P synthase from (*T. maritima*) (PDB code 1RZM).

In the type II DAH7P synthase (*M. tuberculosis*) PEP is bound in a very similar manner to the type I DAH7P synthase enzymes. However, Lys^{133} does not interact with the carboxyl of PEP, as seen in the type I enzymes. There is an interaction between the phosphate of PEP and a main chain nitrogen atom, however this residue is a glutamic acid residue in the type II and an alanine residue in the type I enzymes. Also, like the subfamily Iα enzymes, type II enzymes lack a glutamine to interact with the carboxylate of PEP (**Figure 1.33**).

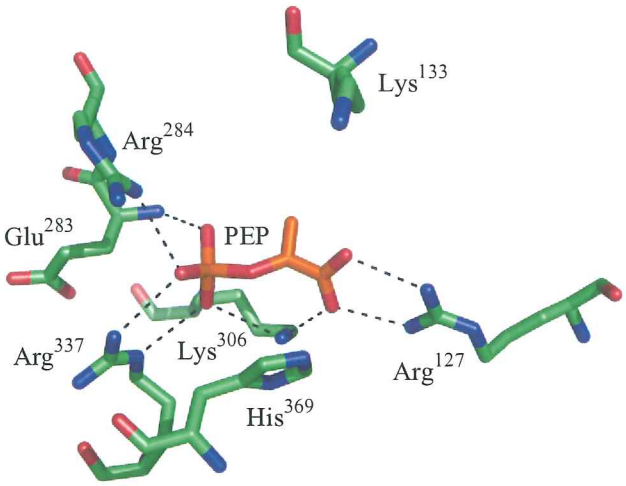

Figure 1.33 Residues that interact with PEP from type II DAH7P synthase (*M. tuberculosis*) (PDB code 2B7O).

In the crystal structure of metallo-KDO8P synthase (*A. aeolicus*), PEP is positioned almost identically to those of DAH7P synthases (**Figure 1.34, A**). Like the type Iβ DAH7P synthase, KDO8P synthase also has a glutamine residue that interacts with the carboxyl of PEP. However, KDO8P synthase has two key differences to DAH7P synthases. Firstly, the carboxyl binding arginine in DAH7P synthases (e.g. Arg^{127}, **Figure 1.33**) is substituted with the functionally related residue, lysine, in KDO8P synthases (Lys^{41}, **Figure 1.34, A**). This may have a different effect on the conformation (for example, rotation of carboxylate) of PEP during reaction. Secondly, one of the arginines (Arg^{284}, **Figure 1.33**) that interacts with the phosphate moiety of PEP, conserved in all DAH7P synthases, is substituted with a hydrophobic phenylalanine residue in KDO8P synthases (Phe^{103}, **Figure 1.34, A**). This results in less salt bridges to the phosphate moiety of PEP, and as mentioned, is proposed to cause PEP to bind in its dianionic form in KDO8P synthases rather than the fully ionised form.

There is no crystal structure of non-metallo KDO8P synthase bound to PEP that is clear enough to unambiguously assign their interactions. However, a phosphate ion binds in the same position in the non-metallo form (*E. coli*) as the phosphate moiety of PEP in the metallo form, and the residues are conserved in both forms in an almost superimposable fashion (**Figure 1.34**). It is therefore assumed that metallo and non-metallo forms of KDO8P synthase have identical binding to PEP.

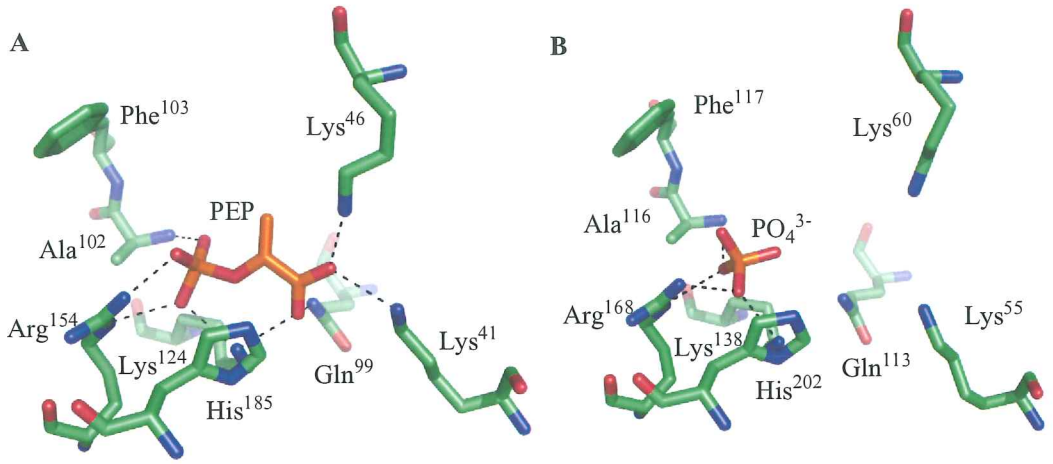

Figure 1.34 Residues that interact with PEP from, **A**, metallo KDO8P synthase (*A. aeolicus*) (PDB code 1FWW) and, **B**, non-metallo KDO8P synthase (*E. coli*) (PDB code 1GGO).

1.7.2 Interaction with E4P and A5P

Taking advantage of the negligible reactivity of thermophilic enzymes at low temperatures (~4°C) crystal structures of DAH7P synthase (from *T. maritima*[15]) and a metallo KDO8P synthase (from *A. aeolicus*[12]) have been solved containing both substrates, PEP and E4P or A5P respectively, and the metal co-factor. The sugar substrates, E4P and A5P, in these structures have slightly different conformations in the different asymmetric units, therefore the exact role of the conserved residues that surround the substrates and the conformation of these substrates during their respective catalysed reactions can only be speculated.

The conformation of E4P in DAH7P synthase (Iβ) from *T. maritima* (**Figure 1.35, A**) is not well defined in the crystal structure by Shumilin and co-workers[15] nevertheless it appears to be held in place by its phosphate moiety *via* interactions with the residues of an arginine (Arg^{134}) and threonine (Thr^{133}), and the main chain nitrogen atom of the threonine (Thr^{133}). These two residues are part of the LysProArgThr motif, conserved in all DAH7P synthases. Also from this motif, the lysine (Lys^{131}), interacts with both the carbonyl oxygen of E4P and the carboxyl of PEP and has been proposed to donate its proton to the carbonyl of E4P during the reaction. The carbonyl oxygen is also shown to be in close proximity to the metal ion, and as mentioned previously, is thought to act as a Lewis acid to activate the carbonyl for attack from PEP.

KDO8P synthase has a similar motif to DAH7P synthase, **Lys**AlaAsn**ArgSer** (compared to **Lys**Pro**ArgThr** in DAH7P synthase), that is conserved and contributes to the key interactions with its corresponding sugar substrate, A5P. From this motif the lysine, arginine and the serine (functionally the same as threonine) appear to interact in the same way as their corresponding residue in the DAH7P synthase motif (**Figure 1.35, B**). However, the asparagine (Asn^{48}) in the KDO8P synthase motif forms an extra interaction with its corresponding sugar substrate, A5P, compared to DAH7P synthase. This is expected to interact with the carbonyl oxygen of A5P, thus, facilitating its activation for catalysis.

In the recently determined structure of the C11N mutant of KDO8P synthase from *A. aeolicus*, where metal-dependant activity is lost, it can be seen that the role of the metal ion is essentially replaced by the asparagine (Asp^{11}) as initially predicted (**Figure 1.35, C**). The interactions of the KDO8P synthase mutant with A5P are identical to those found in wild-type KDO8P synthase, however the conformation of A5P appears more strained, possibly explaining its relatively lower catalytic activity compared to wild-type.

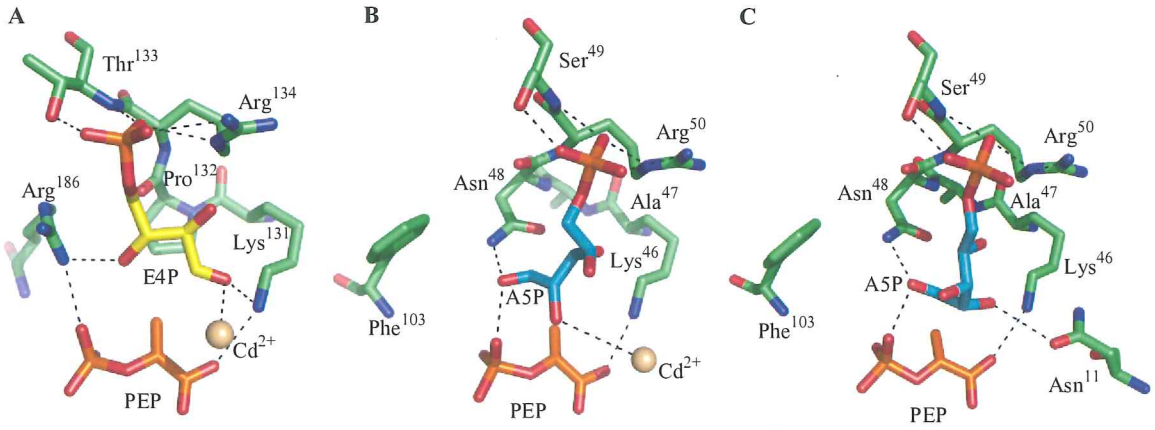

Figure 1.35 Crystal structures of the active site showing interactions of, **A**, E4P in DAH7P synthase from *T. maritima* (PDB code 1RZM), **B**, A5P in KDO8P synthase from *A. aeolicus* (PDB code 1FWW) and, **C**, A5P in the C11N mutant of KDO8P synthase from *A. aeolicus* (PDB code 2NWR).

1.7.3 Source of the Water Reactant in the Enzyme Catalysed Reactions

During the reaction catalysed by both DAH7P synthase and KDO8P synthase, a water molecule attacks C2 of the product (corresponding to the C2 of PEP). There are about 6-8 water molecules found in the enzyme active site from the crystal structures that may take

this role. A likely candidate is a water molecule in close proximity to the *si* face of PEP. This water molecule is conserved amongst the known structures of DAH7P synthase and KDO8P synthase. As mentioned (*vide infra*), DAH7P synthase (*T. maritima*) has a chain of conserved residues and water molecules that provide a proposed mechanism for the protonation of the ex-carbonyl oxygen of E4P, and the deprotonation of the water molecule involved in attack at the C2 of PEP (**Figure 1.36**).[15] The water molecule that interacts with the metal ion has been suggested to be a likely candidate for attack at the C2 of PEP.[16,23] The interaction of the water and the metal ion is thought to lower the pK_a of the water molecule, favouring nucleophilic attack.

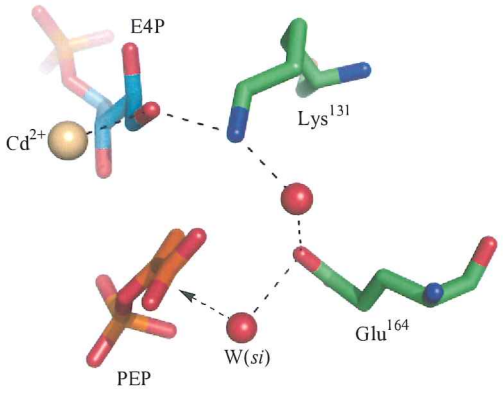

Figure 1.36 Possible movement of protons facilitating the protonation of carbonyl oxygen of E4P and water attack to the *si* face of PEP, in DAH7P synthase from *T. maritima* (PDB code 1RZM).

In the crystal structure of KDO8P synthase (*A. aeolicus*) the carbonyl of A5P is oriented in the opposite direction to the carbonyl of E4P in DAH7P synthase (*T. maritima*), and is in close proximity to the phosphate moiety of PEP (**Figure 1.37, A**). If the phosphate moiety of PEP is mono-protonated, as proposed, a balanced movement of the protons can be envisioned *via* the phosphate of PEP (**Figure 1.37, B**). The deprotonated phosphate of PEP (due to acceptance by the carbonyl of A5P) would be basic enough to accept a proton from the conserved water on the *si* side of PEP, facilitating the attack of C2 of PEP.

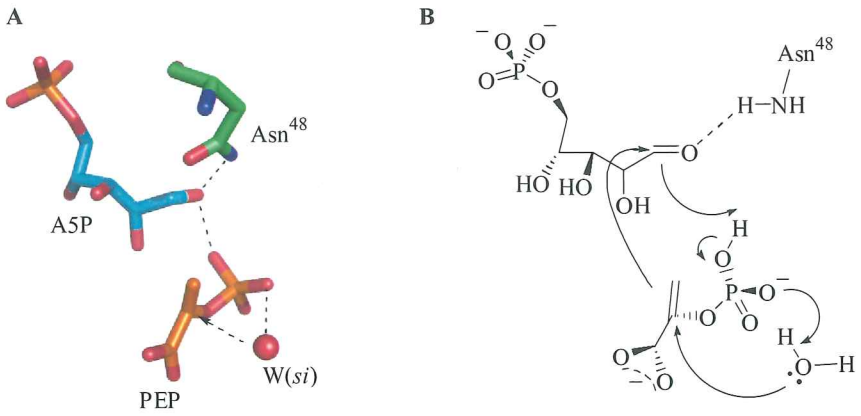

Figure 1.37 Proposed movement of protons in KDO8P synthase with, **A**, the crystal structure from *A. aeolicus* (PDB code 1FWW) and, **B**, a diagram illustrating electron movement.

Recently Kona and co-workers[37] reported a crystal structure of KDO8P synthase (triple mutant from *A. aeolicus*) containing the linear reaction intermediate (**Figure 1.37, A**). The intermediate species has C2 stereochemistry corresponding to hydroxyl attack at the *re* face of PEP, opposite to that shown in **figure 1.34**. The crystal structure of KDO8P synthase from *A. aeolicus* (wild-type) contains a water molecule that coordinates to the metal ion and is located on the *re* face of PEP, however this is not conserved in all structures (**Figure 1.38, B**). The long flexible Lys^{46} residue from this structure coordinates with the water molecule and is capable of moving out of the active site into bulk solvent. This may facilitate the movement of protons away from the active site. This however, does not explain the source of the proton to the carbonyl oxygen of A5P. It must be noted that this intermediate species (**Figure 1.38, A**) is short lived and therefore the validity of the structure reported is questionable.[38]

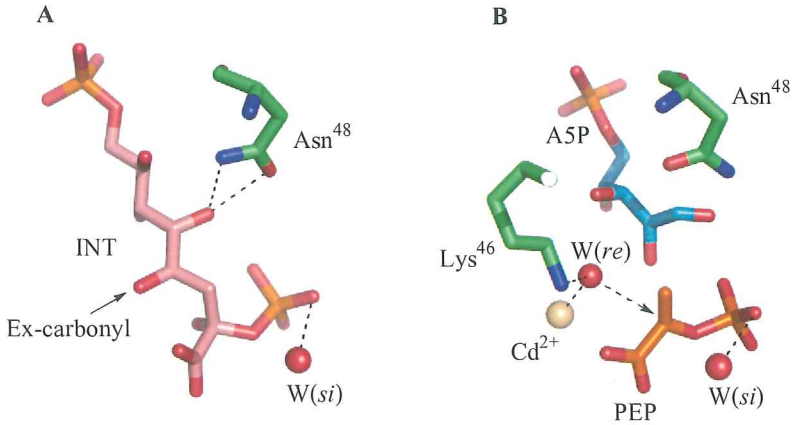

Figure 1.38 Crystal structures of, **A**, reaction intermediate from KDO8P synthase (triple mutant) from *A. aeolicus* (PDB code 2NXG) and, **B**, both substrates in KDO8P synthase (wild-type) from *A. aeolicus* (PDB code 1FWW).

1.8 Phosphoenolpyruvate (PEP)

PEP is the common substrate between DAH7P synthase and KDO8P synthase. The focus of this thesis is on determining the important features of PEP in the catalytic reactions of these two enzymes.

PEP arises from the glycolytic pathway and is an important and very versatile metabolite involved in many metabolic and biosynthetic pathways (**Figure 1.39**). This high importance stems from the fact that it has a very high phosphate group-transfer potential ($\Delta G°$ = -14.8 kcal/mole). PEP can undergo a range of reactions, with enzyme cleavage at either side of the enol oxygen (**Figure 1.39**). Cleavage of the C-O bond gives rise to an 'active' pyruvyl group and cleavage of the P-O bond gives rise to an 'active' phosphoryl group.

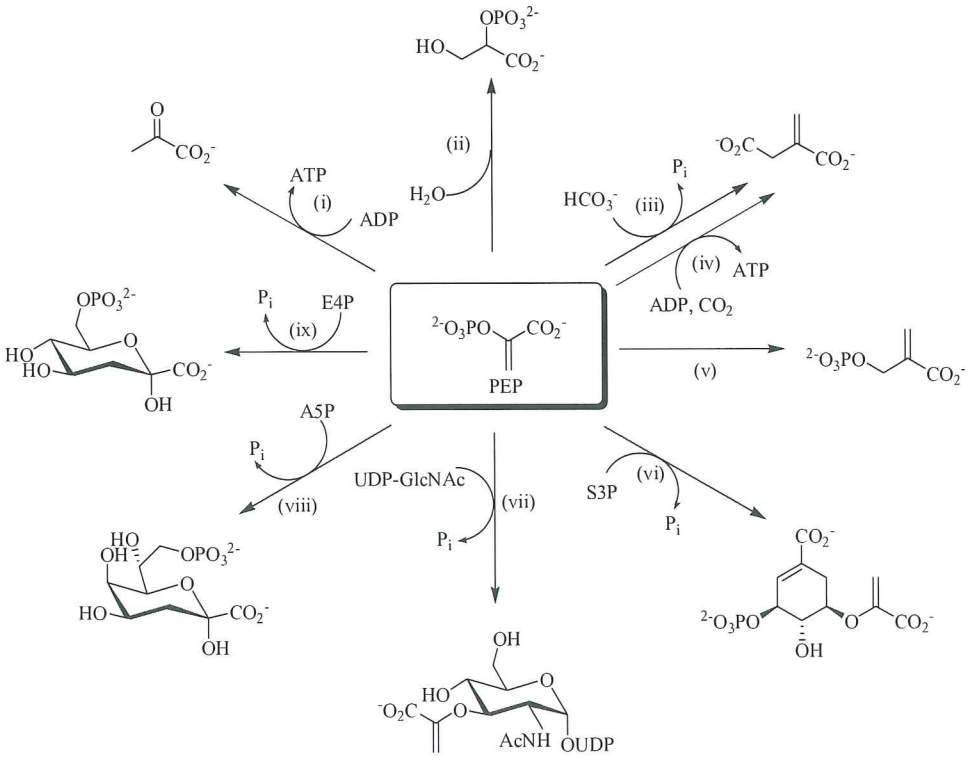

(i) Pyruvate kinase
(ii) Enolase
(iii) PEP carboxylase
(iv) PEP carboxykinase
(v) PEP mutase
(vi) EPSP synthase
(vii) UDP-*N*-acetylglucosamine enolpyruvyl transferase
(viii) KDO8P synthase
(ix) DAH7P synthase

Figure 1.39 Examples of enzymic reactions PEP is involved in.

The reactions for which PEP acts as a substrate can be divided into 4 main types: **(Figure 1.40)**

A. Simple addition to the double bond, eg. enolase.

B. Addition of an electrophile at C-3 with subsequent cleavage of P-O bond. Phosphate group is then eliminated as inorganic phosphate or transferred, for example pyruvate kinase.

C. Addition of an electrophile at C-3 with subsequent cleavage of the C-O bond and elimination of the phosphate as inorganic phosphate, for example DAH7P synthase.

D. Addition followed by elimination to regenerate the enolpyruvyl system and thus transfer this group from phosphate to another molecule. This results in the cleavage of the C-O bond, for example 5-EPS-3-P synthase.

DAH7P and KDO8P synthases both catalyse addition to the C3 of PEP, with the loss of P_i *via* the cleavage of the P-O bond.

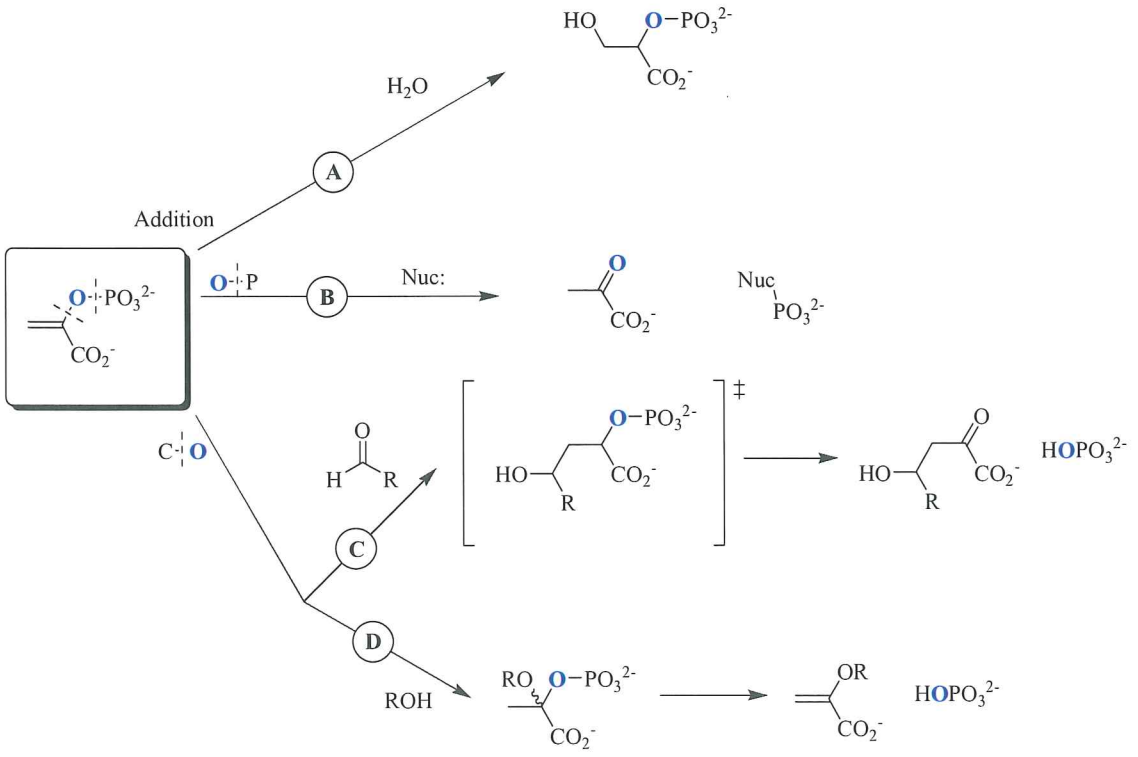

Figure. 1.40 Examples of the four different types of enzyme reactions PEP is involved in.

1.9 Work Described in This Thesis

The aim of this project was to better understand the mechanism of DAH7P synthase and KDO8P synthase. By observing differences between the catalysed reactions to inform the design of strong and specific inhibitors of the enzymes.

To achieve this we have designed and synthesised analogues of the common substrate, PEP, and tested their ability to act as substrates or inhibitors of the two enzymes. The analogues were designed to test different aspects of the binding and catalysis of PEP in the two enzymes.

The synthesised analogues exploited the four functionallities of PEP shown in **figure 1.41**; the vinylic protons on C3 (**A**), the carboxylic acid (**B**), the C2-C3 double bond (**C**) and the phosphonate (**D**). Analogues varying substituents on C3 (**Figure 1.42**) include the chloro **17**, bromo **18**, methyl **19** and fluoro **20** compounds as well as the dideuterated compound **21**. Since there is no free rotation of the double bond (C2-C3), substitution of one vinylic proton produces two possible isomers. Both isomers of each C3 analogue were synthesised and tested against the enzymes.

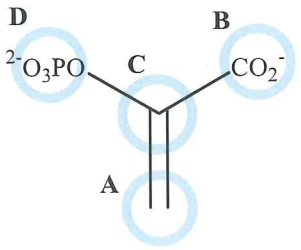

Figure 1.41 Four functional groups of PEP; **A**, vinylic protons, **B**, carboxylic acid, **C**, carbon-carbon double bond, and **D**, phosphate moiety.

A

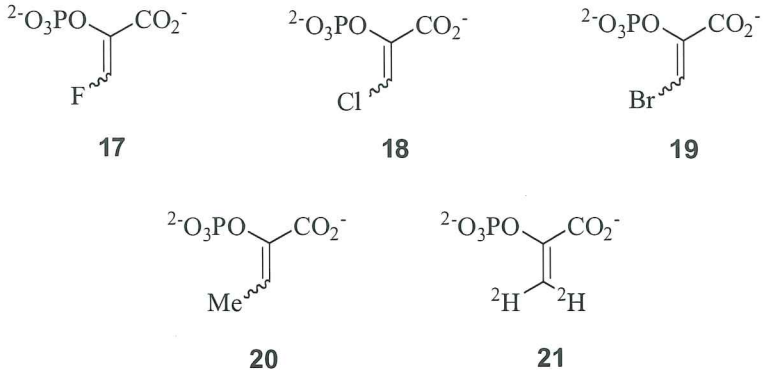

Figure 1.42 C3 analogues of PEP.

Other analogues (**Figure 1.43**) include, substitution of the carboxylate for a methylchloride **22** or a phosphonate moiety **23**, enantiomeric analogues **24**-(*R*) and **24**-(*S*) from reduction of the double bond of PEP, and substitution of the phosphate bridging oxygen for a carbon **25**.

B

C

D

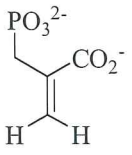

Figure 1.43 Analogues of PEP.

Chapter Two

Synthesis of PEP analogues

2.1 Introduction

The use of substrate analogues has proven to be a very useful tool for probing enzymic reaction mechanisms and for providing information about the interaction substrates have with their enzyme active sites.[54-55]

The high versatility of PEP in biochemical reactions has meant that considerable efforts have been put into the synthesis of analogues of PEP to further understand reactions of PEP-utilising enzymes.[56-57] However, little work has been undertaken on testing PEP analogues against DAH7P synthase and KDO8P synthase.[58,59]

As discussed in Chapter One, the mechanisms of DAH7P synthase and KDO8P synthase were initially thought to be identical due to the high similarity of the reactions they catalyse. Continuing studies have shown that the mechanisms are likely to have significant differences, but these mechanisms are still not fully understood.[33,15,16,28,29,40] It was hoped that analogues to the common substrate, PEP, would help resolve mechanistic differences between the enzymes, and also help determine which structural features of PEP are important for enzyme binding.

2.2 Perkow reaction

The Perkow reaction is a key reaction in the synthesis of many PEP analogues. The general procedure is the reaction of trimethylphosphite ($P(OMe)_3$) with an α-haloketone to yield a vinyl phosphate functionality (**Figure 2.1**).

Figure 2.1 General Perkow reaction.

This reaction has been used in the synthesis of a number of analogues in these studies. The follow section reviews this reaction and discusses the mechanisms for the Perkow reaction.

2.2.1 Mechanism of the Perkow reaction

There is no clear consensus in the literature regarding the mechanism of the Perkow reaction. Four different mechanisms have been reported and these represent the four different areas of the α-haloketone that could be attacked by the lone pair of electrons on $P(OMe)_3$ (**Figure 2.3**).[60-61] The Perkow reaction has been shown to be stereoselective with the (*Z*)-isomer being the major product.[62]

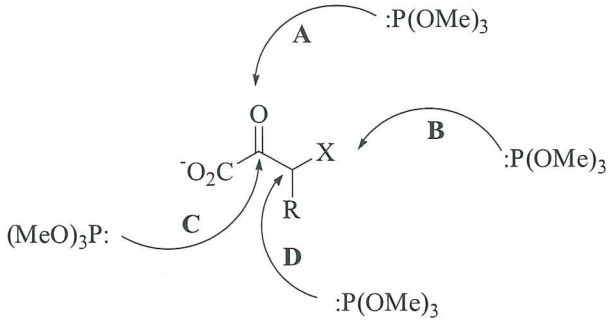

Figure 2.3 Possible areas of attack by $P(OMe)_3$ on an α-halo ketone.

2.2.1.1 Mechanism A: *Attack at the carbonyl oxygen* (Figure 2.3, A)

In 2002, Li and co-workers proposed that attack by $P(OMe)_3$ on the carbonyl oxygen could cause a concerted reaction, forming the C-C double bond with loss of a bromide ion (**Figure 2.4**).[61] The bromide ion may then perform a nucleophilic substitution reaction to generate the phosphate moiety and release methylbromide.

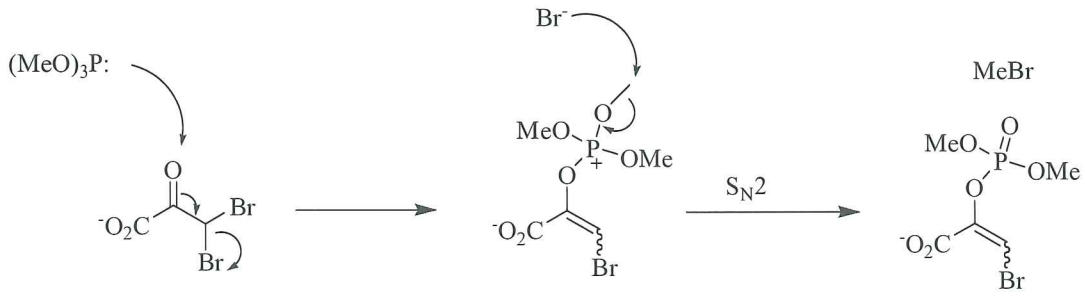

Figure 2.4 Proposed Perkow mechanism with initial nucleophilic attack by $P(OMe)_3$ on the carbonyl oxygen.

However, this mechanism does not provide an explanation for the high stereoselectivity observed, because the reaction occurs in one-step. This is easier to envision with the

Perkow reaction of bromofluoropyruvic acid, which is a racemic mixture of its enantiomers. The expected anti-periplanar loss of bromide, relative to the carbonyl pi orbital, therefore would give a racemic mixture of the diastereoisomers of the Perkow product.

2.2.1.2 Mechanism B: *Attack at the halogen (bromine)* (Figure 2.3, B)

An alternative to mechanism **A**, proposed by Janecki and Bodalski[63] has nucleophilic attack by $P(OMe)_3$ on the electrophilic bromine as the initial step to produce a positively charged bromophosphite species. Nucleophilic attack by the carbonyl oxygen on the bromophosphite species, with subsequent loss of methylbromide, would afford the Perkow product (**Figure 2.5**).

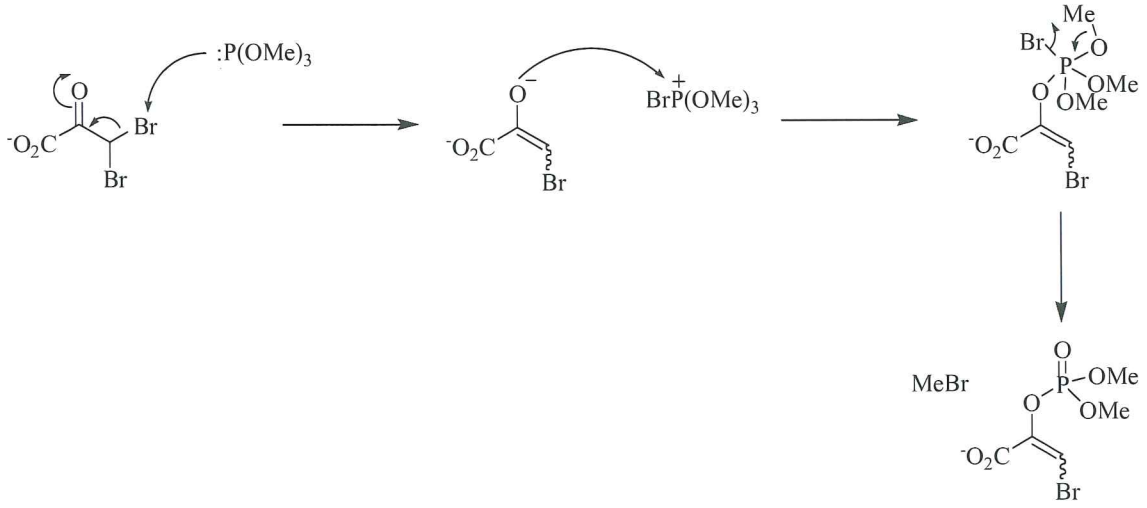

Figure 2.5 Proposed Perkow mechanism with initial nucleophilic attack by $P(OMe)_3$ on the halogen.

To explain the observed stereoselectivity, Janecki and Bodalski[63] proposed that after the bromine is removed, the isomeric bromophosphonium-enolate may have a preference for the substituent (bromine) in the (*Z*)-position (**Figure 2.6**).

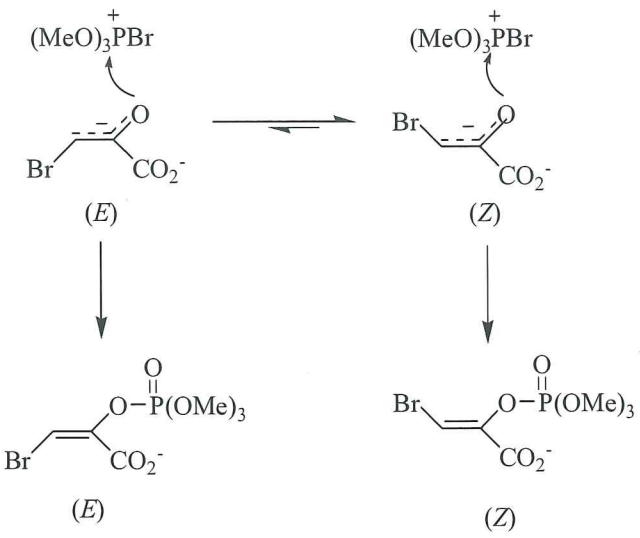

Figure 2.6 Proposed stereoselection from mechanism **B**.

In the literature, there are reports of phosphorus (III) compounds attacking bromine or chlorine from α-haloketones with the formation of an anion stabilised by an adjacent sulfonyl or carbonyl group.[64,65] However, the Perkow reaction has been shown to proceed in the absence of a halogen at the α-carbon, using a trifluoroacetate ester at this position as an alternative leaving group (**Figure 2.7**).[60] Therefore, unless an alternative mechanism is occurring in this case, a mechanism involving initial attack on a halogen seems implausible.

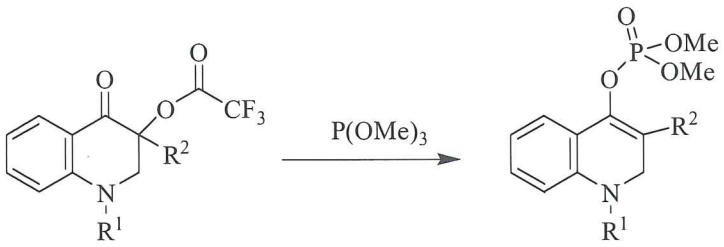

Figure 2.7 Example of a Perkow reaction without an α-halogen.

2.2.1.3 Mechanism C: *Attack at the carbonyl carbon* (Figure 2.3, C)

A common mechanism reported in the literature [60, 66] is nucleophilic attack of $P(OMe)_3$ on the carbonyl carbon followed by migration of the phosphonate and subsequent loss of bromine (**Figure 2.8**).

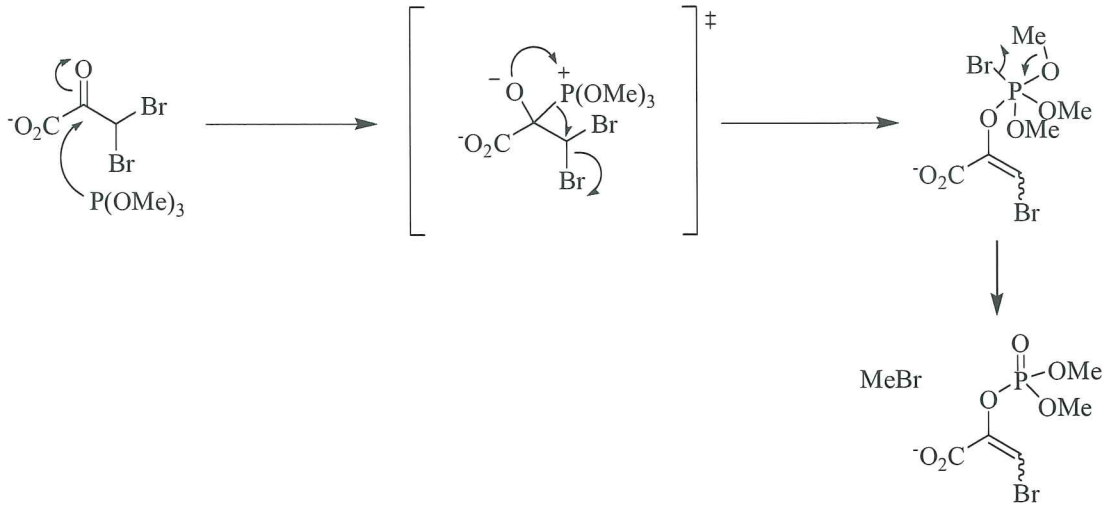

Figure 2.8 Proposed Perkow mechanism with initial nucleophilic attack by $P(OMe)_3$ on the carbonyl carbon.

Synthesis of diphosphoPEP **23** (see Section 2.4.2) is an example of $P(OMe)_3$ attacking at the carbonyl carbon (**Figure 2.9**). In this reaction $P(OMe)_3$ reacts with chloroacetyl chloride **27**, and at the first step has the choice of either a Perkow or a substitution reaction. Only diphosphoPEP **23** is formed, and therefore the rate of substitution is very rapid followed by the slower Perkow reaction.[67]

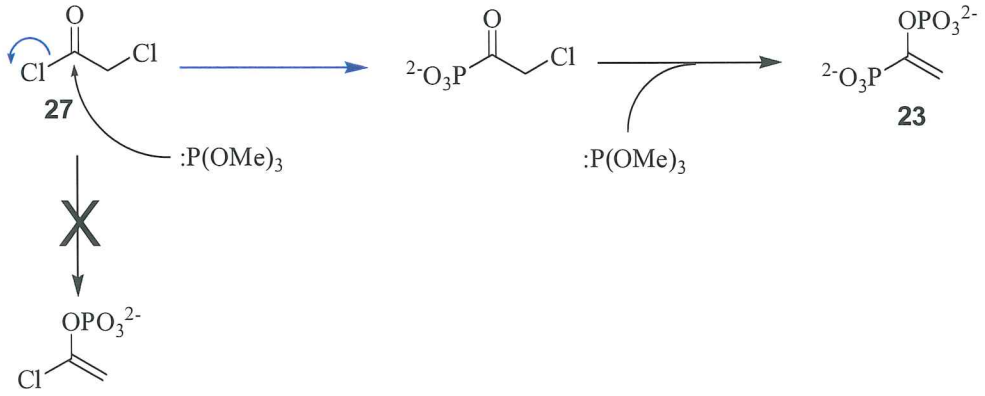

Figure 2.9 Experiment that demonstrates that $P(OMe)_3$ can act as a nucleophile.

To explain the observed stereoselectivity of the Perkow reaction *via* this mechanism requires reversible addition of $P(OMe)_3$ to the carbonyl.[62] The subsequent elimination step requires an anti-periplanar conformation, which is thermodynamically controlled to afford the two isomers (**Figure 2.10**).

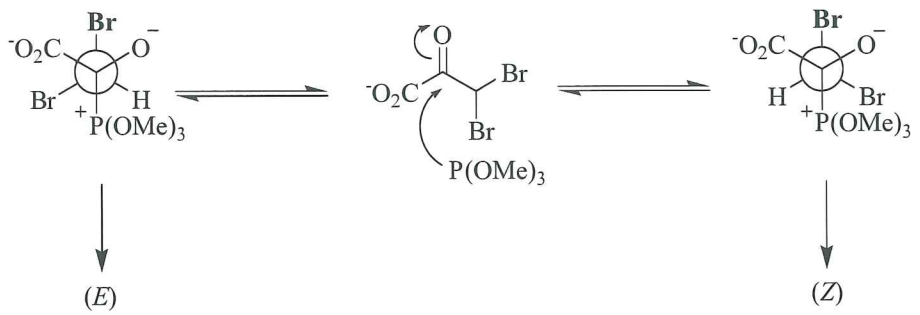

Figure 2.10 Newman projections of the two possible conformations of the transition state that lead to the (*E*)- and (*Z*)-isomers.

2.2.1.4 Mechanism D: *Attack at the halogenated α-carbon* (Figure 2.3, D)

This mechanism proposes an initial S_N2 substitution reaction on the α-carbon that is observed in the similar Arbusov reaction (**Figure 2.11**).[68]

Figure 2.11 Arbusov reaction.

The substitution reaction forms a phosphonium salt intermediate that results in a phosphonate-phosphate rearrangement to yield the substituted vinyl phosphate (**Figure 2.12**).

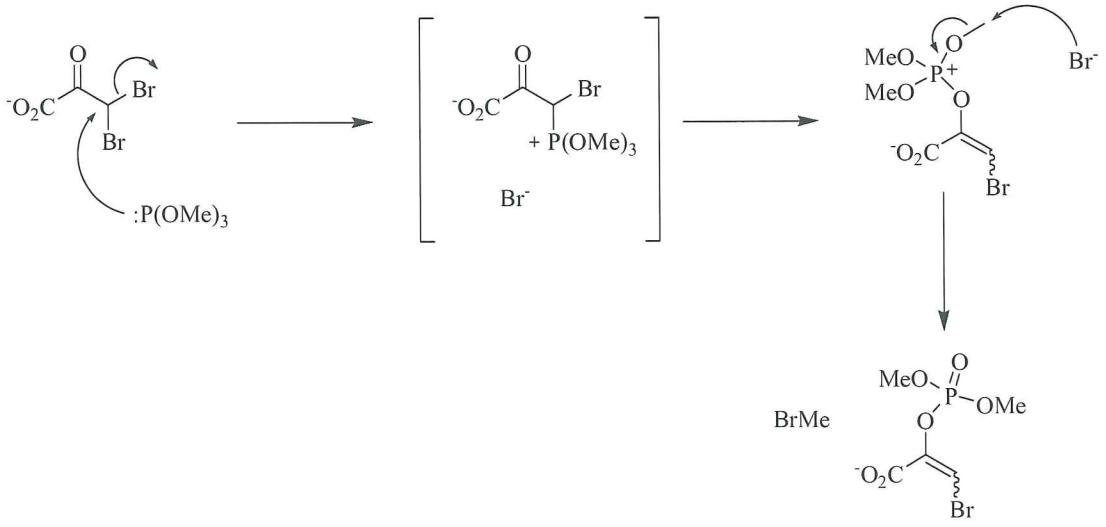

Figure 2.12 Proposed Perkow mechanism with initial nucleophilic attack by $P(OMe)_3$ on the α-carbon.

The point of stereoselection in this mechanism occurs directly after the phosphonate-phosphate rearrangement that forms a carbanion (**Figure 2.13**). The substituent (bromine) can either rotate up (towards the phosphate) to form the (*Z*)-isomer, or down (towards the carboxylic acid) to form the (*E*)-isomer. It is not clear why the substituent would have such a strong preference to rotate to the same side as the phosphate forming the (*Z*)-isomer.

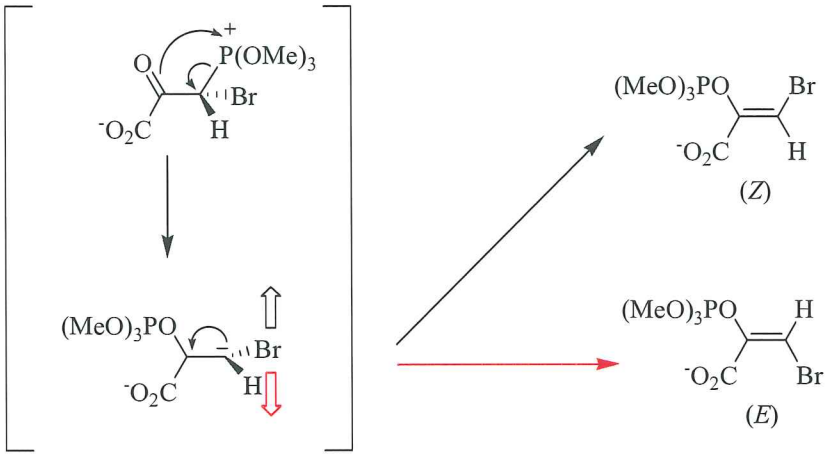

Figure 2.13 Proposed stereoselection in mechanism **D**.

One reaction that supports this mechanism is the reaction between 1-chlorooxirane **28** and $P(OMe)_3$ that forms the same product as found in the Perkow reaction (**Figure 2.14**). Only two of the mechanisms proposed for the Perkow reaction are possible in this reaction, either ring opening (equivalent to mechanism **D**, blue arrows) and chlorine attack (equivalent to mechanism **B**, red arrow), as the other two (mechanism **A** and **C**) involve a carboxylic acid.

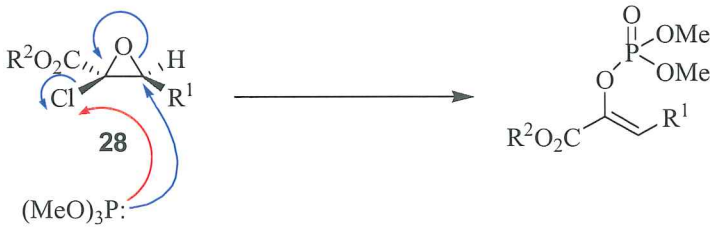

Figure 2.14 Reaction of 1-chlorooxirane **28** and $P(OMe)_3$.

2.2.1.5 Summary

In summary, there is no mechanism that fully resolves the features of the Perkow reaction, such as the high stereoselectivity towards the (*Z*)-isomer, whether the substituent is large, small, electron-withdrawing or electron-donating. Mechanism **D** is attractive, as its initial step is the same as the very similar Arbusov reaction. However, it is possible that the Perkow reaction proceeds *via* more than one route.

2.2.2 The Use of Triethylphosphite in the Perkow Reaction

$P(OMe)_3$ is sensitive to water, and forms dimethylphosphonic acid **26** (**Figure 2.15**). This meant that old stored bottles were found to be useless, due to decomposition, and fresh $P(OMe)_3$ had to be purchased.

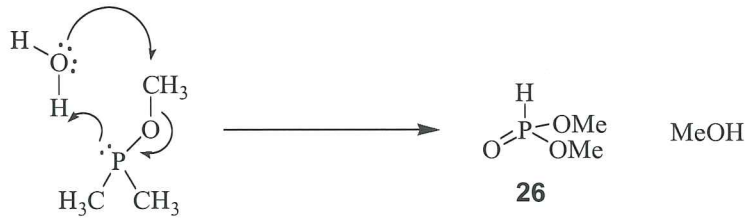

Figure 2.15 Decomposition of $P(OMe)_3$.

In this study, PEP was synthesised from 3-bromopyruvic acid and $P(OMe)_3$ to test the Perkow reaction (**Route A, Scheme 2.1**). Due to the unavailability of pure $P(OMe)_3$ at the early stages of this project, triethylphosphite ($P(OEt)_3$) was investigated as an alternative. Using the same conditions used for $P(OMe)_3$, the reaction of $P(OEt)_3$ and 3-bromopyruvic acid was shown to afford diethylPEP in an approximate 40 % yield (**Route B, Scheme 2.1**).

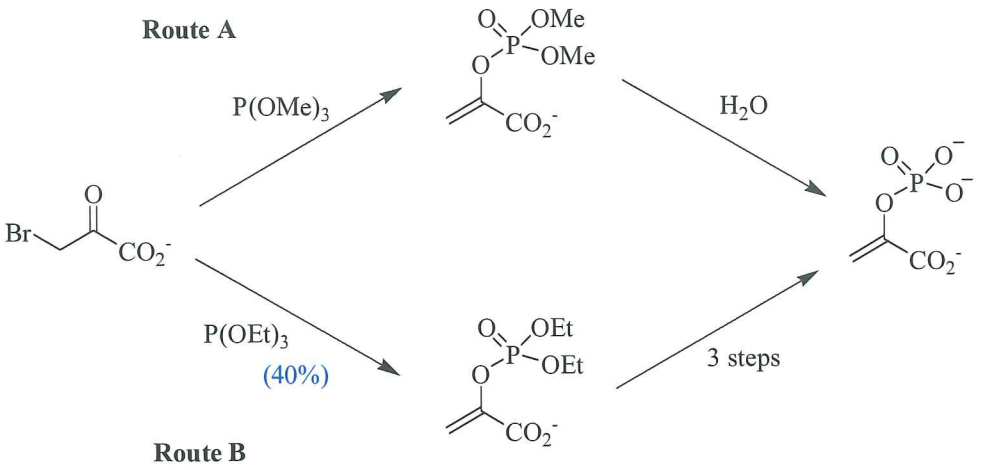

Scheme 2.1 Two possible routes of the Perkow reaction.

However, when $P(OEt)_3$ was reacted with 3,3-dichloropyruvic acid only trace levels of the desired Perkow product were observed by ^1H NMR spectroscopy (**Scheme 2.2**).

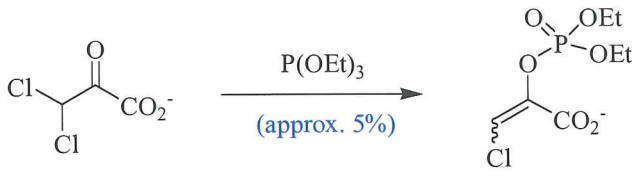

Scheme 2.2 Perkow reaction *via* the use of $P(OEt)_3$.

It was considered possible that the carboxylic acid group on 3,3-dichloropyruvic acid may be responsible for the lack of reactivity with $P(OEt)_3$, and so the carboxylic acid was converted to the corresponding methyl ester. Reaction of the ester with $P(OEt)_3$ yielded the desired Perkow reaction product, diethylchloroPEP in 76% yield (**Scheme 2.3**).

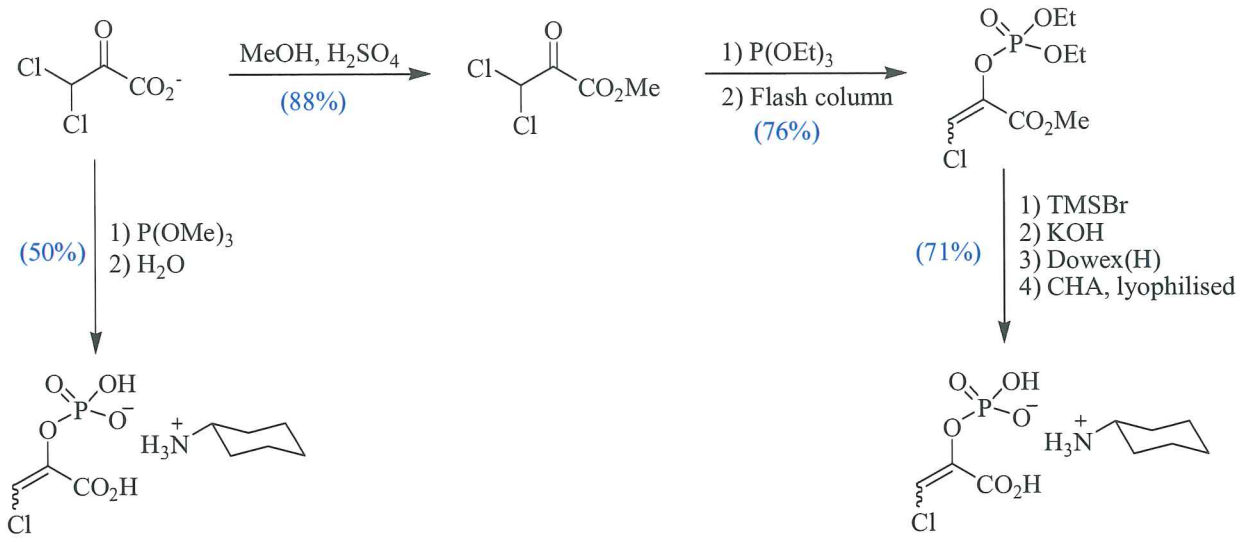

Scheme 2.3 Perkow reaction *via* the use of $P(OEt)_3$ of the esterified reactant.

The advantage of this alternative route is that the esterified carboxylate is suitable for purification by flash chromatography. This purification step is desirable as it removes contaminating phosphonic acid that effects recrystallisation in the final step. However, the lower reactivity of the ethyl esters of the phosphate, means that water can not be used to hydrolyse these esters (as is used in methyl ester hydrolysis). The protected compound was reacted with bromotrimethylsilane (TMSBr) followed by treatment with a solution of aqueous KOH which led to the formation of the desired hydrolysed adduct. Addition of cyclohexylamine, afforded the cyclohexylammonium salt of 3-chloroPEP with an overall yield of 47%. This compares to a 50% yield *via* the direct phosphorylation of dichloropyruvic acid with $P(OMe)_3$.[69] Although this alternate use of $P(OEt)_3$ results in a purer product, more steps are employed and therefore, the sequence is more time consuming and has greater opportunity for product loss.

2.3 3-Substituted Analogues of Phosphoenolpyruvate

2.3.1 Preparation of 3-FluoroPEP

17*Z* **17*E***

In terms of size, fluorine and hydrogen are very similar (Van der waals radii of 1.47 Å and 1.20 Å, respectively)[70] and so substitution of a hydrogen by a fluorine would cause minimal steric implications for substrate binding. Therefore, any observed effects of such a substitution would be caused by the electronic properties of the electronegative fluorine. In the proposed reactions catalysed by both DAH7P synthase and KDO8P synthase, the C3 of PEP acts as a nucleophile, and therefore a fluorine at C3 could alter the activation energy by removal of electron density from the carbon-carbon double bond. In addition, fluorine is capable of hydrogen bonding to residues containing a proton attached to either an oxygen or nitrogen, therefore there is the possibility of altered binding in the active site with respect to PEP.

Both isomers of 3-fluoroPEP (**17*Z*** and **17*E***) have been reported as substrates or inhibitors on a range of PEP-utilising enzymes, for example PEP carboxykinase, pyruvate kinase and PEP carboxylase.[71-72] Furdui and co-workers[59] compared the ability of DAH7P synthase (*E. coli*) and both metallo (*A. pyrophilus*) and non-metallo (*E. coli*) forms of KDO8P synthase to utilise the two isomers of 3-fluoroPEP as substrates. It was demonstrated that both the KDO8P synthase enzymes preferred the (*E*)-isomer of 3-fluoroPEP over the (*Z*)-isomer, whereas DAH7P synthase did not discriminate between the two stereoisomers, and both were consumed by enzyme at a similar rate.

All C3 substituted analogues were prepared using the Perkow reaction. Therefore, the synthesis of 3-fluoroPEP **17** required production of the α-haloketone, 3-bromo-3-fluoropyruvic acid **31**. Sodium ethoxide, diethyl oxalate and ethyl fluoroacetate were reacted to form the enolate of diethyl fluorooxaloacetate **29**. The isolated enolate **29** was then brominated in diethyl ether. This reaction was previously reported to be carried out in toluene but it was found that even at cold temperatures the toluene was being brominated producing benzylbromide.[69] Hydrogen bromide formed in the reaction was removed by washing with water and excess bromine was reduced and removed by washing with an aqueous solution of sodium sulphite. The desired diethyl bromofluorooxaloacetate **30** was obtained in 61% yield.

Hydrolysis and decarboxylation of **30** was achieved by refluxing in concentrated hydrochloric acid to afford 3-bromo-3-fluoropyruvic acid **31**. This was purified by extracting from diethyl ether into a basic solution, acidifying and re-extracting into ethyl

acetate, providing **31** in 46% yield. Omission of this purification step in order to obtain better yields resulted in contaminants being carried through, causing problems when it came to recrystallising the final product. Dimethyl-3-fluoroPEP **32** was synthesised using $P(OMe)_3$ and 3-bromo-3-fluoropyruvic acid **31** in diethyl ether under dry conditions. Hydrolysis was achieved by treatment with water followed by the addition of cyclohexylamine to form the cyclohexylammonium salt. Recrystallisation using methanol/diethyl ether gave 3-fluoroPEP **17** with a (*Z*):(*E*) isomer ratio of 10:1.

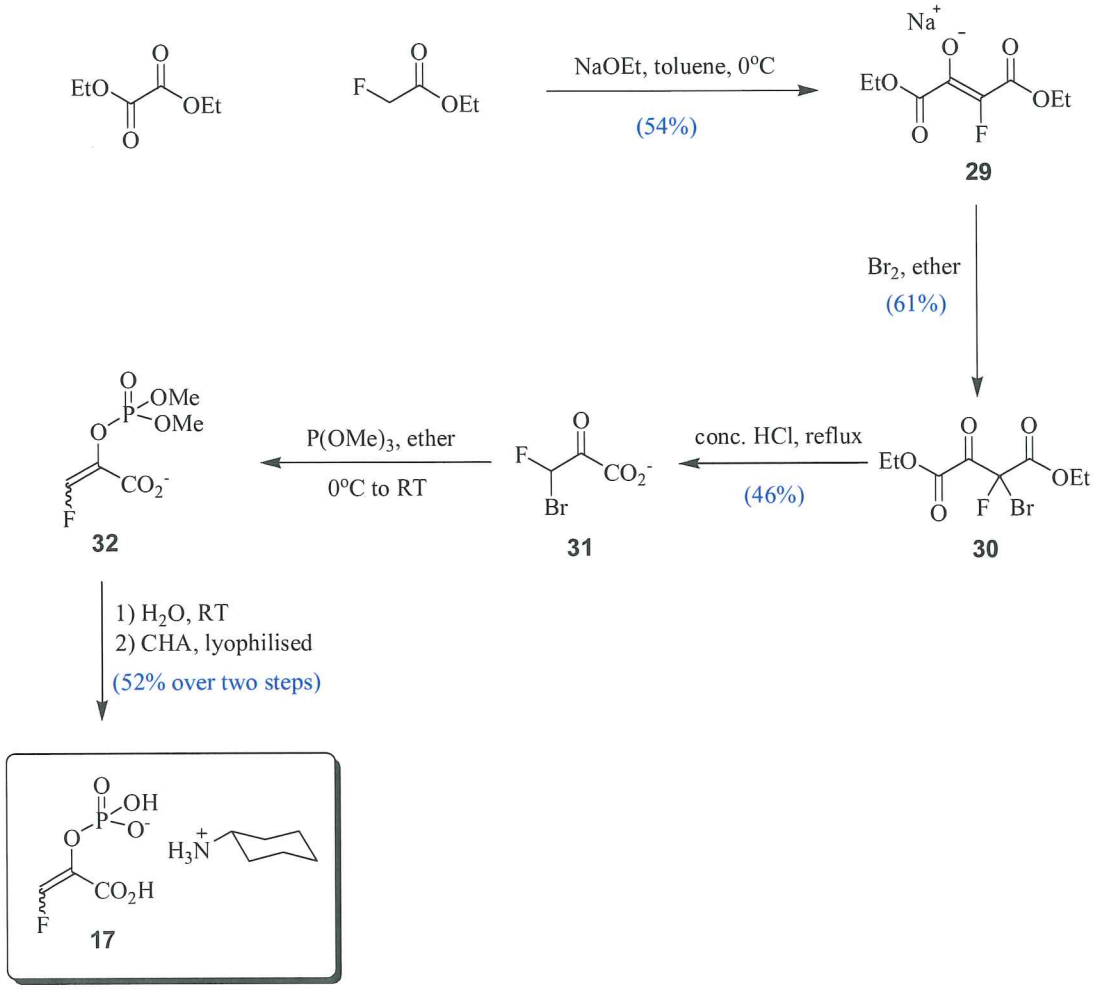

Scheme 2.4 Synthesis of 3-fluoroPEP.

2.3.2 Preparation of 3-ChloroPEP

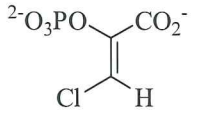

18*Z*

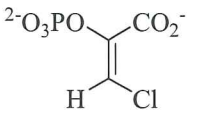

18*E*

Compared to hydrogen, chlorine has much larger Van der waals radii of 1.75 Å (compared to 1.20 Å for hydrogen[70]), therefore the substitution of a hydrogen with a chlorine may have steric effects, reducing its ability to fit in the binding pocket of PEP in the active site. Also, chlorine is electronegative, and consequently, the presence of this substituent reduces the electron density from the carbon-carbon double bond relative to unsubstituted PEP.

Studies with other PEP-utilising enzymes have demonstrated that 3-chloroPEP is a weak competitive inhibitor for PEP, in enzyme I from the bacterial phosphotransferase system (PTS), pyruvate kinase, PEP carboxylase and enolase.[57,73] 3-ChloroPEP has the potential to inactivate PEP utilising enzymes by forming 3-chloropyruvic acid during the reaction, followed by attack by a nucleophilic residue in the active site. Inactivation has been reported in enzyme I from the bacterial PTS by the (*Z*)-isomer of 3-chloroPEP. Pyruvate kinase and PEP carboxylase are able to use 3-chloroPEP as a (poor) substrate. However, PEP carboxylase converts 3-chloroPEP into both its analogous product, chlorooxaloacetate, and chloropyruvic acid in a 1:3 ratio, respectively.

3-ChloroPEP **18** was prepared following the procedure reported by Parker[69], which is a modification of the synthesis by Liu and co-workers.[73] Firstly, the synthesis of 3,3-dichloropyruvic acid **33** was required in order to form the α-haloketone precursor for formation of the chloro-phosphoenol functionality. This was achieved by adding two equivalents of sulfuryl chloride to pyruvic acid. $P(OEt)_3$ was used as an alternative due to the unavailability of $P(OMe)_3$ at the time. Reaction of 3,3-dichloropyruvic acid **33** with $P(OEt)_3$, gave no reaction. However, following esterification to afford methyl 3,3-dichloropyruvate **34**, the reaction with $P(OEt)_3$ yielded the desired product. With the esterification of the carboxylic acid, the Perkow product **35** was suitable for purification by flash chromatography. This had an advantage over the original method by removing any contaminating phosphonic acid, thus, making recrystallisation easier. Removal of the

phosphate and carboxylate esters from **35** was achieved following the method reported by Bartlett[74], *via* reaction with bromotrimethylsilane (TMSBr). The trimethylsilane was hydrolysed by the addition of potassium hydroxide, desalted through a column of Dowex(H) and finally cyclohexylamine added to generate the cyclohexylammonium salt of 3-chloroPEP **18**, with a (*Z*):(*E*) isomer ratio of 4.5 : 1.

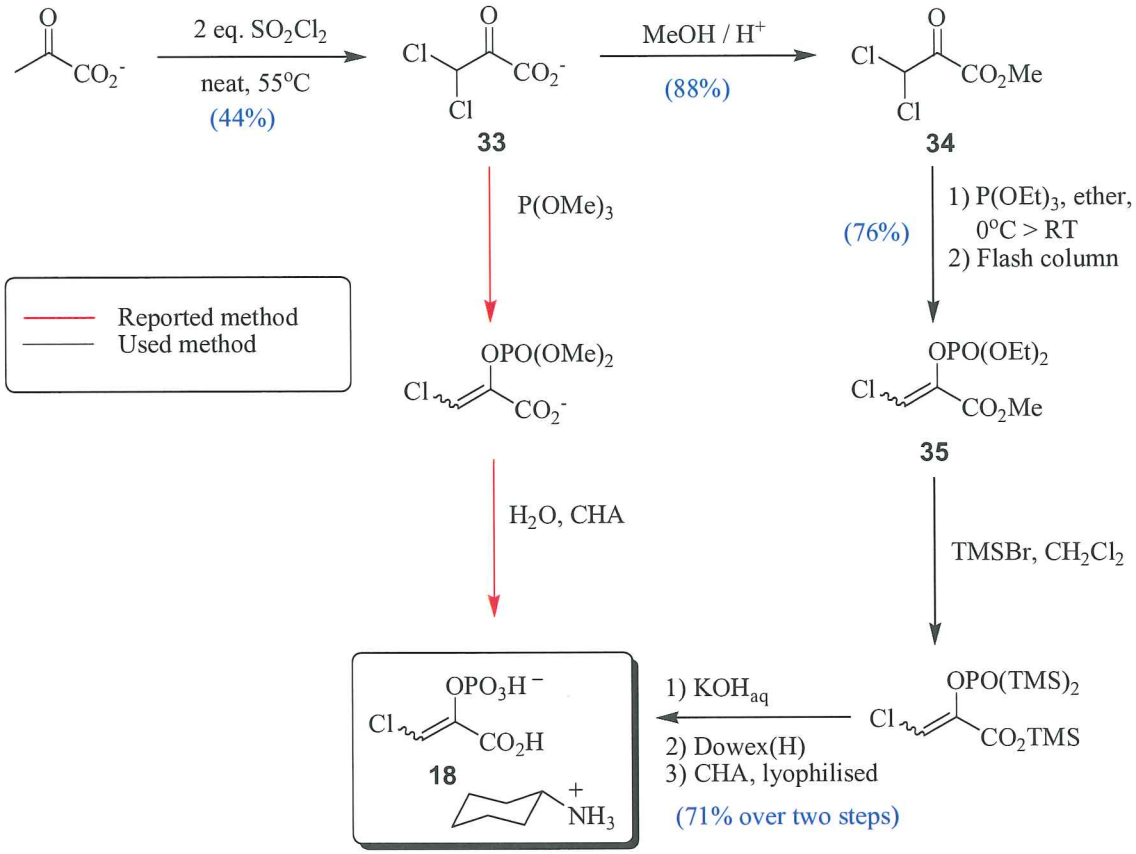

Scheme 2.5 Synthesis of 3-chloroPEP.

2.3.3 Preparation of 3-BromoPEP

In terms of size, bromine is slightly larger than chlorine, with a Van der waals radii of 1.85 Å compared to 1.75 Å.[70] Bromine is less electronegative than chlorine with Pauling units of 2.96 compared to 3.16, respectively.[75] Like chlorine substitution, both steric and electronic effects are possible with bromine substitution at C3 of PEP.

From studies of 3-bromoPEP with other PEP-utilising enzymes, only pyruvate kinase has been observed to utilise it as a substrate, to form 3-bromopyruvic acid, although reaction was considerably slower than with PEP. Inactivation of PEP carboxylase (from maize) has been reported by 3-bromoPEP. However, covalent modification did not occur inside the active site as desired. It was demonstrated that 3-bromoPEP was converted to 3-bromopyruvic acid in the active site, it then dissociates and alkylates at another site of the enzyme by reaction with a sulfhydryl group.[76]

3-BromoPEP **18** was prepared according to the procedure of Parker[69], which is a modification of the synthesis reported by Stubbe and Kenyon.[77] Firstly, 3,3-dibromopyruvic acid **36** was prepared by reaction of two equivalents of bromine with pyruvic acid. The Perkow reaction was then performed by reaction with $P(OMe)_3$ to afford dimethyl-3-bromoPEP **37**. The phosphate methyl esters were hydrolysed with water, and addition of cyclohexylamine provided the cyclohexylammonium salt of 3-bromoPEP **18** with a (*Z*):(*E*) ratio of 10:1.

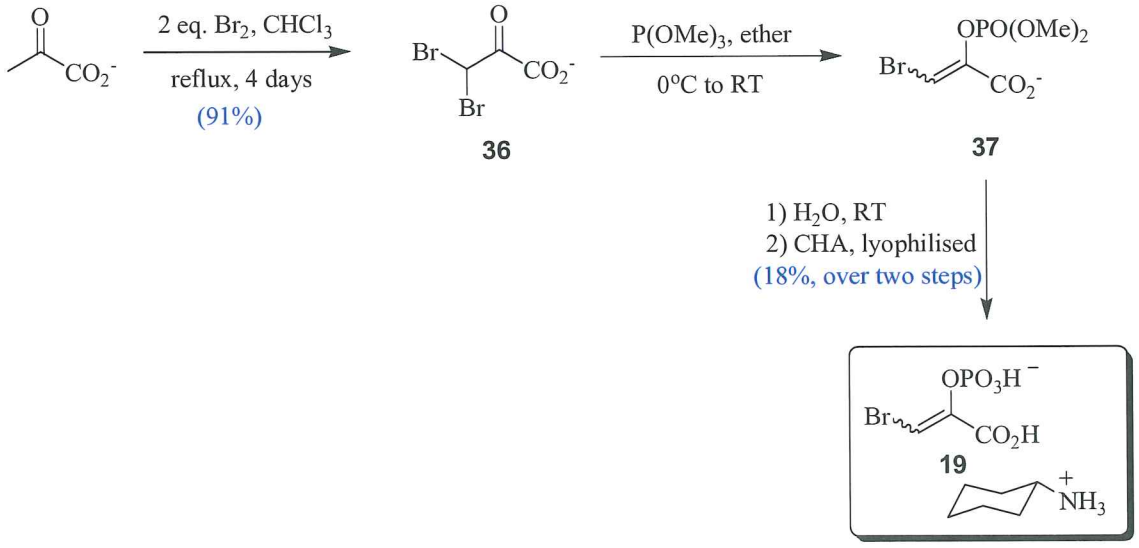

Scheme 2.6 Synthesis of 3-bromoPEP.

For the purpose of better understanding the Perkow reaction mechanism, dibromopyruvic acid **36** was reacted with $P(OMe)_3$ at -70°C. From analysis of the ^1H NMR spectra of the products, it was observed that at -70°C, the proportion of the (*E*)-isomer had more than tripled that of the typical Perkow reaction performed at 0°C (**Figure 2.16**).

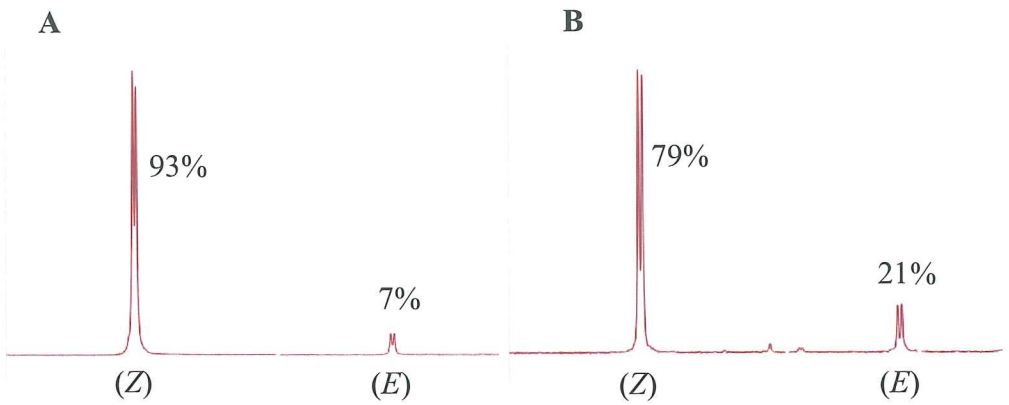

Figure 2.16 ^{1}H NMR spectra showing key signals for the (*Z*) and (*E*) products formed from Perkow reaction of 3,3-dibromopyruvic acid at, **A**, 0°C or, **B**, -70°C.

2.3.4 Preparation of 3-MethylPEP

20*Z* **20*E***

Substitution of the C3 proton with a methyl group differs from the halogenated C3 analogues of PEP in that it is electron-donating rather than electron-withdrawing, therefore the electron density of the carbon-carbon double bond in 3-methylPEP would be greater relative to PEP. In terms of its size, the methyl group is much larger than hydrogen, and slightly larger in size than bromine with a Van der Waals radii of 2.0 Å.[78] Therefore, steric effects may interfere with binding of **20** to the active site.

3-MethylPEP has been reported to show competitive inhibition with some other PEP-utilising enzymes, namely, pyruvate kinase, PEP carboxylase and enolase.[57] Studies of 3-methylPEP with DAH7P synthase (*E. coli*) demonstrated that it was not a substrate for this enzyme but had competitive inhibition with respect to PEP with a K_i of 160 μM. Both (*Z*)- and (*E*)-isomers were demonstrated to have a similar inhibitory effect.[69]

Preparation of 3-methylPEP was achieved utilising the procedure of Parker[69] and Woods and co-workers.[56] Accordingly, α-ketobutyric acid was brominated to afford 3-bromo-2-ketobutyric acid **38**. Previously, Parker[69] had used carbon tetrachloride for this reaction but this was unavailable, and cyclohexane was used as an alternative. Excess bromine was

removed from the reaction mixture by repeatedly dissolving the sample in chloroform and removing the solvent *in vacuo*. Butyric acid **38** was then reacted with $P(OMe)_3$ to afford dimethyl-3-methylPEP **39**. Phosphate methyl esters were hydrolysed with water, and addition of cyclohexylamine provided the cyclohexylammonium salt of 3-methylPEP **20** with a (*Z*):(*E*) isomer ratio of 4.2:1.

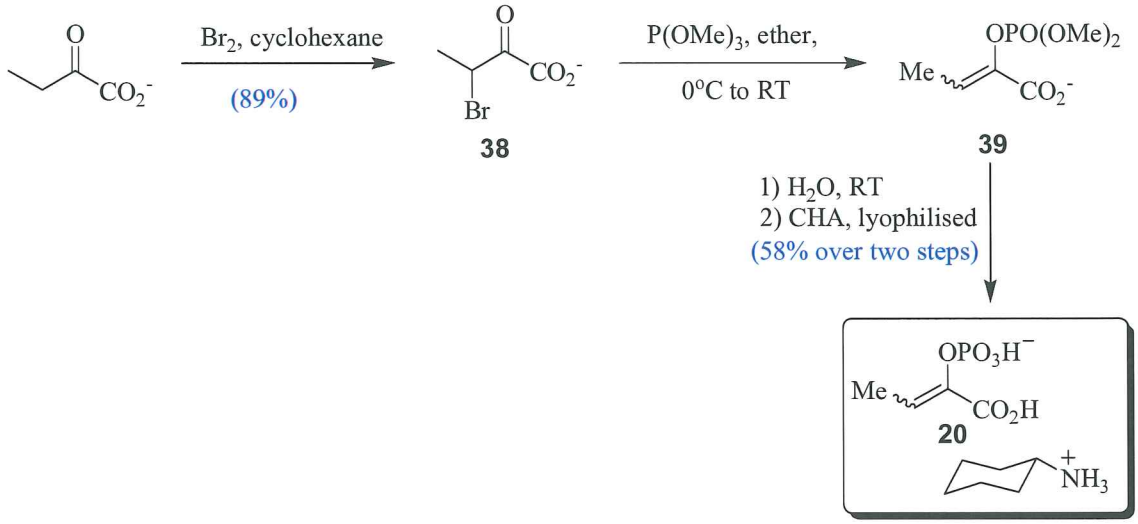

Scheme 2.7 Synthesis of 3-methylPEP.

2.3.5 Preparation of 3,3-DideuteroPEP

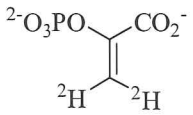

21

During the reaction catalysed by DAH7P synthase and KDO8P synthase the vinylic proton bonds of PEP are not broken. However, the bound carbon undergoes modification from a trigonal to a tetrahedral carbon. Therefore, substitution of the vinylic protons for the heavier isotope, deuterium, would show a secondary kinetic isotope effect on the enzyme catalysed reaction. Classically, this effect can be rationalised by the effect atom mass has on the frequency of the bond vibration, and in the case of a ^1H to ^2H substitution the mass has doubled. Consequently, this would result in a much lower vibrational frequency. It would be interesting to see if there is an observable reduction in the rate that **21** is

catalysed compared to PEP in DAH7P synthase and KDO8P synthase, which would indicate that reaction of C3 of PEP is part of the rate determining step.

3,3-DideuteroPEP **21** was synthesised by stirring 3-bromopyruvic acid in deuterium oxide. Reaction progress was followed by ^{1}H NMR spectroscopy, by observing the loss of the proton peak at 3.5 ppm (**Figure 2.17**). The reaction of dideuterobromopyruvic acid **40** with $P(OMe)_3$ gave dimethyl-3,3-dideuteroPEP **41.** Phosphate methyl esters were hydrolysed with water, and addition of cyclohexylamine afforded the cyclohexylammonium salt of 3,3-dideuteroPEP **21**.

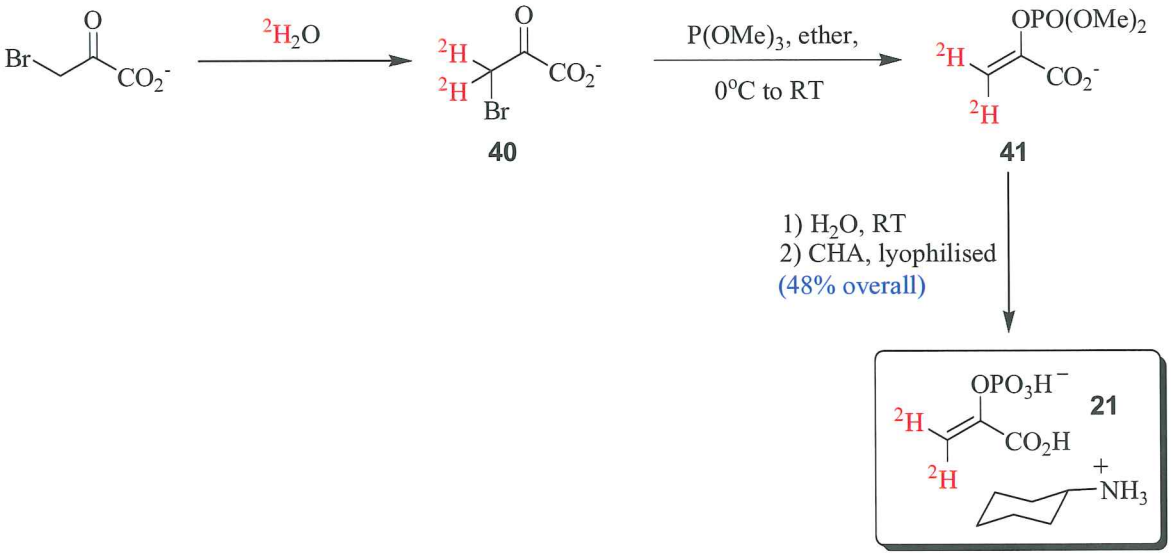

Scheme 2.8 Synthesis of 3,3-dideuteroPEP.

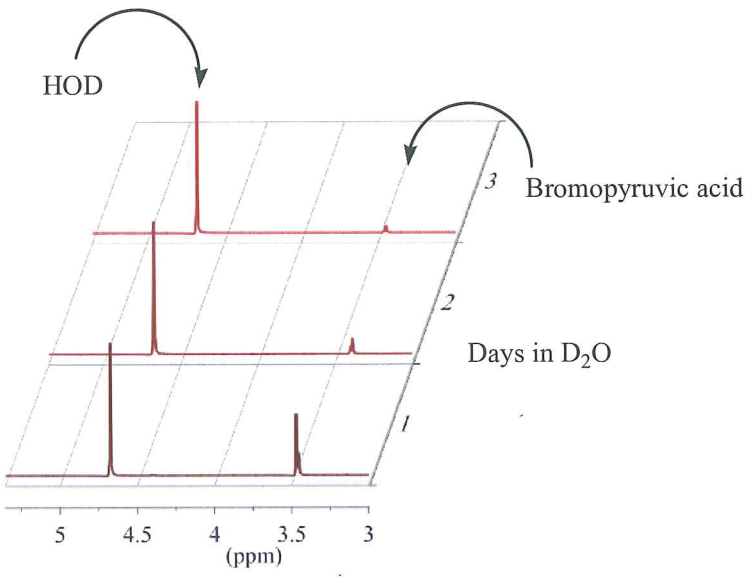

Figure 2.17 Following replacement of the α-hydrogen for deuterium by ^{1}H NMR spectroscopy.

To determine the extent of deuteration in the sample of **21**, ^{1}H and ^{31}P NMR spectroscopy spike experiments were performed. Spiked ^{31}P NMR spectra indicated the amount of both deuterated and non-deuterated PEP, and spiked ^{1}H NMR spectra indicated the amount of non-deuterated PEP. From this information, the percentage of deuteration of PEP in the sample was calculated to be approximately 58%. When this sample was tested as a substrate to *E. coli* DAH7P synthase and *N. meningitidis* KDO8P synthase, no observable difference to PEP was noted. Due to the high content of PEP in the sample, no information could be taken from these tests, and these studies were not pursued further.

2.4 Carboxyl Substituted Analogues of Phosphoenolpyruvate

Crystal structures of DAH7P synthase and KDO8P synthase suggest that the carboxyl group of PEP is important for correct binding of PEP in the active sites. From the proposed mechanisms, the carboxyl group of PEP is twisted out of the plane of PEP by charged residues to disrupt conjugation, making C3 more nucleophilic. After nucleophilic attack by C3 of PEP, the carboxyl group is proposed to stabilise the putative oxocarbenium ion transition state. Therefore, alterations to this functionality may provide insight into the role of the carboxyl group and the importance of its interactions in the active site.

2.4.1 Preparation of 1-(Chloromethyl)vinyl Phosphate

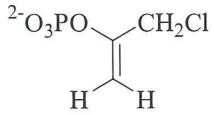

22

1-(Chloromethyl)vinyl phosphate **22**, where the carboxylic acid moiety of PEP is replaced with a methylchloride is considered a possible suicide inhibitor. It has been proposed that the relatively unreactive **22** may be made reactive due to interactions in the active site leading to enzyme inactivation.[57] Removal of the ionic carboxylic acid may however have drastic effects in its ability to bind in the active site.

A study of 1-(chloromethyl)vinyl phosphate **22** on other PEP-utilising enzymes demonstrated that PEP carboxylase was inactivated in its presence.[57] After 2 hours of

incubation 25% less activity was observed in PEP carboxylase. Interestingly, addition of 1-(chloromethyl)vinyl phosphate **22** to the enzyme PEP carboxylase increased the activity.

To synthesise 1-(chloromethyl)vinyl phosphate **22**, commercially available 1,3-dichloro acetone **42** was reacted with $P(OMe)_3$ to generate dimethyl-1-(chloromethyl)vinyl phosphate **43**. TMSBr was used to hydrolyse the phosphate methyl esters and the sample was immediately dissolved in a methanol/diethyl ether mixture, and cyclohexylamine was added. A white precipitate was formed of the cyclohexylammonium salt of 1-(chloromethyl)vinyl phosphate **22** (57% overall yield).

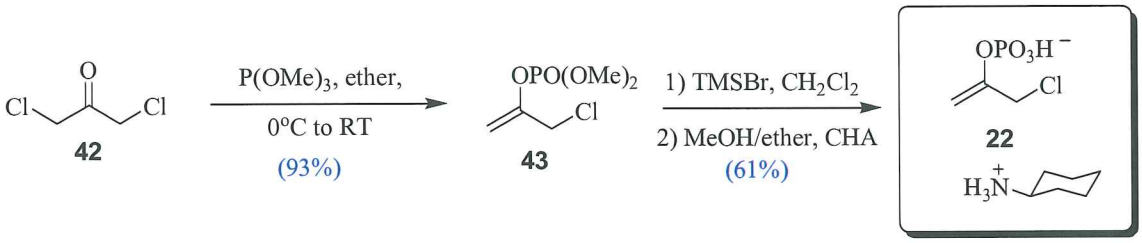

Scheme 2.9 Synthesis of 1-(chloromethyl)vinyl phosphate.

2.4.2 Preparation of 1-(Dihydroxyphosphinyl)vinyl Phosphate

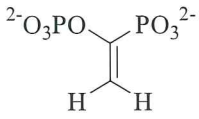

23

1-(Dihydroxyphosphinyl)vinyl phosphate (diphosphoPEP) **23**, where the carboxylate functionality is substituted for the isosteric phosphonate, $-PO_3^{2-}$, is expected to bind to electrostatic receptors in the active site. The difference in the structure of the phosphonate (tetrahedral), compared to the carboxylate (trigonal planar) would alter the alignment of the molecule in the active site and effect its ability to bind to the enzyme active sites and hence, its ability to be a substrate. If diphosphoPEP **23** acted as a substrate for DAH7P synthase or KDO8P synthase it would produce an electrophilic acyl phosphonate moiety that would be susceptible to covalent modification by attack of a nucleophile in the active site. This would disable the catalytic activity of the enzyme (**Figure 2.18**).

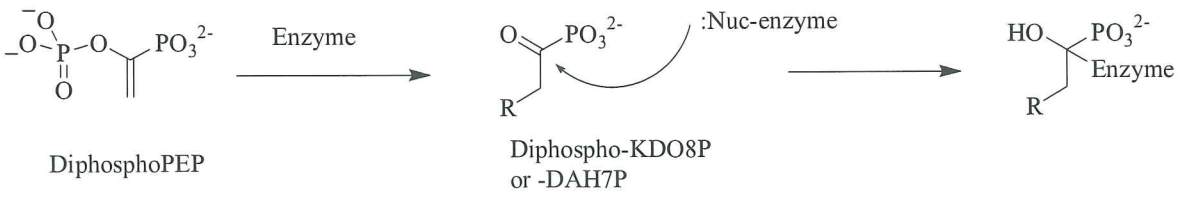

Figure 2.18 Mechanism of diphosphoPEP as a potential suicide inhibitor.

DiphosphoPEP **23** has been found to be a weak competitive inhibitor of other PEP-utilising enzymes, namely pyruvate kinase, PEP carboxylase and enolase.[57,79] A study by Benenson and co-workers demonstrated that diphosphoPEP **23** was a slow binding substrate of KDO8P synthase (a non-metallo form, *E. coli*) in pH conditions that caused diphosphoPEP **23** to be in its dianionic form (pH 5). However, formation of the analogous KDO8P product ($t_{1/2}$ = 567 min) had about 0.26% of the rate observed for PEP ($t_{1/2}$ = 10.5 min) under the same conditions. Inhibition studies also showed pH dependence, with K_i values of 60 and 360 μM at pH 5 and 7, respectively.[58]

DiphosphoPEP **23** was synthesised using chloroacetyl chloride **44** and two equivalents of $P(OMe)_3$ as reported by Sekine and co-workers.[67] In the reaction, $P(OMe)_3$ reacts with chloroacetyl chloride **44** in two ways; nucleophilic attack on the carbonyl followed by a Perkow reaction to afford tetramethyldiphosphoPEP **45**. The reaction was performed neat, in accordance with the procedure reported by Sekine, but instead of reacting for 30 minutes at 90°C, the reaction was performed overnight at room temperature. Hydrolysis of the phosphate esters was achieved using TMSBr, followed by treatment with aqueous KOH. The crude material was eluted through a Dowex(H) column, then cyclohexylamine was added to afford the cyclohexylammonium salt of diphosphoPEP **23**.

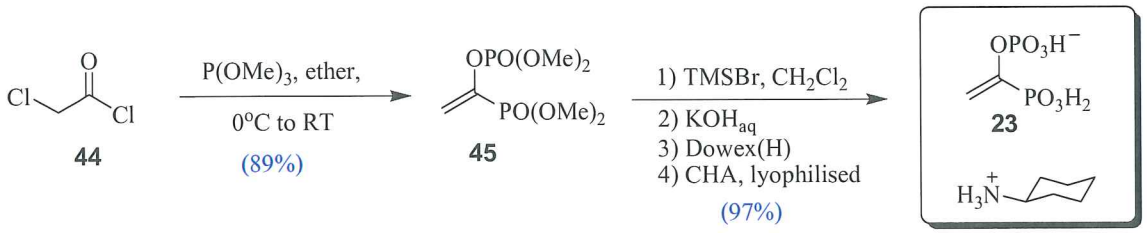

Scheme 2.10 Synthesis of diphosphoPEP.

2.5 2-Phospholactic Acid

24*R* **24*S***

The 2-phospholactic acid analogue **24** differs from PEP in that the double bond has been reduced, resulting in the formation of a stereocentre. This closely resembles the (partial) structure of the proposed intermediate species formed during the reactions catalysed by both DAH7P synthase and KDO8P synthase (**Figure 2.19**).

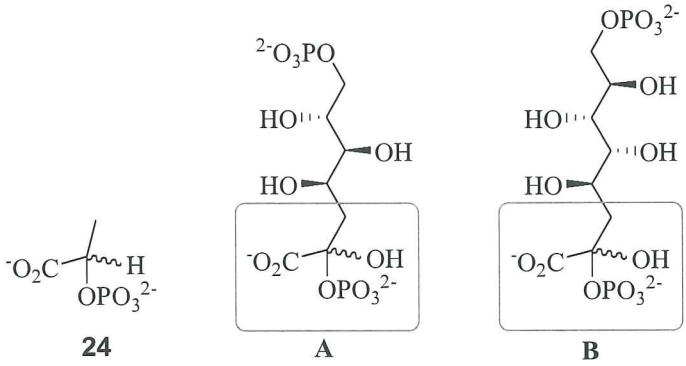

24 **A** **B**

Figure 2.19 Comparison of analogue **24** and the proposed linear intermediate from the DAH7P synthase reaction, **A**, and the KDO8P synthase reaction, **B**.

2.5.1 Preparation of 2-Phospholactic Acid

The two enantiomers of 2-phospholactic acid **24** were synthesised by phosphorylation of either (*R*)- or (*S*)-methyl lactate. Previously reported procedures[69,80] use diphenylchlorophosphate to phosphorylate methyl lactate, resulting in formation of methyl-2-(diphenylphospho)lactate **46**. To avoid the hydrogenolysis reaction using hydrogen gas and a metal catalyst, diethylchlorophosphate was used as an alternative to phosphorylate methyl lactate to afford methyl-2-(diethylphospho)lactate **47**. The phosphate ethyl esters were removed with TMSBr and then treated with aqueous KOH to afford 2-phosphomethyl lactate **48**. Removal of the carboxylate methyl ester was achieved by heating (80°C) in water overnight, followed by the addition of cyclohexylamine to afford the cyclohexylammonium salt of 2-phospholactic acid **24**.

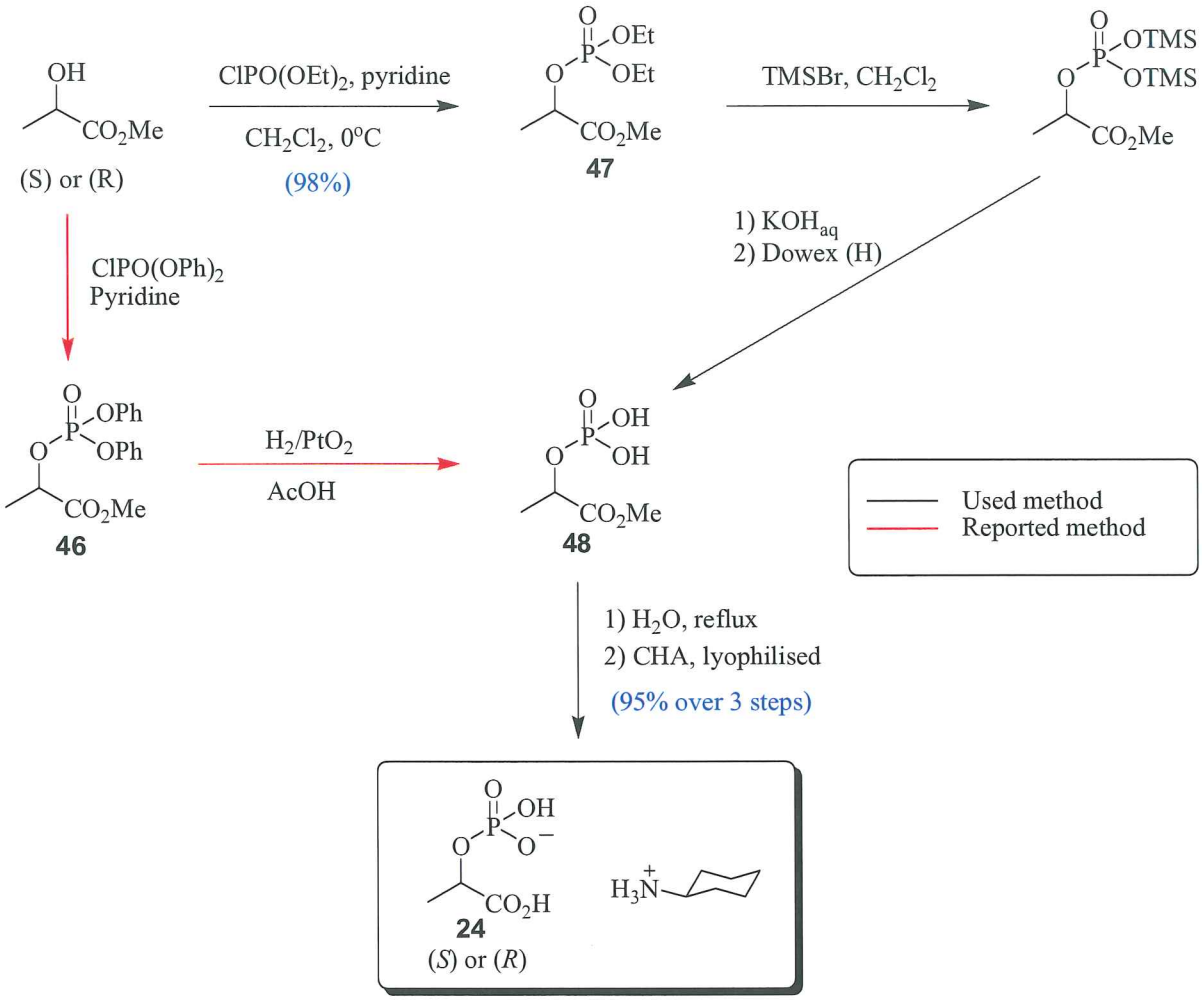

Scheme 2.11 Synthesis of 2-phospholactic acid.

2.6 2-(Phosphonomethyl)acrylic Acid

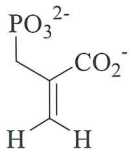

25

Substitution of the phosphate bridging oxygen for a methylene carbon gives the isosteric phosphonate analogue of PEP **25**. The enzyme catalysed reaction involves cleavage of the phosphate of PEP at the C-O bond, corresponding to the C-C bond of the phosphonate **25**, therefore this analogue is not expected to be a substrate for DAH7P synthase or KDO8P synthase. The effect of substituting the electron-withdrawing oxygen, for the electron-donating methylene group, is a reduced ability of the phosphate moiety to stabilise the

negative charge and therefore the phosphonate analogue **25** will have a higher pK_a (more basic). In addition, there is evidence from crystal structures that the bridging oxygen of PEP may be involved in hydrogen bonding in the active site of the enzymes and these interactions would be eliminated by substitution with a methylene group.[12,14]

Previous inhibition studies on other PEP-utilising enzymes showed weak competitive inhibition in the presence of the phosphonate analogue of PEP **25**, with pyruvate kinase, PEP carboxylase and enolase.[57,77] The phosphonate **25** was also found to be a slow reacting substrate in enolase, with a V_{max} 1.6% of that obtained with PEP.[81]

2.6.1 Preparation of 2-(Phosphonomethyl)acrylic Acid

The synthesis of phosphonate **25** was based on the procedure of Parker.[69] This route involves formation of the bromomethyl acrylate derivative **50**, which then undergoes an Arbusov reaction with $P(OMe)_3$ to afford the phosphonate.

Diethyl bis(hydroxymethyl) malonate **49** was synthesised by reacting diethyl malonate and two equivalents of formalin solution with the addition of potassium bicarbonate to act as the base. Heating diethyl bis(hydroxymethyl) malonate **49** to reflux with HBr yielded a solution of α-(bromomethyl)acrylic acid **50**. Volatile compounds were removed *in vacuo* and the residue cooled to 0°C to facilitate crystallisation of **50**. Filtering provided an orange slush that was extracted into hot pentane giving 5% (over two steps) of pure α-(bromomethyl)acrylic acid **50**.

α-(Bromomethyl) acrylic acid **50** was reacted with $P(OMe)_3$ to afford the dimethyl ester of the phosphonate **51**. The methyl esters were removed by treatment with 100 mM formic acid to afford 2-(phosphonomethyl)acrylic acid **25**.

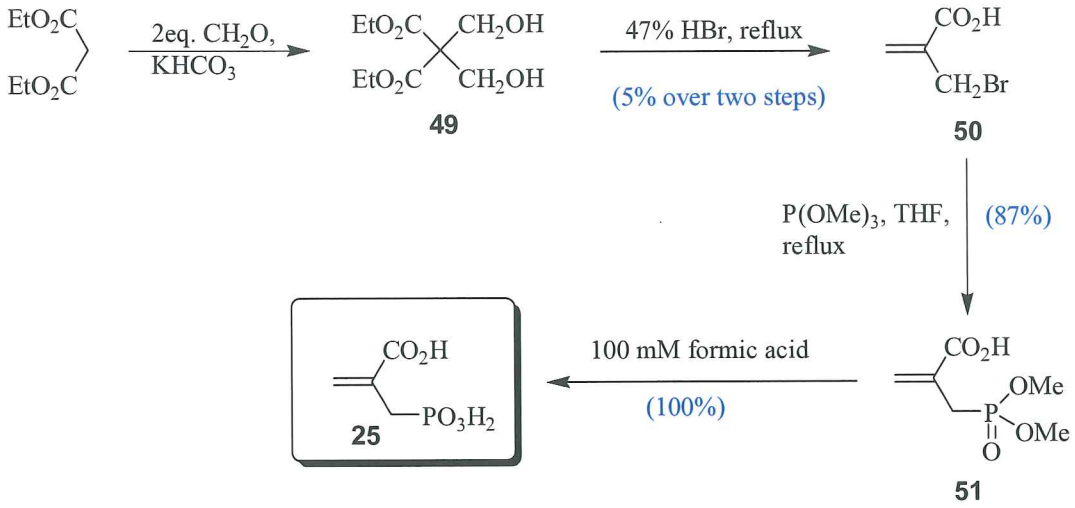

Scheme 2.12 Synthesis of the phosphonate analogue of PEP.

Chapter Three

Testing of PEP Analogues with DAH7P and KDO8P synthases

3.1 Introduction

The aim of this thesis was to test the ability of DAH7P synthase and KDO8P synthase to interact with PEP analogues. A range of analogues of PEP were synthesised as discussed in Chapter Two. These were then tested as competitive inhibitors or as substrates with DAH7P synthase and KDO8P synthase. The source of the DAH7P synthase enzyme used in this study is from *E. coli*, which is one of many species of bacteria that reside in the lower intestine of mammals, and can cause both intestinal and extra-intestinal infections.[75] DAH7P synthase from *E. coli* is a member of the Iα DAH7P synthase subfamily. There are three isozymes expressed in this organism. In this study the most abundant of these, the phenylalanine sensitive isozyme, was used. This enzyme has been highly studied, and its crystal structure has been solved.[14,49]

The source of the KDO8P synthase used in this study is from *N. meningitidis*, a Gram-negative bacterium that causes meningitis in humans.[75] While all DAH7P synthases and some KDO8P synthases require a divalent metal ion for activity, KDO8P synthase from *N. meningitidis* does not. The crystal structure of this enzyme has recently been solved. (PDB code 2QKF)

To test for inhibition, enzyme assays were performed at two or three PEP analogue concentrations with a range of PEP concentrations. The initial rates were then entered into GraFit© computer software (Appendices 2 and 3). From analysis of the data, it appears that all reversible inhibition observed of these enzymes in this study were competitive, as the maximum rate (V_{max}) was unaffected by the PEP analogues. The inhibition constant (K_i) was calculated by the GraFit software using non-linear least squares fitting to the data.

Molecular modeling was used in this study as a tool to help rationalise the observed experimental inhibition of the two enzymes by the PEP analogues. The active site crystal structure of phenylalanine sensitive DAH7P synthase from *E. coli* (PDB code 1N8F) and KDO8P synthase from *E. coli* (PDB code 1GG0) were used as molecular models of the enzymes. The crystal structure of KDO8P synthase from *E. coli* was chosen as the model structure as this contains identical active site residues to that from *N. meningitidis*, and the *N. meningitidis* crystal structure had some active site residues that were not defined. Using

modeling software (as described in experimental), the analogues of PEP were docked into the rigid enzyme models and the most energetically favoured orientation of the PEP analogue was calculated.

3.2 Testing 3-Substituted Analogues Against DAH7P and KDO8P Synthases

3.2.1 3-FluoroPEP

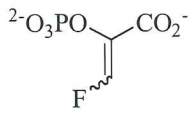

17

*DAH7P synthase (*E. coli*)*

3-FluoroPEP **17** was synthesised with a (*Z*):(*E*) ratio of 9:1, and then photo-isomerised to give a (*Z*):(*E*) ratio of 4:3. The photo-isomerised mixture of 3-fluoroPEP was tested as a substrate for DAH7P synthase and the reaction was followed *via* ^{19}F NMR spectroscopy. It was observed that both (*Z*)- and (*E*)-isomers of 3-fluoroPEP were substrates for DAH7P synthase, producing (3*R*)-[3-fluoro]DAH7P and (3*S*)-[3-fluoro]DAH7P, respectively. Both isomers of 3-fluoroPEP were converted to their corresponding 3-fluoroDAH7P product at the same rate (**Figure 3.1**).

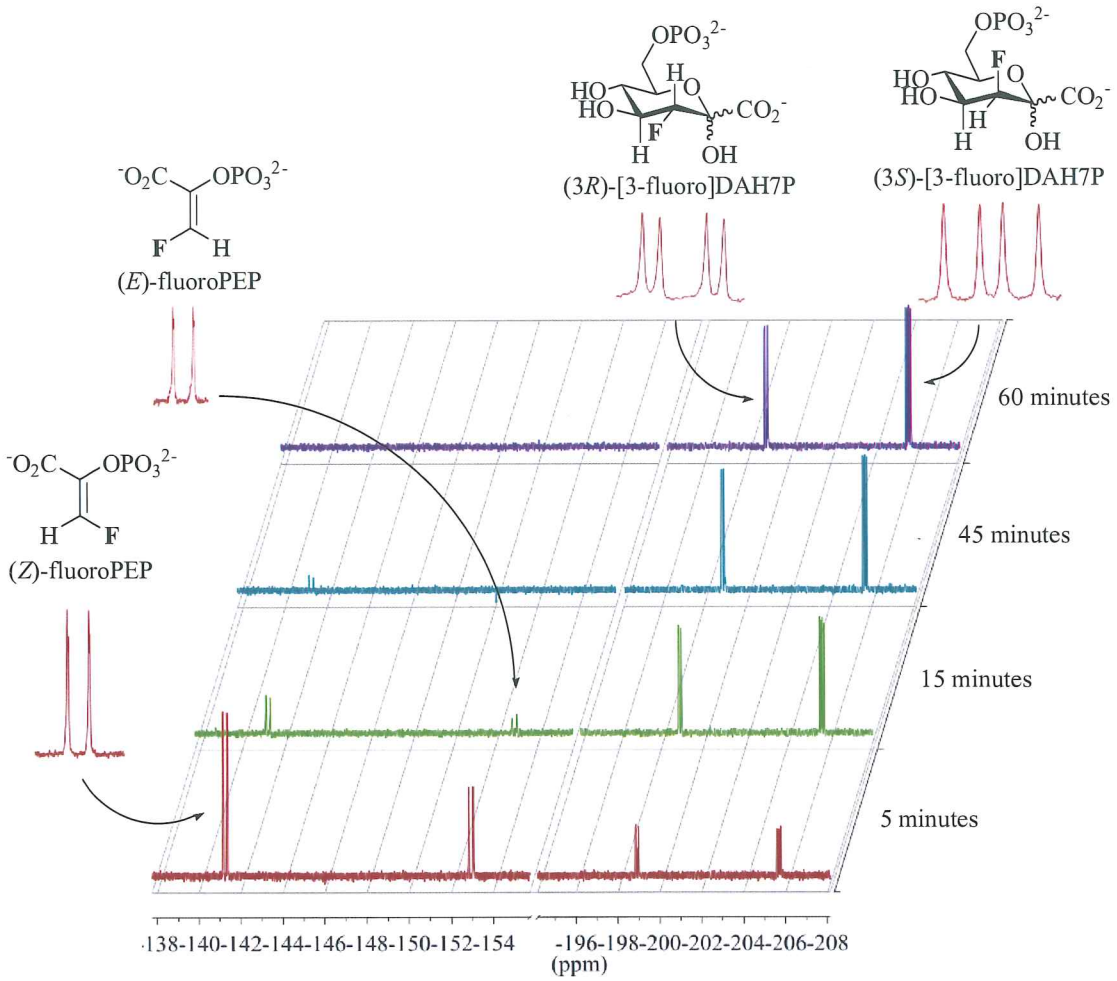

Figure 3.1 ^{19}F NMR spectroscopy reaction time course of the two isomers of 3-fluoroPEP catalysed by DAH7P synthase.

*KDO8P synthase (*N. meningitidis*)*

The photo-isomerised mixture of 3-fluoroPEP was tested as a substrate for KDO8P synthase and the reaction was followed *via* ^{31}F NMR spectroscopy. It was observed that 3-fluoroPEP is a substrate for KDO8P synthase. Interestingly, the (*E*)-isomer is processed much faster than the (*Z*)-isomer. **Figure 3.2**, **A**, shows the gradual loss (over 1 hour) of the peak that corresponds to (*E*)-3-fluoroPEP (from literature)[59,69], with a gain in the peak that corresponds to its product (3*R*)-[3-fluoro]KDO8P. The (*Z*)-fluoroPEP peak is effectively unchanged over this time scale, but as can be seen in **Figure 3.2**, **B**, the (*Z*)-3-fluoroPEP peak (over 9 hours) diminishes slowly, with the gradual increase in the peaks that correspond to its product (3*S*)-[3-fluoro]KDO8P. The different peaks observed for (3*S*)-[3-fluoro]KDO8P correspond to different cyclisation conformations that arise due to the C5 hydroxyl group being in the unfavourable axial position.

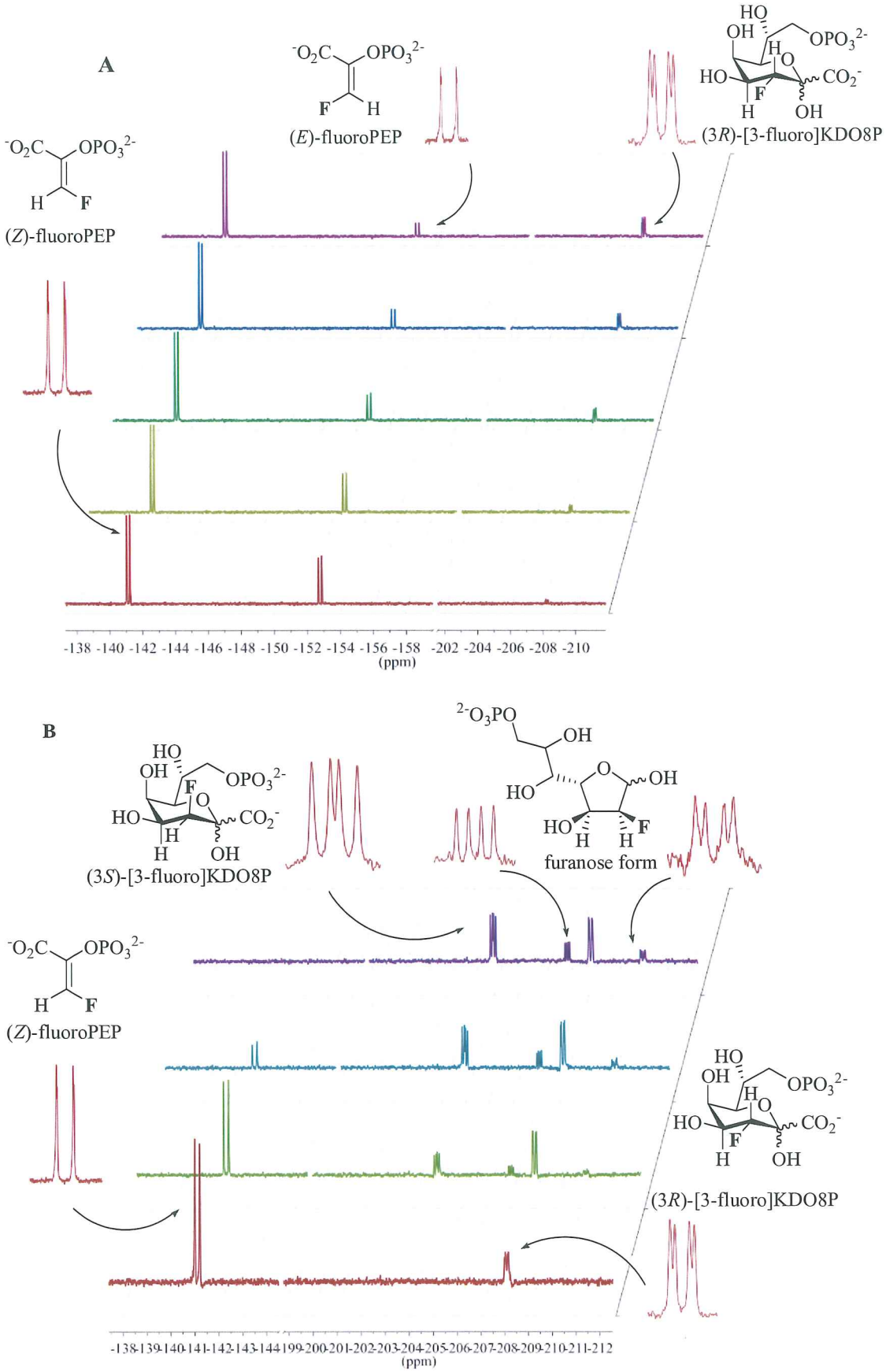

Figure 3.2 ^{19}F NMR spectroscopy reaction time course of the two isomers of 3-fluoroPEP catalysed by KDO8P synthase.[59]

Comparison / Discussion

Both isomers of 3-fluoroPEP **17** were shown to act as a substrate for both DAH7P synthase (from *E. coli*) and KDO8P synthase (from *A. pyrophilus* and *E. coli*), as was previously done by Garcia-Alles and co-workers.[57] Interestingly, the *N. meningitidis* KDO8P synthase showed the same high preference for the (*E*)-isomer of 3-fluoroPEP **17** over the (*Z*)-isomer, whereas the *E. coli* DAH7P synthase did not discriminate between the two isomers of **17**.

It has been proposed[57] that (*E*)-3-fluoroPEP is more electronegative than (*Z*)-3-fluoroPEP in solution, because of its greater retention time on an anion-exchange HPLC column, and as the ^{31}P NMR shifts show greater shielding by (*E*)-3-fluoroPEP than (*Z*)-3-fluoroPEP (-152.8 and -141.1 ppm, respectively). This was proposed to explain the greater reactivity of (*E*)-3-fluoroPEP observed in the KDO8P synthase reaction, as the higher net charge of (*E*)-3-fluoroPEP is expected to increase its binding to the positively charged residues in the active site. In addition, the higher negative charge density at C3 of (*E*)-3-fluoroPEP would make it more nucleophilic, promoting the aldol-type reaction.

However, it is not clear why this stereoisomer preference is not observed in the DAH7P synthase reaction, or whether this difference in stereoisomer preference between DAH7P synthase and KDO8P synthase is caused by mechanistic differences or by differences in their active sites.

One possible explanation for why the (*Z*)-3-fluoroPEP is a weaker substrate in KDO8P synthase than (*E*)-3-fluoroPEP, is that it is conceivable a mono-protonated phosphate group (as proposed in the mechanism) can form a hydrogen bond with the fluorine of (*Z*)-3-fluoroPEP, altering the preferred catalytic conformation (**Figure 3.3**). A fluorine in the (*E*)-position would be too far for interaction to occur. In DAH7P synthase the phosphate of 3-fluoroPEP is predicted to be unprotonated, therefore, it might be unaffected by the position of the fluorine.

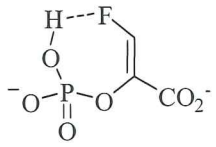

Figure 3.3 A possible conformation of (*Z*)-3-fluoroPEP to explain its unusual weak reactivity in KDO8P synthase.

3.2.2 Chloro-, Bromo- and Methyl-PEP

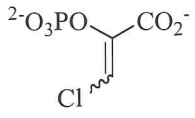

18

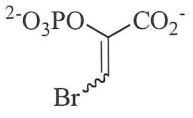

19

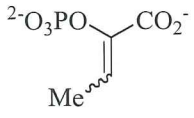

20

*DAH7P synthase (*E. coli*)*

When testing the PEP analogues as inhibitors, the initial rate of the enzymic reaction (containing both substrates) is measured by monitoring the rate of loss of PEP (at 232 nm), and the effect the added analogue has in lowering this rate is measured. The C3-substituted analogues have an absorbance maximum close to that of PEP, and therefore the concentrations of these species can not be too high, due to the error limitations of absorbance spectroscopy. This restriction of lower concentrations leads to less accurate results in some cases, especially for those analogues which exhibit poorer inhibition.

The chloro- **18**, bromo- **19** and methyl- **20** C3 analogues of PEP were synthesised and analysis of their ^{1}H NMR spectra established a (*Z*)-isomer percentage of 81, 93 and 90%, respectively. When tested as inhibitors against DAH7P synthase (*E. coli*) they were shown to exhibit moderate inhibition, with the greatest inhibition achieved by 3-chloroPEP **18**, followed by 3-methylPEP **20** and then 3-bromoPEP **19** (K_i values 240, 300 and 390 μM, respectively).

These compounds were then photo-isomerised by irradiation with ultraviolet light to increase the proportion of (*E*)-isomer. This gave a (*Z*)-isomer percentage of 60, 59 and 57% for chloro **18**, bromo **19** and methyl **20** C3-analogues of PEP respectively. These isomeric mixtures were tested against DAH7P synthase and were all shown to exhibit

greater inhibition than their unphoto-isomerised counterparts, with K_i values of 100, 180 and 180 μM, respectively. These follow a similar trend to the unphoto-isomerised samples.

	(*Z*)-isomer %	
	Isolated following synthesis	After photo-isomerisation
3-FluoroPEP	90	57
3-ChloroPEP	81	60
3-MethylPEP	90	57
3-BromoPEP	93	59

Table 3.1 Percentage of the (*Z*)-isomers of the mono-C3 substituted analogues before and after photo-isomerisation.

*KDO8P synthase (*N. meningitidis*)*

The chloro- **18**, bromo- **19** and methyl- **20** C3 analogues of PEP (mainly (*Z*)-isomeric mixture) were tested as inhibitors for *N. meningitidis* KDO8P synthase and these showed a similar inhibition trend to the results with DAH7P synthase. The greatest inhibition was observed with 3-chloroPEP **18**, followed by 3-methylPEP **20** and then 3-bromoPEP **19** (K_i values 150, 240 and 530 μM, respectively).

Mixtures of the (*Z*)- and (*E*)-isomers of **18**, **19** and **20** were tested to see if these showed altered inhibition of the enzyme. The inhibition by the isomeric mixture 3-chloroPEP **18** (K_i 140 μM) was similar to the inhibition observed with the mainly (*Z*)-3-chloroPEP **18** mixture (K_i 150 μM). The inhibition by the isomeric mixture of 3-bromoPEP **19** (K_i 210 μM) was considerably greater than that of the mainly (*Z*)-3-bromoPEP **19** mixture (K_i 530 μM). Interestingly, the inhibition by the isomeric mixture of 3-methylPEP **20** (K_i 400 μM) was nearly double that of the mainly (*Z*)-3-methylPEP **20** mixture (K_i 240 μM). These results suggest that the (*E*)-isomer of 3-bromoPEP **19** is significantly more inhibitory than the (*Z*)-isomer, whereas the (*Z*)-isomer of 3-methylPEP **20** is significantly more inhibitory than the (*E*)-isomer, and for 3-chloroPEP **18** there is no significant difference in inhibition between the isomers.

Comparison / Discussion

It was observed that the mixtures of C3 analogues that are mostly (*Z*)-isomers show a similar trend for both *E. coli* DAH7P synthase and *N. meningitidis* KDO8P synthase, in that strongest inhibition is observed by 3-chloroPEP, followed by 3-methylPEP and then 3-bromoPEP. The isomeric mixture of the C3 analogues showed a reduction in their K_i values against DAH7P synthase in comparison to their mostly (*Z*)-isomer mixtures, suggesting (*E*)-isomers of **18**, **19** and **20** were better inhibitors of the enzyme. In contrast, the inhibition of KDO8P synthase with the isomeric mixtures of the C3 analogues gave varied results (**Table 3.2** and illustrated in **Figure 3.4**).

	DAH7P synthase		KDO8P synthase	
	Mainly (*Z*)-isomer	Mixture of isomers	Mainly (*Z*)-isomer	Mixture of isomers
3-ChloroPEP	240 ± 40	100 ± 20	150 ± 20	140 ± 20
3-MethylPEP	300 ± 30	180 ± 20	240 ± 40	410 ± 100
3-BromoPEP	390 ± 50	180 ± 20	530 ± 110	210 ± 40

Table 3.2 Inhibition constants (μM) of the C3 substituted analogues.

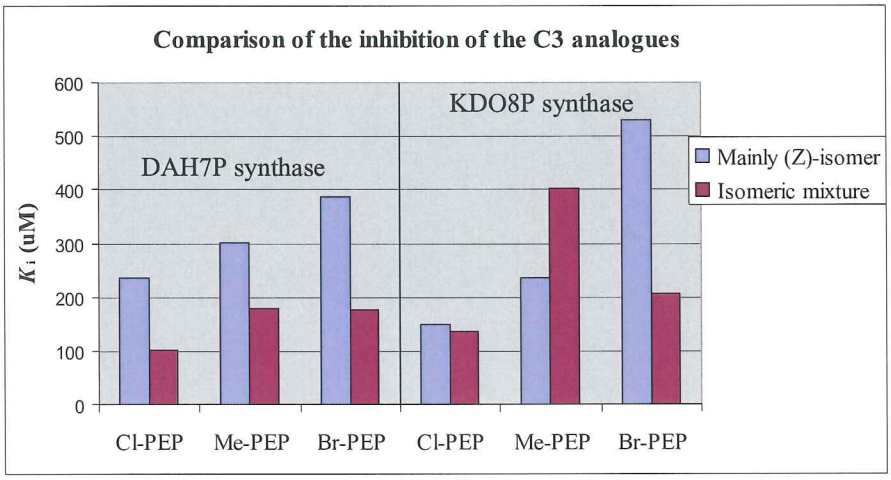

Figure 3.4 Relative inhibition of C3 analogues. Mainly (*Z*)-isomers were 81, 90 and 93% (*Z*)-isomer of chloro-, methyl- and bromo-PEP, respectively. Isomeric mixtures were 60, 57 and 59% (*Z*)-isomer of chloro-, methyl- and bromo-PEP, respectively.

Molecular modelling of 3-chloroPEP **18** into a KDO8P synthase model (PDB code 1GG0, *E. coli*) showed similar orientations for both isomers to that of PEP, indicating that chlorine can be accommodated in both positions. This is consistent with experimental observations as no significant difference in inhibition was observed between the two isomers in KDO8P synthase. In DAH7P synthase, the two isomers showed different

conformations, the (*E*)-3-chloroPEP was predicted to bind in a manner similar to the binding observed with PEP (**Figure 3.5**), and the C3 of (*Z*)-3-chloroPEP points towards the cavity opening due to steric effects by an arginine residue (**Figure 3.6**). This may account for the greater inhibition observed by (*E*)-3-chloroPEP over (*Z*)-3-chloroPEP in DAH7P synthase.

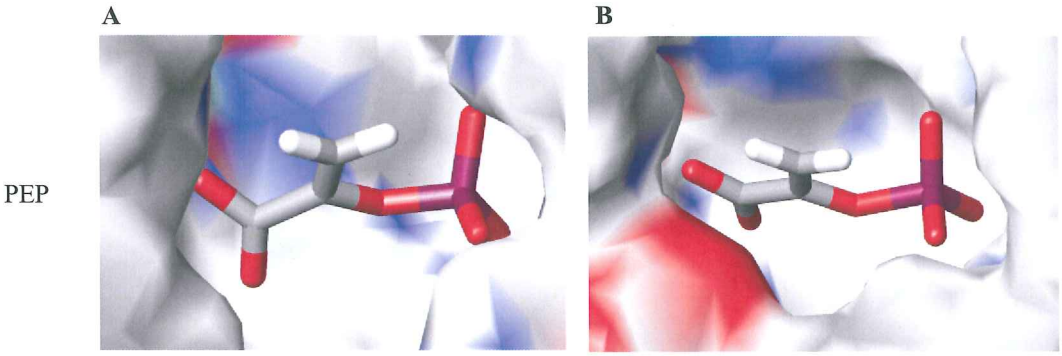

Figure 3.5 Molecular model of , **A**, PEP bound in the active site of *E. coli* DAH7P synthase from the crystal structure (PDB code 1N8F) and, **B**, PEP docked into the active site of *E. coli* KDO8P synthase (PDB code 1GG0).

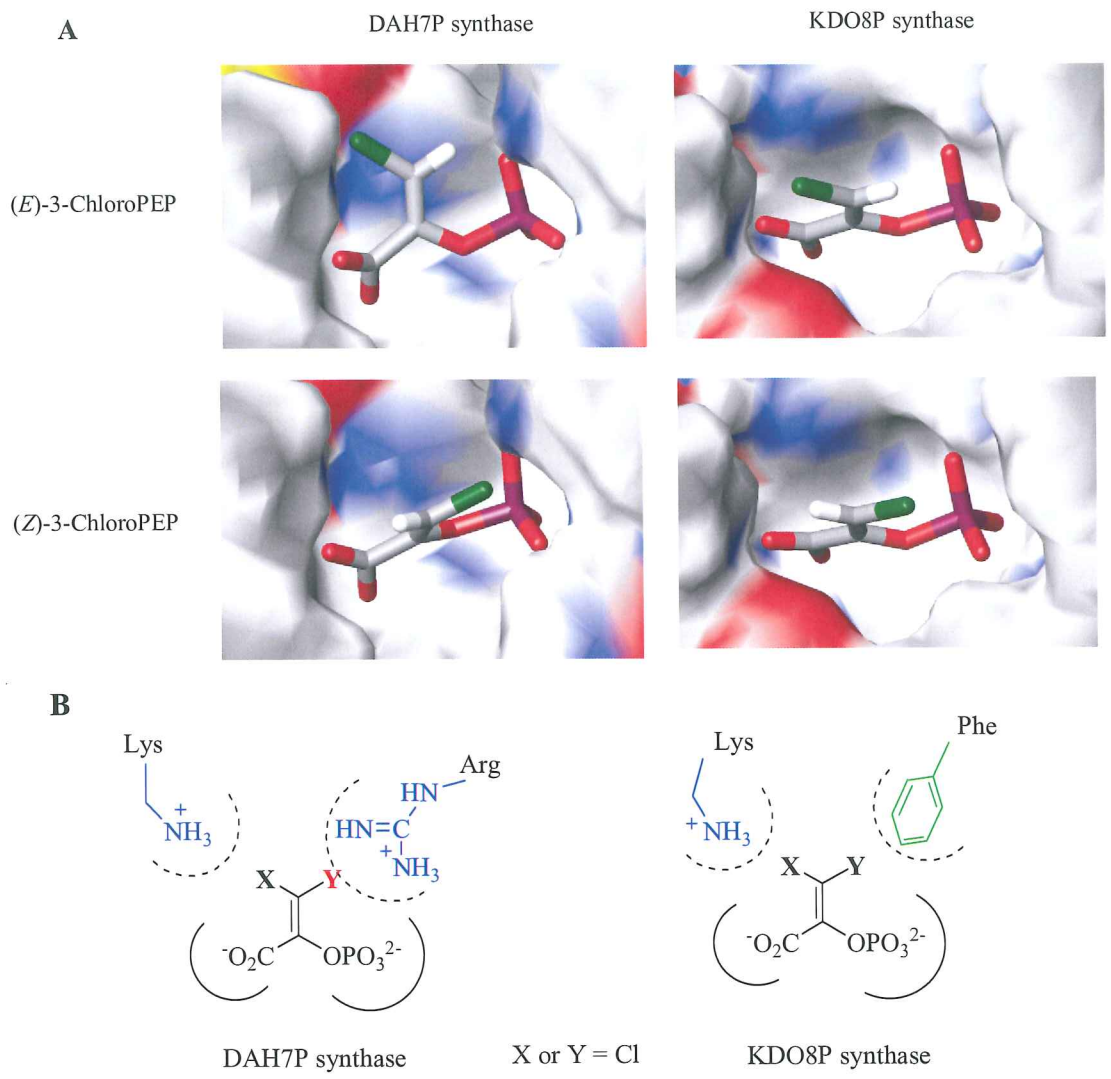

Figure 3.6 Molecular model, **A**, and schematic diagram, **B**, of the active site of DAH7P synthase and KDO8P synthase containing the two isomers of 3-chloroPEP. Red indicates the position of chlorine observed to have significantly weaker inhibition.

Modelling the two isomers of 3-bromoPEP into DAH7P synthase indicates that they adopt similar conformations to that of PEP. However, the phosphate of (*Z*)-3-bromoPEP is slightly kinked due to an interaction between the bromine and an arginine residue. This may account for the greater inhibition observed by (*E*)-3-bromoPEP over (*Z*)-3-bromoPEP in DAH7P synthase. Modelling of the two isomers in KDO8P synthase predicted very similar conformations were adopted by both the enzyme active sites, suggesting that there was sufficient room for the bromine in both isomers (**Figure 3.7**). However, experimentally, greater inhibition was found with the isomeric mixture compared to the mixture containing mostly (*Z*)-3-bromoPEP, suggesting the (*E*)-isomer is a stronger inhibitor of this enzyme.

Comparing the inhibition of 3-bromoPEP with 3-chloroPEP in KDO8P synthase, the inhibition of (*E*)-3-bromoPEP was 50% less than that observed for (*E*)-3-chloroPEP, and (*Z*)-3-bromoPEP was approximately 3.5 times weaker than the inhibition observed with (*Z*)-3-chloroPEP. This suggests that the active site of KDO8P synthase can accommodate a chlorine at the (*Z*)-position of PEP but does not readily accomodate the slightly larger bromine is in this position.

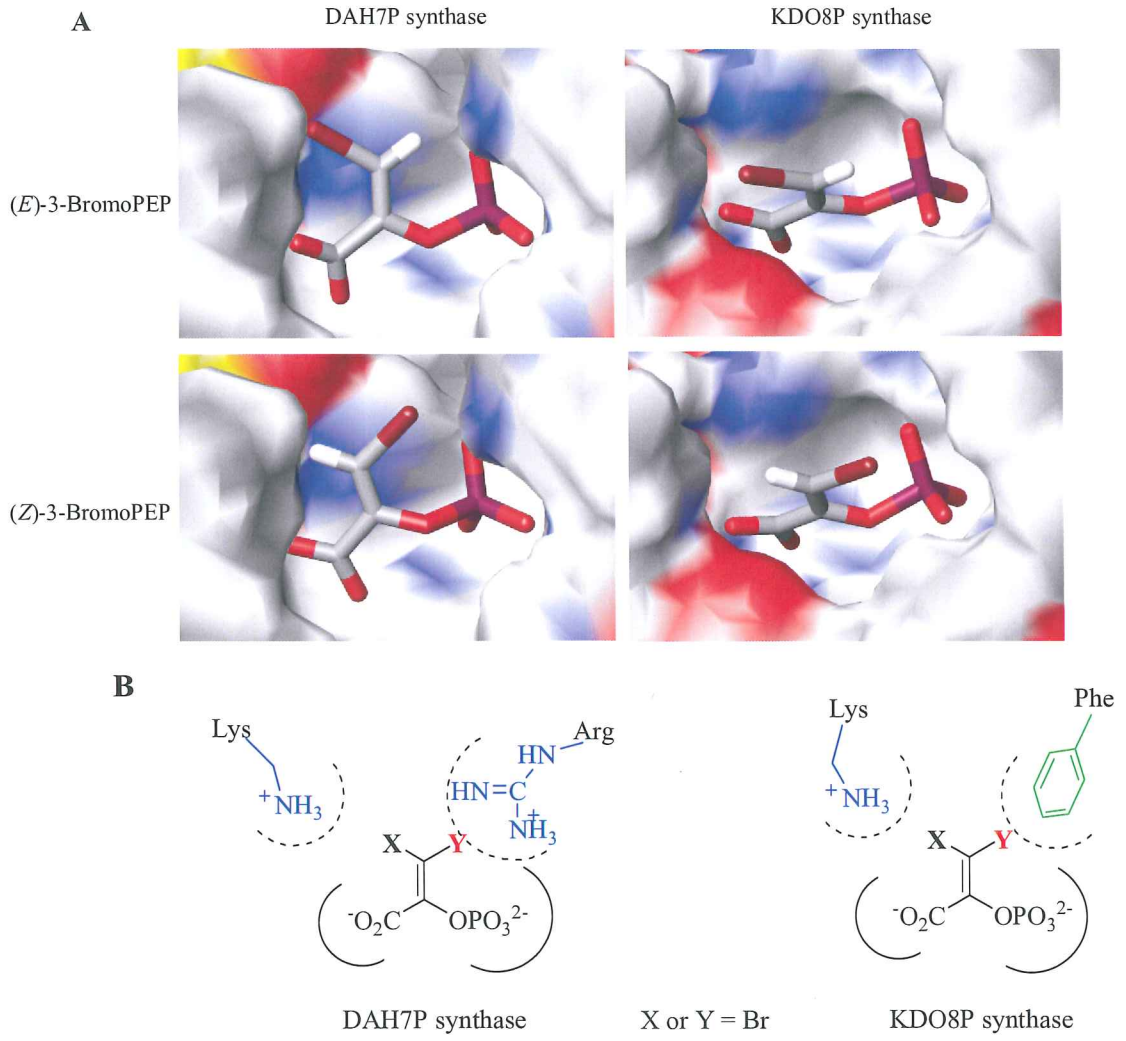

Figure 3.7 Molecular model, **A**, and schematic diagram, **B**, of the active site of DAH7P synthase and KDO8P synthase containing the two isomers of 3-bromoPEP. Red indicates the position of bromine observed to have significantly weaker inhibition.

Modelling the two isomers of 3-methylPEP into DAH7P synthase, indicates that (*E*)-3-methylPEP binds in a conformation similar to that of PEP, and the (*Z*)-3-methylPEP has a kinked orientation due to interaction of the methyl group with an arginine group (**Figure 3.8**). This may account for the greater inhibition observed with (*E*)-3-methylPEP over (*Z*)-3-methylPEP in DAH7P synthase. Interestingly, the opposite isomeric preference is

observed in KDO8P synthase, where greater inhibition of the enzyme was observed with (*Z*)-3-methylPEP. Modelling the two isomers into KDO8P synthase indicates that they bind to the enzyme with similar conformations, and one rational explanation for the greater inhibition with (*Z*)-3-methylPEP is that the methyl group appears to have hydrophobic interactions with a phenylalanine residue that favours its binding.

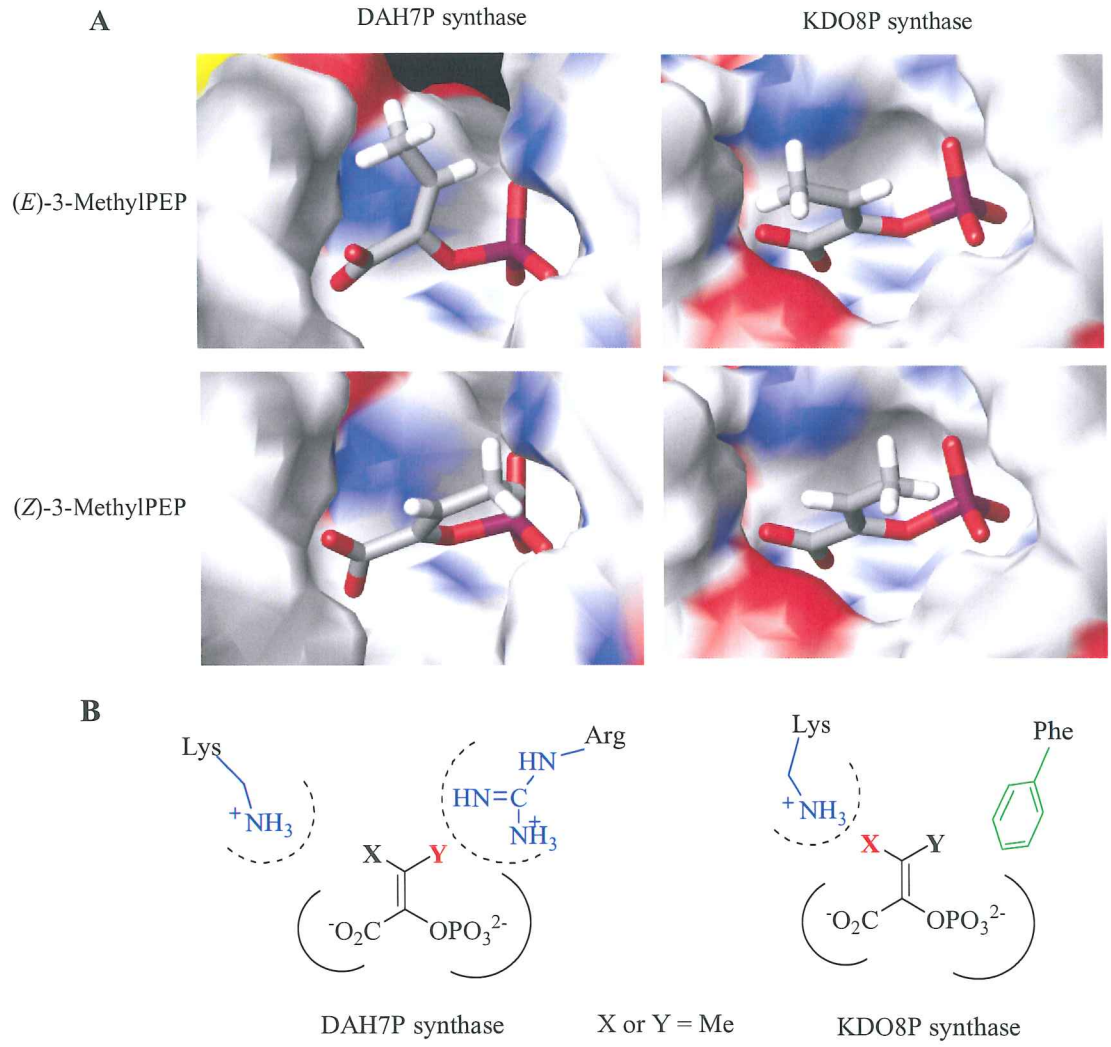

Figure 3.8 Molecular model, **A**, and schematic diagram, **B**, of the active site of DAH7P synthase and KDO8P synthase containing the two isomers of 3-methylPEP. Red indicates the position of the methyl group observed to have significantly weaker inhibition.

Molecular modelling indicates that the weaker inhibition observed by the (*Z*)-isomers of 3-chloroPEP, 3-bromoPEP and 3-methylPEP in DAH7P synthase, may be due to an arginine residue that sterically hinders substituents in the (*Z*)-position. Docking 3-chloroPEP, 3-bromoPEP and 3-methylPEP into a KDO8P synthase model showed similar conformations with little help in rationalising the observed inhibition differences. The molecular models suggest that KDO8P synthase has a larger PEP binding pocket to that of DAH7P synthase.

3.3 Testing Carboxyl Substituted Analogues Against DAH7P and KDO8P Synthases

3.3.1 1-(Chloromethyl)vinyl Phosphate

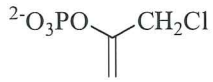

22

*DAH7P synthase (*E. coli*)*

1-(Chloromethyl)vinyl phosphate **22** was tested as an inhibitor for DAH7P synthase and was found to be a very poor inhibitor with a K_i value of 2.6 ± 0.7 mM. The high error arises from the difficulties of testing this analogue at high concentrations, as it absorbs at the same wavelength as PEP.

It was proposed that 1-(chloromethyl)vinyl phosphate **22** may act as a time-dependent inhibitor, so this was tested as a irreversible inhibitor. This was achieved by incubating *E. coli* DAH7P synthase with **22** or buffer (as a control) and using samples of these mixtures to catalyse the reaction of PEP and E4P at different time intervals. It was observed that a gradual loss of activity occurred in the enzyme incubated in **22**, and after approximately five hours activity was reduced to 5% (**Figure 3.9**).

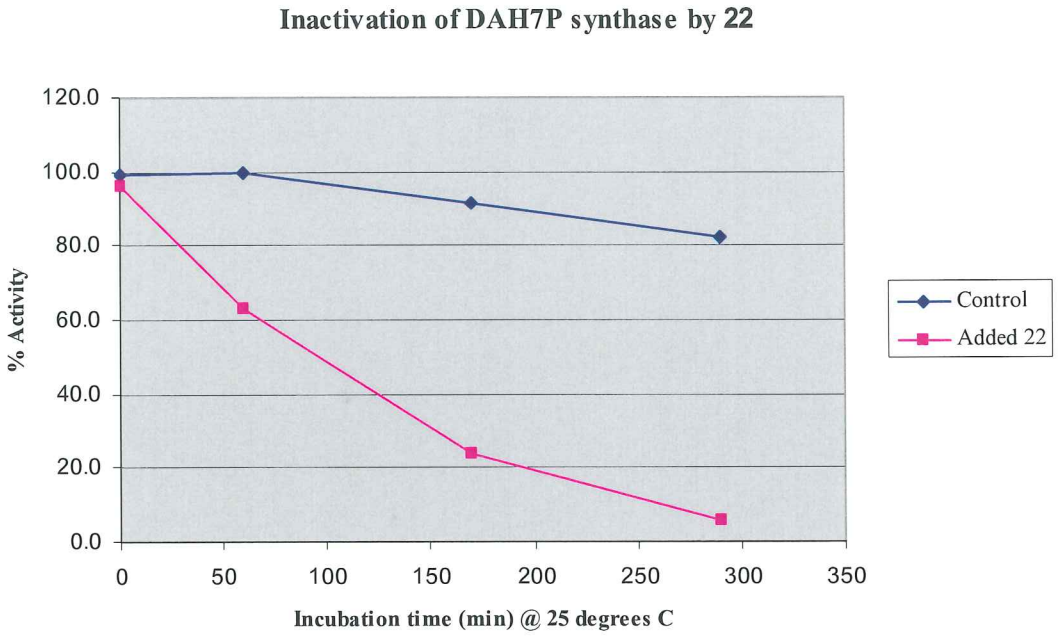

Figure 3.9 Time dependent inactivation of *E. coli* DAH7P synthase with **22**.

To further investigate the nature of this time dependent inactivation, the enzyme samples were analysed with mass spectrometry. It was evident by comparison of the control (**Figure 3.10, A**), that the enzyme incubated in **22** had multiple modifications (**Figure 3.10, B**).

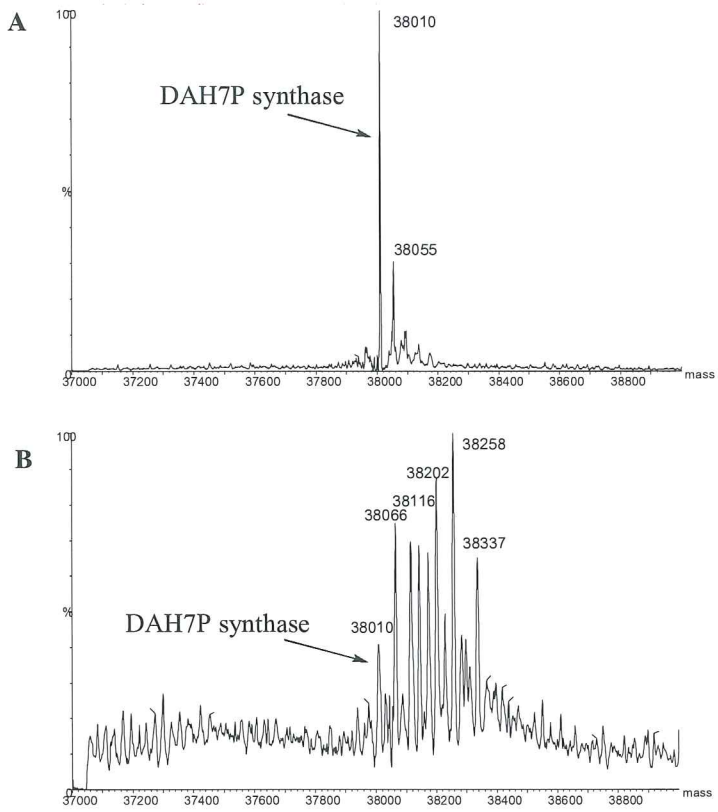

Figure 3.10 Mass spectra of, **A**, *E. coli* DAH7P synthase and, **B**, *E. coli* DAH7P synthase incubated in **22**.

The observed modifications to *E. coli* DAH7P synthase, are expected to be caused by the nucleophilic substitution by a nucleophilic enzyme residue at the C1 carbon of **22**, and followed by phosphate hydrolysis (**Figure 3.11**). This forms the two proposed types of modification with a phosphoenol moiety (M_r = 135 Da) or a pyruvyl moiety (M_r = 57 Da).

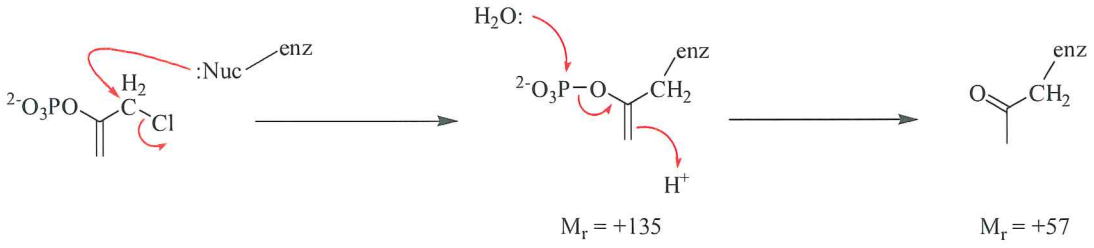

Figure 3.11 Diagram of proposed modification that leads to increases in mass to the enzyme.

*KDO8P synthase (*N. meningitidis*)*

In a similar manner to *E. coli* DAH7P synthase, 1-(chloromethyl)vinyl phosphate **22** was found to be a very poor competitive inhibitor of KDO8P synthase with a K_i value of 2.8 ± 0.5 mM.

An inactivation experiment was performed in the same way as DAH7P synthase, using *N. meningitidis* KDO8P synthase incubated with either **22** or buffer (as a control), and using samples of these to catalyse the reaction of PEP and A5P at different time intervals. It was observed that a gradual loss of activity occurred in the enzyme incubated in **22**, and after approximately five hours activity was reduced to 30% (**Figure 3.12**).

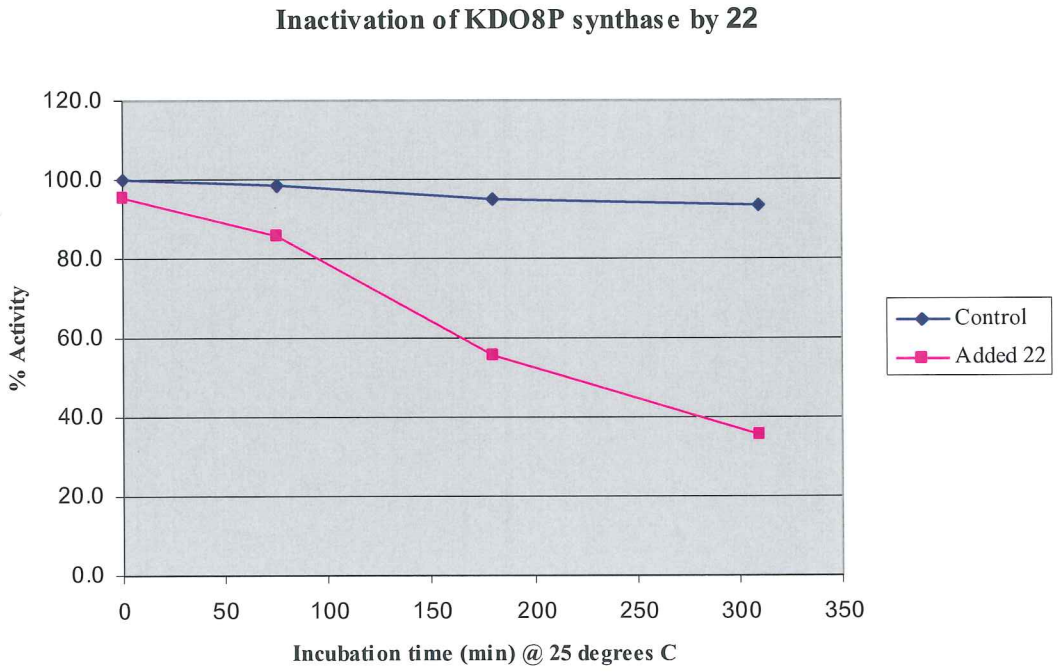

Figure 3.12 Time dependent inactivation of *N. meningitidis* KDO8P synthase with **22**.

Analysis of the enzyme samples with mass spectrometry showed that covalent modification of the enzymes had occurred, with masses of 55 and 135 Da added to the mass of the enzyme (**Figure 3.13**). These peaks correspond to the covalent substitution of a pyruvyl moiety (57 Da) and a phophoenol moiety (135 Da), and suggest only one site on the enzyme was modified.

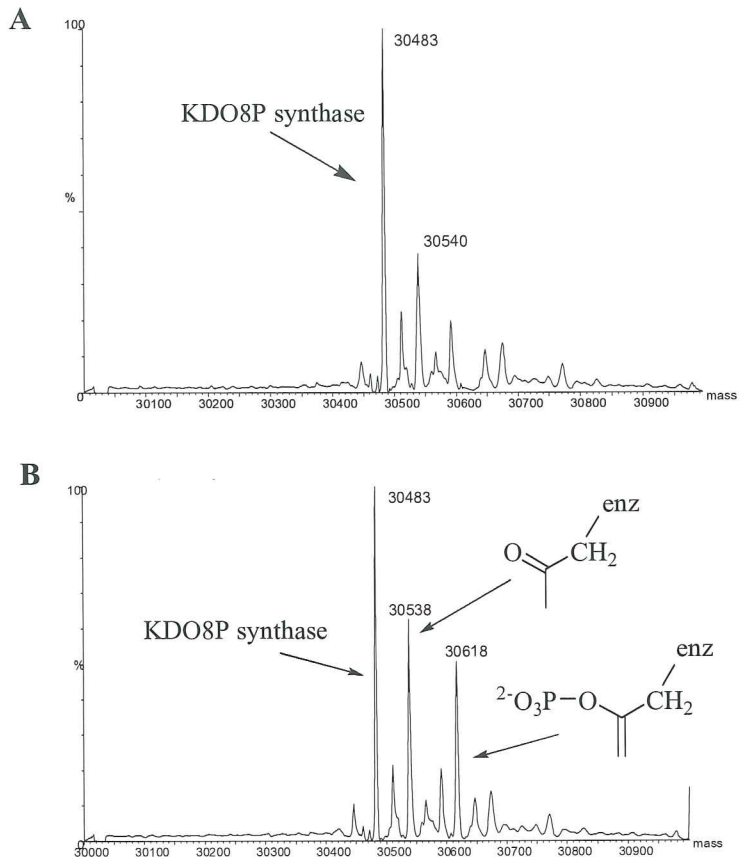

Figure 3.13 Mass spectra of, **A**, *N. meningitidis* KDO8P synthase and, **B**, *N. meningitidis* KDO8P synthase incubated in **22**.

Comparison / Discussion

1-(Chloromethyl)vinyl phosphate **22** was a poor inhibitor of both *E. coli* DAH7P synthase and *N. meningitidis* KDO8P synthase, with K_i values of 2.6 ± 0.7 and 2.8 ± 0.5 mM. This was reflected by docking of 1-(chloromethyl)vinyl phosphate **22** into DAH7P synthase and KDO8P synthase molecular models, which both indicated different binding to that of PEP. Therefore, the interactions of the carboxylic acid group in PEP that occur in the active site of both DAH7P synthase and KDO8P synthase must be important for correct and tight binding.

Time dependent modification of both DAH7P synthase and KDO8P synthase were observed after incubation with **22**. DAH7P synthase was inactivated at a faster rate than KDO8P synthase, with activity after five hours incubation of 5 and 30%, respectively. Analysis of the mass spectrum of DAH7P synthase showed multiple peaks, suggesting that there are many sites on this enzyme that can react with **22**. Interestingly, KDO8P synthase

appears to have a single site of modification, and since it was observed that activity was lost due to the modification, it is likely that this covalent modification occurred in the active site.

3.3.2 1-(Dihydroxyphosphinyl)vinyl Phosphate

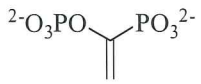

23

*DAH7P synthase (*E. coli*)*

The diphosphoPEP analogue **23**, where the carboxyl in PEP is substituted with a phosphonate moiety, was observed to be a good inhibitor of DAH7P synthase, with a K_i value of 150 ± 20 μM. This PEP analogue absorbs light at a lower wavelength to that of PEP, and therefore greater concentrations of diphosphoPEP could be used in the enzyme assay giving more accurate inhibition results.

DiphosphoPEP was tested as a substrate for DAH7P synthase by following the reaction of E4P and diphosphoPEP with ^{31}P NMR spectroscopy. No change was observed in the ^{31}P NMR spectra, indicating diphosphoPEP was not a substrate for DAH7P synthase.

*KDO8P synthase (*N. meningitidis*)*

The diphosphoPEP analogue was a poor inhibitor of KDO8P synthase at pH 6.5 with a K_i value of 1.6 mM. The pK_{a2} of both the phosphate and phosphonate groups of diphosphoPEP have been previously estimated by proton decoupled ^{31}P NMR measurements of chemical shifts to be 5.8 (± 0.3).[58] Therefore, at pH 6.5 diphosphoPEP is expected to be mostly in its tetraanionic form (**Figure 3.14, A**). PEP bound in the active site of KDO8P synthase, has been proposed to be in its dianionic form (**Figure 3.14, C**)[33], therefore inhibition with diphospho PEP was tested at pH 5.3, where it would be mostly in its dianionic form (**Figure 3.14, B**). It was observed at pH 5.3 that diphosphoPEP was significantly more inhibitory, with a K_i value of 690 μM.

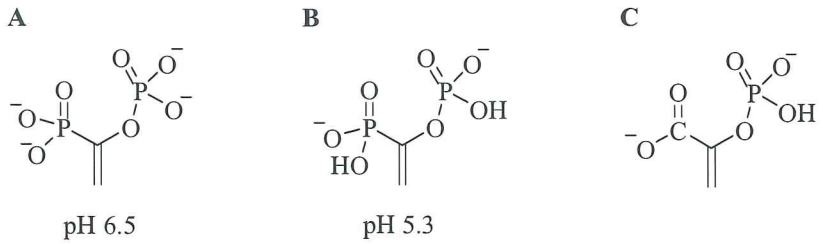

Figure 3.14 Schematic diagram of diphosphoPEP at, **A**, pH 6.5, **B**, pH 5.3 and, **C**, PEP in its proposed ionised form in the active site of KDO8P synthase.

DiphosphoPEP was tested as a substrate for KDO8P synthase by following the reaction of A5P and diphosphoPEP with ^{31}P NMR spectroscopy. No change was observed in the ^{31}P NMR spectra, indicating diphosphoPEP was not a substrate for KDO8P synthase.

Comparison / Discussion

	DAH7P synthase	KDO8P synthase	
	(pH 6.8)	(pH 6.5)	(pH 5.3)
DiphosphoPEP **23**	150 ± 20	1600 ± 300	690 ± 80

Table 3.3 Inhibition constants (μM) of diphosphoPEP.

E. coli DAH7P synthase was inhibited significantly more by diphosphoPEP **23** in comparison to *N. meningitidis* KDO8P synthase (**Table 3.3**). However, when the inhibition conditions were performed at a lower pH with KDO8P synthase, significant increased inhibition was observed. *E. coli* DAH7P synthase lost all activity at pH values between 5 and 6, so a comparison of the effect of pH could not be made readily.

Interestingly, when diphosphoPEP **23** was docked into KDO8P synthase the phosphonate sat in the phosphate binding site preferentially over the phosphate, whereas in DAH7P synthase the phosphonate sat in the carboxylic acid pocket (**Figure 3.15**). This reversed binding observed in KDO8P synthase resulted in reduced hydrogen bonding interactions. This may account for the much weaker inhibition observed by diphosphoPEP in KDO8P synthase over DAH7P synthase.

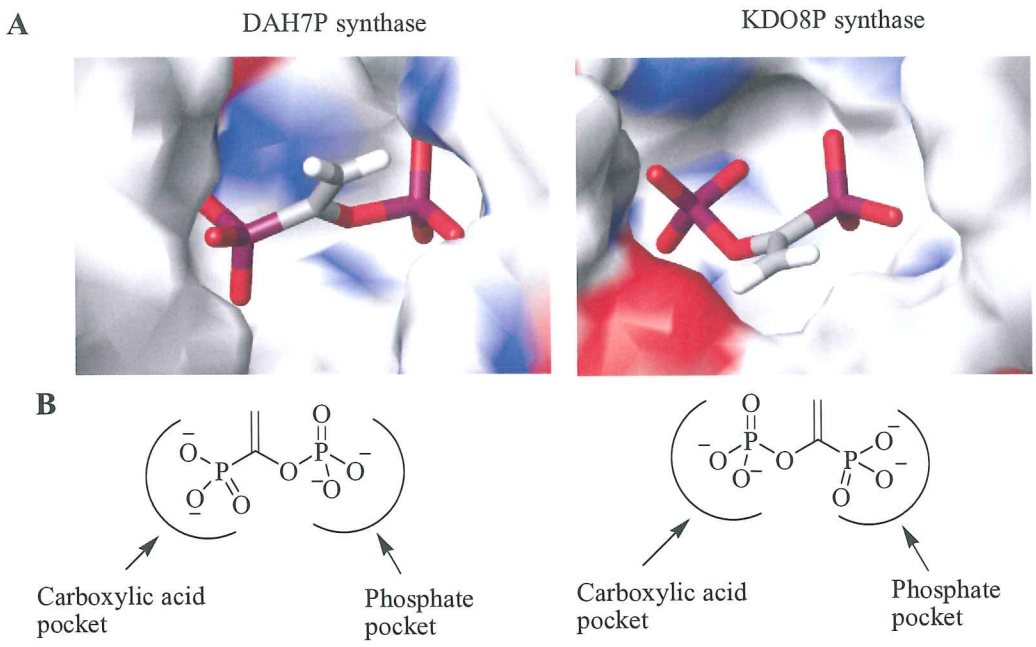

Figure 3.15 Molecular model, **A**, and schematic diagram, **B**, of the active site of DAH7P synthase and KDO8P synthase containing diphosphoPEP.

3.4 Testing 2-Phospholactic Acid Against DAH7P and KDO8P Synthases

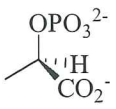

24*R*

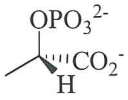

24*S*

*DAH7P synthase (*E. coli*)*

The (*R*)-isomer of 2-phospholactic acid **24** showed the best inhibition of all analogues with a K_i value of 57 ± 3 μM. Interestingly, the (*S*)-isomer gave significantly (6-fold) weaker inhibition, with a K_i value of 340 ± 14 μM.

*KDO8P synthase (*N. meningitidis*)*

Both isomers of 2-phospholactic acid **24** were found to have poor inhibition, with slightly stronger inhibition observed with the (*R*)-isomer over the (*S*)-isomer. The K_i values were 870 and 1200 μM, respectively. Like diphosphoPEP **23**, 2-phospholactic acid **24** has the

advantage of absorbing away from the testing absorbance, of 232 nm, allowing more accurate results at higher inhibitor concentrations.

Comparison / Discussion

2-Phospholactic acid	DAH7P synthase	KDO8P synthase
(*R*)-isomer	57 ± 3	870 ± 90
(*S*)-isomer	340 ± 14	1200 ± 150

Table 3.4 Inhibition constants (μM) of phospholactic acid.

In DAH7P synthase, the (*R*)-isomer of phospholactic acid is a significantly better competitive inhibitor than the (*S*)-isomer. In contrast, the (*R*)-isomer is only a slightly better inhibitor than the (*S*)-isomer in KDO8P synthase, and both isomers are weaker inhibitors in KDO8P synthase than with DAH7P synthase. These results indicate that the active site in DAH7P synthase is more accepting of a phosphate species connected to an sp^3 carbon atom than KDO8P synthase.

The greater ability of the (*R*)-isomer over the (*S*)-isomer to inhibit both DAH7P synthase and KDO8P synthase, could be rationalised as the (*R*)-isomer binding in the PEP binding pocket and mimicking the stereochemistry observed in a proposed crystal structure of the linear intermediate (KDO8P synthase triple-mutant from *A. aeolicus*) (**Figure 3.16**).

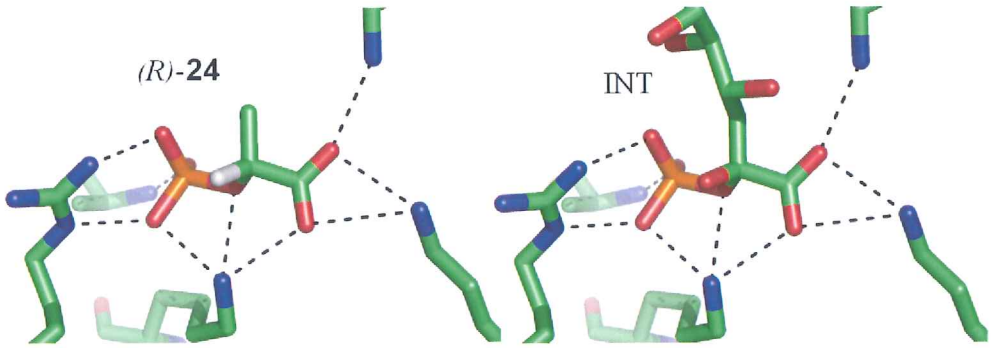

Figure 3.16 (*R*)-Phospholactic acid modelled into the active site from the crystal structure of the triple mutant from KDO8P synthase (*A. aeolicus*) containing the linear intermediate. The hydrogen at the C2 of (*R*)-**24** is grey and was added for clarity of stereochemistry (PDB 2NXG).

Assuming the methylene group of (*R*)-**24** acts like the extended chain of the intermediate, this would support a reaction mechanism in both DAH7P synthase and KDO8P synthase that involves nucleophilic attack of a water molecule (at the C2 of PEP) to the *re* face,

rather than the expected *si* face (discussed in chapter 1.7.3). However, molecular modelling of the two isomers of phospholactic acid in DAH7P synthase and KDO8P synthase showed no preference to either the (*R*)- or the (*S*)-isomer.

3.5 Testing PEP Phosphonate Against DAH7P and KDO8P Synthases

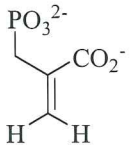

25

*DAH7P synthase (*E. coli*)*

The phosphonate analogue of PEP **25** was tested as an inhibitor and it was observed to have reasonable competitive inhibition against DAH7P synthase with a K_i value of 270 ± 50 μM at pH 6.8.

*KDO8P synthase (*N. meningitidis*)*

The phosphonate analogue of PEP **25** tested as an inhibitor of KDO8P synthase showed close to no observable inhibition at pH 6.5. However, at pH 5.3 some competitive inhibition of KDO8P synthase was observed with a K_i value of 1080 ± 120 μM.

Comparison / Discussion

	DAH7P synthase	KDO8P synthase	
	(pH 6.8)	(pH 6.5)	(pH 5.3)
Phosphonate	270 ± 50	4300 ± 2000	1080 ± 120

Table 3.5 Inhibition constants (μM) of PEP phosphonate.

The phosphonate analogue of PEP **25** had reasonable inhibition against DAH7P synthase, whereas very little inhibition was observed in KDO8P synthase. This suggests that the

bridging oxygen in PEP makes very important interactions in the active site of KDO8P synthase, that are disrupted when it is substituted for the hydrophobic methylene group. A lysine residue is expected to interact with the phosphate bridging oxygen of PEP in KDO8P synthase, however, this residue is also present in DAH7P synthase in a similar position and therefore would be expected to make similar interactions.

Similar to the inhibition of diphosphoPEP **23**, greater inhibition was observed by the phosphonate of PEP at a lower pH in KDO8P synthase. Which suggest that the phosphate moieties on these analogues have greater binding when they carry only one negative charge, supporting the hypothesis that PEP binds in the active site of KDO8P synthase as the dianion (**Figure 3.17**).[33] *E. coli* DAH7P synthase lost all activity at pH values between 5 and 6, so a comparison of the effect of pH could not be made readily.

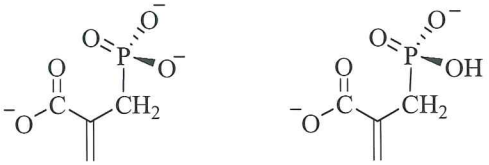

Figure 3.17 Ionisation states of the PEP phosphonate at pH 6.5 and pH 5.3.

Interestingly, when PEP phosphonate was modelled into DAH7P synthase and KDO8P synthase, with KDO8P synthase the phosphonate was orientated in a similar way to what is observed with, PEP whereas in the DAH7P synthase model the C3 is pointed towards a hydrophobic glycine (**Figure 3.18**). This can be interpreted as the cavity of KDO8P synthase providing a good fit for the phosphonate of PEP. However, weakened interactions prevents it sitting in the active site long enough to cause significant inhibition. In DAH7P synthase, this additional hydrophobic interaction may be the reason for its greater inhibition.

DAH7P synthase KDO8P synthase

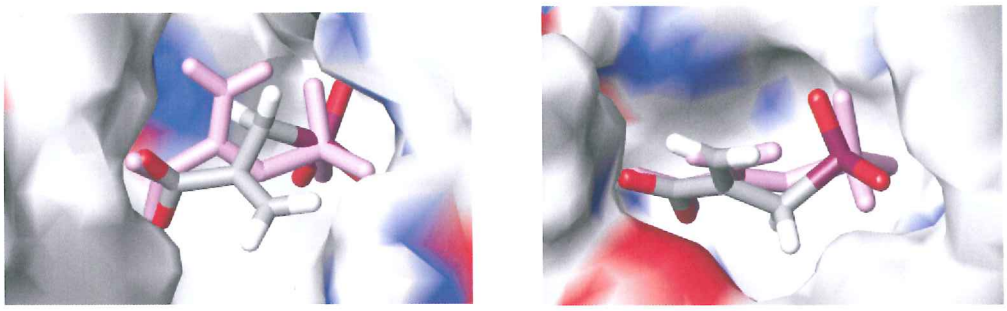

Figure 3.18 Molecular model of PEP phosphonate (grey) and PEP (pink) in the active site of DAH7P synthase and KDO8P synthase.

3.6 Implication of Results to Inhibitor Design

DAH7P synthase

In designing an inhibitor for DAH7P synthase, it appears that a charged species is critical to bind in the carboxylic acid pocket, this is evident by the weak inhibition observed by 1-(chloromethyl)vinyl phosphate **22**. However, this charged species may not necessarily need it be a carboxylic acid functionality, as the phosphonate at this position, as in diphosphoPEP **23**, was a reasonable inhibitor. The phosphonate of PEP **25** was a reasonable inhibitor of DAH7P synthase, suggesting that the more stable phosphonate moiety may be used to replace the phosphate group in inhibitor design. If a longer chain inhibitor is designed to contain a phosphoenol functionality, the (*E*)-isomer would be expected to be a better inhibitor to the (*Z*)-isomer, as better inhibition was observed by (*E*)-3-methylPEP over (*Z*)-3-methylPEP.

The (*R*)-isomer of phospholactic acid **24**, had the best inhibition of the PEP analogues tested against DAH7P synthase. Therefore, extended chains with this functionality at one end may prove to be good inhibitors.

KDO8P synthase

In KDO8P synthase it appears crucial for an inhibitor to contain a carboxyl group, as substituting the carboxyl group for a methyl chloride (1-(chloromethyl)vinyl phosphate **22**), or for a phosphonate moiety (diphosphoPEP **23**) resulted in very poor inhibition of

the *N. meningitidis* enzyme. The phosphonate of PEP **25** was found to be the poorest inhibitor tested suggesting the bridging oxygen is critical for binding to the active site of KDO8P synthase. Interestingly, lowering the pH from 6.5 to 5.3 significantly increased the inhibition of KDO8P synthase with diphosphoPEP **23** and the phosphonate of PEP **25**.

Unlike the results obtained for DAH7P synthase, both enantiomers of phospholactic acid **24** were poor inhibitors of KDO8P synthase, suggesting that inclusion of an sp^2 α-carbon will achieve more significant inhibition. The (*Z*)-isomer of 3-methylPEP was a better inhibitor than the (*E*)-isomer, therefore an inhibitor with an extended chain would be expected to be better as the (*Z*)-isomer.

3.7 Future Work

DAH7P synthase

The most potent inhibition was observed with (*R*)-phospholactic acid **24** against DAH7P synthase. It would be interesting to determine if this preference for the (*R*)-isomer extends to longer molecules, as it may prove the stereochemistry of the linear intermediate, and in doing so, indicate which side of PEP is nucleophilically attacked by water during the enzymic reaction.

The simplest analogue is 2-phosphobutyric acid **52**, which is a one carbon extension, and can be readily synthesised from optically pure 2-hydroxybutyric acid **53**. A more extended analogue is (2*R*,4*S*)-4-hydroxy-2-(phosphonatooxy)pentanoate **54**, that contains the C4 hydroxyl group, and may be readily synthesised in a few steps from optically pure (*R*)-2-hydroxy-4-oxopentanoate **56**. Though it may be difficult, the best way to check the stereochemistry of the intermediate is to test both enantiomers of **57**, which is essentially the intermediate without the C2 hydroxyl group. Also, this would be predicted to be a strong inhibitor of the enzyme.

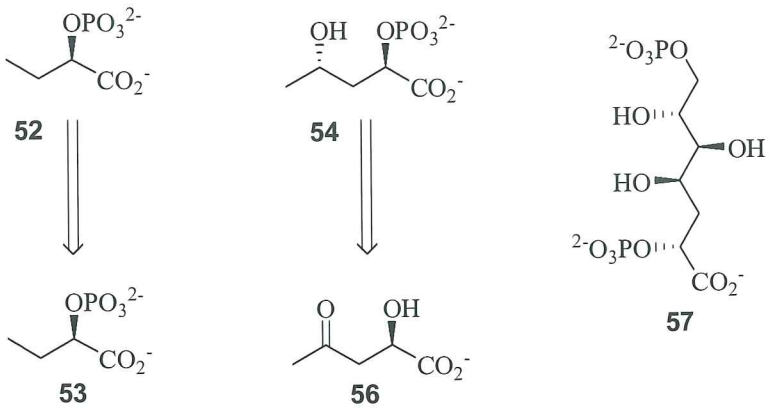

KDO8P synthase

An interesting result obtained with *N. meningitidis* KDO8P synthase, is that the competitive inhibition by diphosphoPEP **23** and PEP phosphonate **25** increased at lower pH conditions. It would be interesting to further investigate this phenomenon, by testing a range of PEP analogues at lower pH conditions.

It was observed in the molecular docking model that the phosphonate of diphosphoPEP **23** sat in the phosphate pocket preferentially over the phosphate in the analogue. Thus, it would be interesting to replace the phosphate for a phosphonate inphospholactate. This could be synthesised from optically pure lactic acid to give 2-phosphonopropanoic acid **58**.

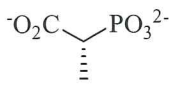

58

Only the C3 substituted analogues gave reasonable inhibition against KDO8P synthase, with all other PEP analogues with alterations to the carboxylic acid functionality (1-(chloromethyl)vinyl phosphate **22** and diphosphoPEP **23**), the bridging oxygen (PEP phosphonate **25**) or the carbon-carbon double bond of PEP were found to be poor inhibitors.

Therefore, it would be interesting to synthesise extended analogues of PEP and test these as inhibitors of KDO8P synthase, for example **59** or **61**. Alternatively, since there is a possibility that 1-(chloromethyl)vinyl phosphate **22** is a suicide inhibitor, the same

analogues could be made with a methylchloride instead of the carboxyl group, for example **60** or **62**. However, some competitive studies with PEP would need to be performed to determine if 1-(chloromethyl)vinyl phosphate **22** does cause covalent modification in the active site. This involves testing whether addition of PEP to the mixture of KDO8P synthase and **22** slows the rate of covalent modification, as observed by mass spectrometry.

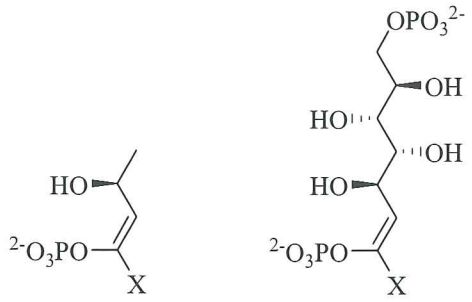

59 (X=CO_2^-) **61** (X=CO_2^-)

60 (X=CH_2Cl) **62** (X=CH_2Cl)

Inhibitors containing the phosphoenol functionality would be expected to show greater inhibition as the (*Z*)-isomer, as (*Z*)-3-methylPEP was observed to be a better inhibitor than (*E*)-3-methylPEP in KDO8P synthase. This proposed (*Z*)-isomer preference is ideal, as the Perkow reaction that may be required to produce the phosphoenol functionality, is highly stereoselective for the (*Z*)-isomer.

Chapter Four

Experimental

4.1 General Procedures

NMR spectroscopy

^{1}H NMR spectra were obtained on either a Bruker 500 (Massey university), a Varian Inova 500 (Canterbury university), or a Varian Unity 300 in deuterated solvents, as indicated. For samples dissolved in D_2O, spectra were referenced to HOD at 4.7 ppm, and in $CDCl_3$, spectra were referenced to $CHCl_3$ at 7.25 ppm.

^{31}P NMR spectra were obtained on a Varian Unity 300, operating at 121 MHz. Samples were referenced to phosphate at 0.0 ppm.

^{19}F NMR spectra were obtained on a Bruker 400, operating at 376 MHz. Externally referenced to $CFCl_3$ at 0.0 ppm.

Chemical shifts are reported in parts per million (ppm) on the δ scale.

UV light source

A Rayonet RPR 100 UV photochemical reactor was used for photo-isomerisation.

pH measurements

pH measurements were made using a Denver Instrument pH meter fitted with a pH/ATC electrode, Ag/AgCl reference and equilibrated with 3 M aqueous KCl solution.

Freeze drying

Samples to be freeze-dried were frozen in liquid nitrogen and placed for 1-2 days on a Christ® freeze dryer, model Alpha I/5.

Solvents

All solvents used in reactions were freshly distilled prior to use. Dichloromethane and toluene were distilled from calcium hydride. Diethyl ether and THF were distilled from sodium metal and benzophenone.

Reagents

Sodium ethoxide was prepared by adding sodium metal to ethanol, and after sodium had fully reacted excess ethanol was removed *in vacuo*. $P(OMe)_3$ and $P(OEt)_3$ were purified by treatment with sodium wire for a few hours followed by distillation.

Chromatography

Analytical thin layer chromatography (TLC) was performed on silica 60 F_{254} plates. Spots on silica plates were visualised by UV then $KMnO_4$ dip. Flash chromatography was performed on Merck silica gel 60, 230 – 400 mesh.

Determining the amount of grams per mole of the PEP analogues

A measured mass of the PEP analogue (~6 mg) was dissolved in 800 μL of a solution containing potassium phosphate (21.4 μM) in D_2O. A ^{31}P NMR spectrum (proton decoupled) was obtained of the solution, and the integral ratio of the phosphate ion and the PEP analogue was used to calculate the amount of grams per mole of the PEP analogue in the solution. To ensure correct assignment of the peaks, a second ^{31}P NMR spectrum was obtained after additional potassium phosphate had been added.

UV photo-isomerisation of mono C3 substituted analogues

A concentrated solution of the sample was dissolved in 1 mL of D_2O and put into a 5 mm quartz NMR tube. This was then irradiated with UV light, and the isomerisation progress was followed by ^1H NMR spectroscopy.

Protein 3-dimensional structures

3-Dimension structural images of enzymes were generated using PyMOL molecular graphics software[82] using files downloaded from the protein data bank (PDB).

4.2 General Biochemical Methods

Buffers

Buffer reagents were purchased from AppliChem. Enzyme assays of *E. coli* DAH7P synthase and *N. meningitidis* KDO8P synthase were performed in 50mM Bis Tris propane buffer at pH 6.8 and 6.5, respectively. KDO8P synthase assays carried out at pH 5.3 were

performed in 50 mM sodium acetate buffer. Buffers were stirred in Chelex-100 resin (Bio-Rad) for approximately one hour, filtered and the pH were adjusted with dilute HCl.

Enzyme assay solutions

$MnSO_4$ solution was prepared by dissolving solid $MnSO_4$ in Chelex treated water and stored at 4°C. Stock solutions of PEP, E4P, A5P and the PEP analogues were prepared by dissolving the appropriate salts in 50 mM BTP buffer at pH 6.8, the solutions were then filtered and stored at -20°C. Aliquots of these solutions were then diluted and stored at 4°C for a maximum 3 weeks, after which a fresh aliquot solution was prepared.

Enzymes

DAH7P synthase (*E. coli*) was over expressed and purified by Fiona Cochrane (Massey University) and was found to have a specific activity of 11.2 U/mg. KDO8P synthase (*N. meningitidis*) was over expressed and purified by Tim Allison (University of Canterbury) and was found to have a specific activity of 5.0 U/mg. Stock enzymes were stored frozen at -80°C. When required, a fraction of DAH7P synthase or KDO8P synthase was diluted with 50 mM BTP buffer (pH 6.8 and 6.5, respectively), stored at 4°C and used within 1 week.

General enzyme assays

All enzyme assays were performed at 25°C in a 1 cm path length quartz cuvette made up to a total volume of 1 mL. Enzyme assays were performed in a Varian Cary 100 UV Visible spectrophotometer. The Michalis-Menten constants (K_M), the inhibition constants (K_i) and their associated errors were determined by Grafit© software.[83]

4.3 Experimental for Chapter 2

Phosphoenolpyruvate 1 (*via* trimethylphosphite) [69, 84 77]

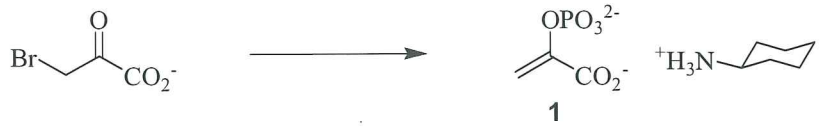

1

Trimethylphosphite (0.35 mL, 3.0 mmol) was added to a solution of 3-bromopyruvic acid (0.384 g, 2.3 mmol) in diethyl ether (20 mL) at 0°C. After stirring the solution for 30 minutes the reaction mixture was warmed to room temperature and stirred overnight. Solvent was then removed *in vacuo* and the residue was dissolved in water (15 mL) and stirred overnight. Cyclohexylamine (0.23 mL, 2.0 mmol) was then added and the solution was frozen with liquid nitrogen and lyophilised. The crude solid was recrystallised from methanol/diethyl ether providing the cyclohexylammonium salt of the title compound as a white solid (0.33 g, 54 %).

^{1}H NMR (300 MHz, D_2O): δ 5.23 (1H, t, J = 1.5 Hz, C*H*H), 5.05 (1H, d, J = 1.5 Hz, CH*H*), 3.04 (1H, m, C*H*NH_3^+), 1.87 (2H, m), 1.70 (2H, m), 1.54 (1H, m), 1.23 (5H, m).

Triethylphosphoenolpyruvate 57

57

Triethylphosphite (1.51 mL, 8.8 mmol) was added to a solution of ethyl 3-bromopyruvate (1.55 g, 7.9 mmol) in diethyl ether (20 mL) at 0°C. After stirring the solution for 30 minutes the reaction mixture was warmed to room temperature and stirred overnight. Solvent was then removed *in vacuo* and the crude material purified *via* flash chromatography, on silica eluting with 50% petroleum ether/hexane, to provide the title compound as a pale yellow oil (1.61 g, 81 %).

R_F (1:1 EtOAc:pet ether) 0.66 (UV / $KMNO_4$).

^{1}H NMR (300 MHz, $CDCl_3$): δ 5.87 (1H, m, C*H*H), 5.53 (1H, m, CH*H*), 4.15 (6H, two overlapping quartets, CH_2CH_3), 1.23 (9H, two overlapping triplets, CH_2CH_3).

Phosphoenolpyruvate 1 (*via* triethylphosphite)[74]

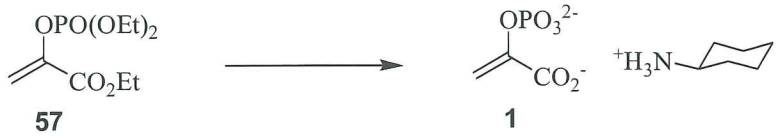

57 **1**

Bromotrimethylsilane (1.30 mL, 10.0 mmol) was added to a solution of triethylphosphoenolpyruvate **57** (0.628 g, 2.5 mmol) in CH_2Cl_2 (15 mL) at 0°C. After 3 hours solvent was removed *in vacuo*, and the residue redissolved in 1 M aqueous KOH solution (15 mL) and stirred for a further 40 minutes. The solution was then eluted through a Dowex(H) column with water. Cyclohexylamine (0.15 mL, 1.3 mmol) was added and the solution was frozen with liquid nitrogen and lyophilised. Recrystallisation of the drude solid from methanol/diethyl ether provided the cyclohexylammonium salt of the title compound as a white solid (0.48 g, 73%).

^{1}H NMR (300 MHz, D_2O): δ 5.23 (1H, t, J = 1.5 Hz, C*H*H), 5.05 (1H, d, J = 1.5 Hz, CH*H*), 3.04 (1H, m, C*H*NH_3^+), 1.87 (2H, m), 1.70 (2H, m), 1.54 (1H, m), 1.23 (5H, m).

Diethyl fluorooxaloacetate (sodium salt) 29[69, 77]

29

Diethyl oxalate (17.6 mL, 130 mmol) was added dropwise over 5 minutes to a suspension of sodium ethoxide (8.84g, 130 mmol) in toluene at 0°C. Ethyl fluoroacetate (12.7 mL, 130 mmol) was then added and the resulting solution was stirred overnight at room temperature. After this time a precipitate had formed. The solid material was filtered off and washed with diethyl ether until the filtrate was colourless. The solid was dried *in vacuo* affording the title compound as a pale yellow solid (15.6 g, 54%).

^{1}H NMR (500 MHz, D_2O): δ 4.16 (2H, q, J = 7 Hz, CH_2CH_3), 4.04 (2H, q, J = 7.5 Hz, CH_2CH_3), 1.19 (3H, t, J = 7.5 Hz, CH_2CH_3), 1.11 (3H, t, J = 7 Hz, CH_2CH_3).

Diethyl bromofluorooxaloacetate 30[69, 77]

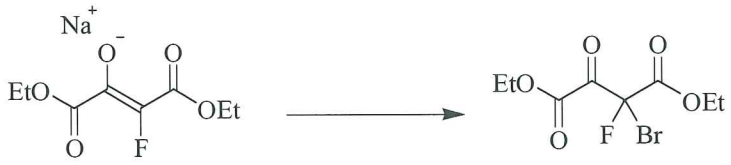

Bromine (1.9 mL, 37 mmol) was added dropwise to a suspension of diethyl fluorooxaloacetate **29** (8.15 g, 36 mmol) in diethyl ether (40 mL). The resulting solution was then washed with water followed by saturated aqueous sodium sulphite solution. The combined aqueous layers were extracted with diethyl ether (x3). The organic extracts were combined, dried ($MgSO_4$) and solvent removed *in vacuo* to provide the title compound as a pale yellow oil (6.19 g, 61%).

R_F (1:1 EtOAc:hexane) 0.65 (UV / $KMNO_4$).

^{1}H NMR (500 MHz, $CDCl_3$): δ 4.37 (4H, 2 overlapping quartets, CH_2CH_3), 1.35 (6H, 2 overlapping triplets, CH_2CH_3).

^{19}F NMR (376 MHz): δ -125.44 (s).

3-Bromo 3-fluoropyruvic acid 31[69, 77]

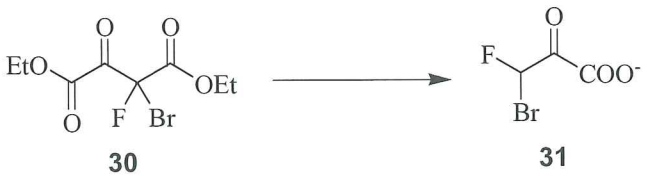

A solution of diethyl bromofluorooxaloacetate (6.19 g, 22 mmol) in concentrated HCl (50 mL) was heated at refluxed overnight. Excess hydrochloric acid was removed *in vacuo* to give a black/brown oil. This oil was dissolved in diethyl ether and extracted into 0.1 M aqueous NaOH solution. The aqueous layer was acidified to pH 1, with concentrated HCl,

and extracted with ethyl acetate (x5). The combined organic extracts were dried and evaporated *in vacuo* to provide the title compound as a white solid (1.55 g, 46%).

R_F (5% AcOH in ethanol) 0.73 (UV / $KMNO_4$).

^{1}H NMR (500 MHz, D_2O): δ 6.27 (d, J_{FCH} = 49 Hz).

^{19}F NMR (376 MHz, D_2O): δ -150.3 (d, J_{FCH} = 50 Hz).

3-Fluorophosphoenolpyruvate 17[69]

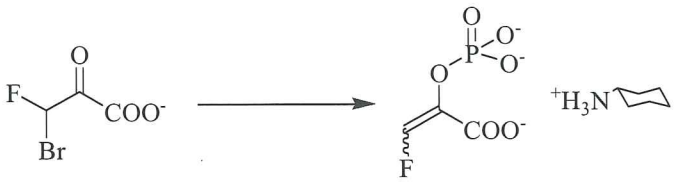

31 **17**

Trimethylphosphite (1.24 mL, 10.5 mmol) was added to a solution of 3-bromo 3-fluoropyruvic acid (1.54 g, 9.9 mmol) in diethyl ether (20 mL) at 0°C. After stirring the solution for 30 minutes the reaction mixture was warmed to room temperature and stirred overnight. Solvent was then removed *in vacuo* and the residue was dissolved in water (20 mL) and stirred overnight. Cyclohexylamine (0.23 mL, 2.0 mmol) was then added and the solution was frozen with liquid nitrogen and lyophilised. The crude solid was recrystallised twice from methanol/diethyl ether providing the cyclohexylammonium salt of the title compound as a white solid (1.47 g, 52 %). Analysis of the ^{1}H NMR spectrum established a (*Z*):(*E*) isomer ratio of 10:1.

R_F (5% AcOH in ethanol) 0.57 (UV / $KMNO_4$).

^{1}H NMR (500 MHz, D_2O): δ 7.53 (1H, dd, J = 73.5 and 2.5 Hz, (*Z*)-isomer), 7.34 (1H, dd, J = 75.0 and 3.5 Hz, (*E*)-isomer), 3.04 (1H, m, C*H*NH_3^+), 1.87 (2H, m), 1.70 (2H, m), 1.54 (1H, m), 1.23 (5H, m).

^{19}F NMR (376 MHz): δ -132.6 (dd, J = 73.4 and 5.8 Hz, (*Z*)-isomer) -137.6 (dd, J = 74.9 and 7.7 Hz, (*E*)-isomer).

3,3-Dichloropyruvic acid 33[69, 73]

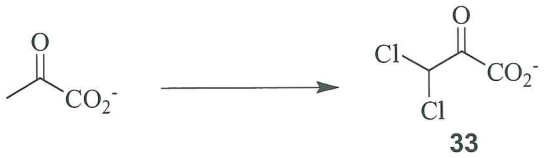

33

Pyruvic acid (5.27 g, 58 mmol) was added to SO_2Cl_2 (12.1 mL, 145 mmol) and stirred at 55°C under a drying tube ($CaCl_2$). After 4 days, water was added and the reaction mixture stirred at room temperature for 1.5 hours. The solution was then extracted with diethyl ether (x3), the combined extracts dried ($MgSO_4$), and the solvent was removed *in vacuo*. Recrystallisation of the crude material from diethyl ether/chloroform provided the title compound as a white solid (3.97 g, 44 %).

^{1}H NMR (500 MHz, D_2O): δ 5.81 (s, C*H*Cl_2).

Methyl 3,3-dichloropyruvate 34[69, 73]

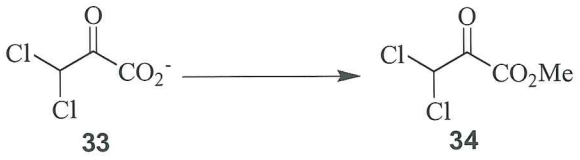

33 **34**

A few drops of sulphuric acid were added to a solution of 3,3-dichloropyruvic acid **33** (0.66 g, 4.2 mmol) in methanol (15 mL) at room temperature. The reaction progress was monitored by TLC. After 3 days, when no starting material was visible (baseline), the solvent was removed *in vacuo*. Purification of the crude material *via* flash chromatography on silica, eluting with 50% petroleum ether/hexane, provided the title compound as a colourless oil (0.63 g, 88%).

R_F (1:1 EtOAc:pet ether) 0.56 (UV / $KMNO_4$).

^{1}H NMR (500 MHz, $CDCl_3$): δ 5.93 (1H, s, C*H*Cl_2), 3.86 (3H, s, OC*H*$_3$).

Methyl 3-chloro(diethyl)phosphoenolpyruvate 35[69, 73]

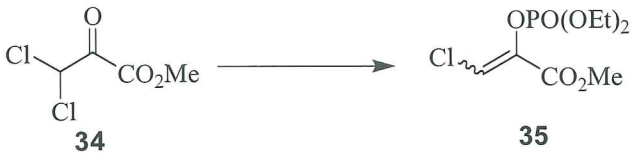

34 **35**

Triethylphosphite (0.72, ml, 4.2 mmol) was added to a solution of methyl 3,3-dichloropyruvate **34** (0.63 g, 3.7 mmol) in diethyl ether (15 mL) at 0°C. After stirring the solution for 30 minutes the reaction mixture was warmed to room temperature and stirred overnight. The solvent was removed *in vacuo* and the crude material purified *via* flash chromatography on silica, eluting with 33% pet ether/EtOAc, to provide the title compound as a colourless liquid (0.66 g, 76 %).

R_F (2:1 EtOAc:pet ether) 0.50 (UV / $KMNO_4$).

^{1}H NMR (500 MHz, $CDCl_3$): δ 6.98 (1H, d, J = 2 Hz, (*Z*)-isomer), 6.74 (1H, d, J = 3 Hz, (*E*)-isomer), 4.21 (4H, dq, J = 7.0 and 2.0 Hz, CH_2CH_3), 3.74 (3H, s, OCH_3), 1.29 (6H, dt, J = 7.0 and 1.0 Hz, CH_2CH_3).

3-Chlorophosphoenolpyruvate 18[73, 74]

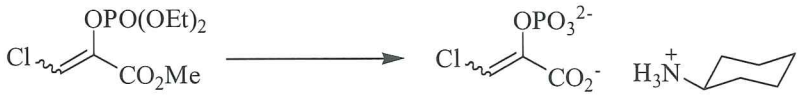

35 **18**

Bromotrimethylsilane (1.30 mL, 10.0 mmol) was added to a solution of methyl 3-chloro(diethyl)phosphoenolpyruvate **35** (0.66 g, 2.4 mmol) in CH_2Cl_2 (15 mL) at 0°C. After 3 hours, the solvent was removed *in vacuo*, and the residue redissolved in 1 M aqueous KOH solution (15 mL) and stirred for a further 40 minutes. The solution was then eluted through a Dowex(H) column with water. Cyclohexylamine (0.32 mL, 2.8 mmol) was added, and the solution frozen with liquid nitrogen and lyophilised. Recrystallisation of the crude solid from methanol/diethyl ether provided the cyclohexylammonium salt of the title compound as a white solid (0.61 g, 71%). Analysis of the ^{1}H NMR spectrum established a (*Z*):(*E*) isomer ratio of 4.5:1.

^{1}H NMR (500 MHz, D_2O): δ 6.65 (1H, d, J = 2 Hz, (*Z*)-isomer), 6.08 (1H, d, J = 3 Hz, (*E*)-isomer), 3.05 (1H, m, C*H*NH_3^+), 1.88 (2H, m), 1.71 (2H, m), 1.54 (1H, m), 1.23 (5H, m).

3,3-Dibromopyruvic acid 36[69, 85]

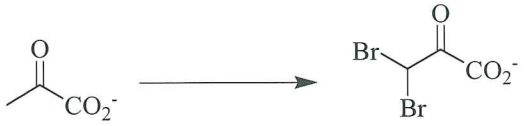

36

Bromine (5.13 mL, 100 mmol) was added dropwise to a solution of pyruvic acid (3.93 g, 44.6 mmol) in chloroform (35 ml). The solution was then heated to reflux under a drying tube ($CaCl_2$) and after 4 days the solvent was removed *in vacuo*. The residue was redissolved in chloroform and evacuated. This process was repeated twice to provide the title compound as a white solid (9.99 g, 91%).

^{1}H NMR (500 MHz, D_2O): δ 5.92 (s, C*H*Br_2).

3-Bromophosphoenolpyruvate 19[69, 71]

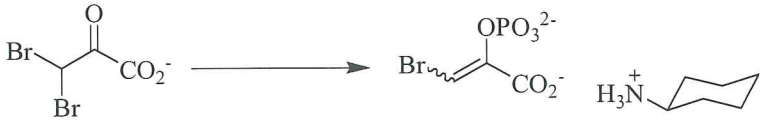

36 **19**

Trimethylphosphite (3.45 mL, 14.0 mmol) was added to a solution of 3,3-dibromopyruvic acid **36** (3.45 g, 14.0 mmol) in diethyl ether (20 mL) at 0°C. After stirring the solution for 30 minutes the reaction mixture was warmed to room temperature and stirred overnight. The solvent was removed *in vacuo* and the residue was dissolved in water (20 mL) and stirred overnight. Cyclohexylamine (1.39 mL, 14.0 mmol) was then added and the solution was frozen with liquid nitrogen and lyophilised. The crude solid was recrystallised twice from methanol/diethyl ether providing the cyclohexylammonium salt of the title compound as a white solid (0.84 g, 18 %). Analysis of the ^{1}H NMR spectrum established a (*Z*):(*E*) isomer ratio of 13:1.

^{1}H NMR (500 MHz, D_2O): δ 7.03 (1H, d, J = 2.5 Hz, (*Z*)-isomer), 6.36 (1H, d, J = 2.5 Hz, (*E*)-isomer), 3.04 (1H, m, C*H*NH_3^+), 1.87 (2H, m), 1.70 (2H, m), 1.54 (1H, m), 1.23 (5H, m).

3-Bromo-2-ketobutyric acid 38[69, 71]

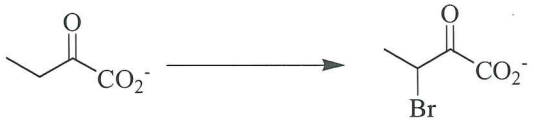

38

Bromine (0.13 mL, 2.6 mmol) was added dropwise to a solution of 2-ketobutyric acid (0.24 g, 2.4 mmol) in cyclohexane (15 ml) at room temperature. After 30 minutes the solvent was removed *in vacuo* to provide a pale orange solid. The solid was redissolved in CH_2Cl_2 then evacuated. This process was repeated providing the title compound as a creamy white solid (0.39 g, 89%).

^{1}H NMR (500 MHz, D_2O): δ 4.31 (1H, q, J = 6.9, C*H*(Br)CH_3), 1.55 (3H, d, J = 6.9, CH(Br)C*H*$_3$).

3-Methylphosphoenolpyruvate 20[56, 69]

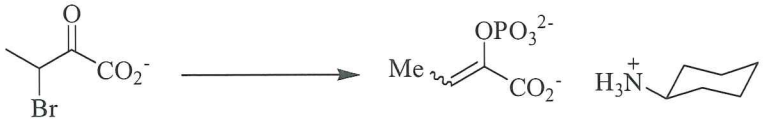

38 **20**

Trimethylphosphite (0.28 mL, 2.4 mmol) was added to a solution of 3-bromo-2-ketobutyric acid **38** (0.39 g, 2.14 mmol) in diethyl ether (8 mL) at 0°C. After stirring the solution for 30 minutes the reaction mixture was warmed to room temperature and stirred overnight. The solvent was removed *in vacuo* and the residue was dissolved in water (15 mL) and stirred overnight. Cyclohexylamine (0.29 mL, 2.5 mmol) was then added and the solution was frozen with liquid nitrogen and lyophilised. The crude solid was recrystallised from methanol/diethyl ether to provide the cyclohexylammonium salt of the title

compound as a white solid (0.35 g, 58 %). Analysis of the ^{1}H NMR spectrum established a (*Z*):(*E*) isomer ratio of 4.2:1.

^{1}H NMR (300 MHz, $CDCl_3$, **Before hydrolysis**): δ 6.62 (1H, dq, *J* 7.5 and 1.8 Hz, C*H*, (*Z*)-isomer), 6.26 (1H, dq, *J* = 7.5 and 3 Hz, C*H*, (*E*)-isomer), 3.92 (6H, d, *J* = 14.1 Hz, $P(OCH_3)_2$), 2.09 (3H, dd, *J* = 7.8 and 3.3 Hz, CH_3, (*E*)-isomer), 1.87 (3H, dd, *J* = 7.2 and 3 Hz, CH_3, (*Z*)-isomer).

^{1}H NMR (300 MHz, D_2O, **Final product**): δ 6.26 (1H, dq, *J* = 7.0 and 2.1 Hz, C*H*, (*Z*)-isomer), 5.82 (1H, dq, *J* = 7.5 and 3 Hz, C*H*, (*E*)-isomer), 3.05 (1H, $CHNH_3^+$), 1.87 (2H, m), 1.81 (3H, dd, *J* = 7.5 and 2.4 Hz, CH_3, (*E*)-isomer), 1.68 (3H, dd, *J* = 7.2 and 3 Hz, CH_3, (*Z*)-isomer), ~1.70 (2H, m, peak is hidden), 1.55 (1H, m), 1.25 (5H, m).

3-Bromo-3,3-dideuteropyruvic acid 40

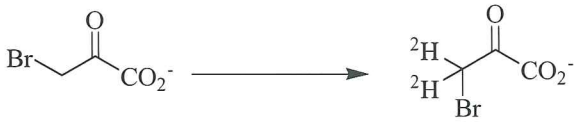

40

A solution of 3-bromopyruvic acid (1.04 g, 6.23 mmol) in deuterium oxide (15 mL) was stirred at room temperature, and the reaction progress followed by ^{1}H NMR spectroscopy, by observing the loss of the α-proton peaks. After 5 days, the solvent was removed *in vacuo* to provide the title compound as a colourless oil. The residue was immediately used for the subsequent step.

^{1}H NMR (400 MHz, D_2O): observed loss of a peak at: δ 3.54 (s, $CBrH_2$).

3,3-Dideuterophosphoenolpyruvate 21

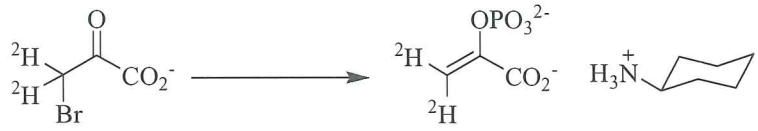

40 **21**

Trimethylphosphite (0.76 mL, 6.4 mmol) was added to a solution of 3-bromo-3,3-dideuteropyruvic acid (1.04 g, 6.23 mmol) in diethyl ether (8 mL) at 0°C. After stirring the solution for 30 minutes the reaction mixture was warmed to room temperature and stirred overnight. The solvent was removed *in vacuo* and the residue was dissolved in water (15 mL) and stirred overnight. Cyclohexylamine (0.78 mL, 6.8 mmol) was then added and the solution was frozen with liquid nitrogen and lyophilised. The crude solid was then recrystallised from methanol/diethyl ether providing the cyclohexylammonium salt of the title compound as a white solid (0.71 g, 43 % over two steps).

^{1}H NMR (500 MHz, D_2O): δ 3.04 (1H, m, C*H*NH_3^+), 1.87 (2H, m), 1.70 (2H, m), 1.54 (1H, m), 1.23 (5H, m).

Dimethyl-1-(chloromethyl)vinyl phosphate 43[57]

42 **43**

Trimethylphosphite (0.71 mL, 6.0 mmol) was added to a solution of 1,3-dichloroacetone **42** (0.70 g, 5.5 mmol) in diethyl ether (20 ml) at 0°C. After stirring the solution for 30 minutes the reaction mixture was warmed to room temperature and stirred overnight. The solvent was removed *in vacuo* to provide the title compound as a colourless oil (1.03 g, 93%).

^{1}H NMR (400 MHz, D_2O): δ 5.02 (1H, s, H_aH_bC), 4.94 (1H, s, H_aH_bC), 4.13 (2H, s, CH_2Cl), 3.81 (6H, d, J = 1.2 Hz, $(OCH_3)_2$).

1-(Chloromethyl)vinyl phosphate 22[57]

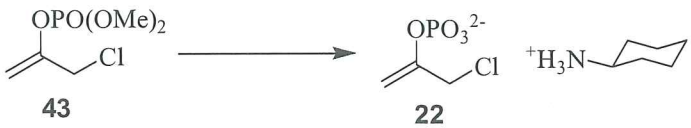

43 **22**

Bromotrimethylsilane (1.34 mL, 10.2 mmol) was added to a solution of dimethyl-1-(chloromethyl)vinyl phosphate **43** (1.03 g, 5.1 mmol) in CH_2Cl_2 (15 mL) at 0°C. After 2.5 hours the solvent was removed *in vacuo* and the residue redissolved in a mixture of 1:5 methanol/diethyl ether (50 mL). Addition of cyclohexylamine (1.25 mL, 11 mmol) gave an instant white precipitate, which was filtered and washed with diethyl ether to provide the cyclohexylammonium salt of the title compound as a white solid (1.16 g, 61%).

^{1}H NMR (500 MHz, D_2O): δ ~4.7 (Hidden under HOD peak, 1H, s, C*H*H), 4.60 (1H, s, CH*H*), 3.99 (2H, s, CH_2Cl), 3.04 (1H, m, C*H*NH_3^+), 1.87 (2H, m), 1.68 (2H, m), 1.55 (1H, m), 1.23 (5H, m).

Dimethyl-1-(dimethylphosphinyl)vinyl phosphate 45[67,79]

44 **45**

Trimethylphosphite (2.61 mL, 22.1 mmol) was added dropwise to chloroacetyl chloride (1.19 g, 10.5 mmol) at 0°C. The reaction mixture was then warmed to room temperature and stirred overnight. Methylchloride produced in the reaction was removed *in vacuo* to provide the title compound as a yellow oil (2.45 g, 89%).

^{1}H NMR (500 MHz, $CDCl_3$): δ 5.90 (1H, d, J = 35 Hz, C*H*H), 5.84 (1H, dd, J = 2.5 and 11 Hz, CH*H*), 3.63 (12H, m, OCH_3).

1-(Dihydroxyphosphinyl)vinyl phosphate (DiphosphoPEP) 23[74]

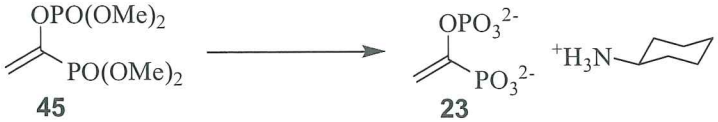

45 **23**

Bromotrimethylsilane (0.91 mL, 7.0 mmol) was added to a solution of dimethyl-1-(dimethylphosphinyl)vinyl phosphate **45** (0.257 g, 1.0 mmol) in CH_2Cl_2 (7 mL) at 0°C. After 3 hours the solvent was removed *in vacuo*, and the residue redissolved in 1M

aqueous KOH solution (7 mL) and stirred for a further 40 minutes. The solution was then eluted through a Dowex(H) column with water to give a total volume of 45 mL. Cyclohexylamine (0.15 mL, 1.3 mmol) was added, and the solution frozen with liquid nitrogen and lyophilised. Recrystallisation of the crude solid from methanol/diethyl ether provided the cyclohexylammonium salt of the title compound as a white solid (0.36 g, 97%).

^{1}H NMR (500 MHz, D_2O): δ 5.18 (1H, d, J = 33 Hz, CH_EH_Z), 5.11 (1H, dt, J = 2 and 11 Hz, CH_EH_Z), 3.04 (1H, m, $CHNH_3^+$), 1.87 (2H, m), 1.68 (2H, m), 1.55 (1H, m), 1.23 (5H, m).

^{31}P NMR (121 MHz, D_2O):

(Proton decoupled): δ 6.22 (d, J = 24 Hz, CPO_3), -1.64 (d, J = 23.8 Hz, OPO_3)

(Proton coupled): δ 6.22 (m, CPO_3), -1.64 (d, J = 24 Hz, OPO_3)

Methyl-2-(diethylphospho)lactate 47[69,80]

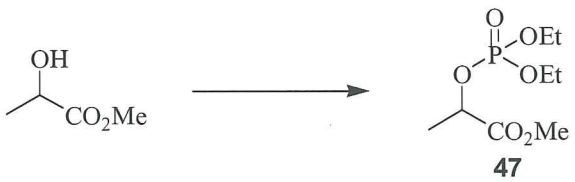

47

Diethyl chlorophosphate (1.26 g, 7.3 mmol) was added dropwise to a solution of methyl lactate (0.76 g, 7.3 mmol) and pyridine (2 mL, 25 mmol) in CH_2Cl_2 (10 mL) at 0°C. After 20 hours, the solvent was removed *in vacuo* and the residue redissolved in chloroform (50 mL), washed with water, 10% aqueous HCl solution (v:v) then again with water. The aqueous portions were extracted with chloroform (x3), and combined organic extracts dried ($MgSO_4$) and solvent removed *in vacuo* to provide the title compound as a colourless oil (1.54 g, 98 %).

^{1}H NMR (500 MHz, D_2O): δ 4.55 (1H, dq, J = 8.5 and 7.0 Hz, $CHCH_3$), 4.08 (4H, m, $P(O)(CH_2CH_3)_2$), 3.68 (3H, s, CO_2CH_3), 1.46 (3H, d, J = 7.0 Hz, $CHCH_3$), 1.25 (6H, dt, J = 4.0 and 7.0 Hz, $P(O)(CH_2CH_3)_2$).

2-Phospholactic acid 24[74]

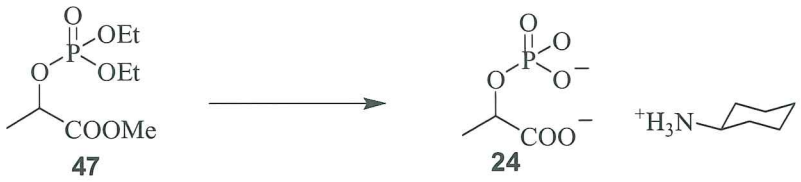

Bromotrimethylsilane (1.70 g, 11.1 mmol) was added to a solution of methyl-2-(diethylphospho)lactate **47** (0.49 g, 1.85 mmol) in CH_2Cl_2 (7 mL) at room temperature. After stirring for 3 hours the solvent was removed *in vacuo* and the residue was redissolved in 1 M aqueous KOH solution (7 mL) and stirred for 30 minutes. The mixture was eluted through a Dowex(H) column with water to desalt, then the solution was heated overnight at 80°C. After cooling to room temperature, the solution was evacuated for 10 minutes to remove volatile compounds. Cyclohexylamine (0.23 mL, 2.0 mmol) was added before the solution was frozen with liquid nitrogen and lyophilised to provide the cyclohexylammonium salt of the title compound as a white solid (0.52 g, 95 %).

^{1}H NMR (500 MHz, D_2O): δ 4.55 (1H, dq, J = 9.0 and 7.5 Hz, -C*H*CH_3), 3.04 (1H, m, C*H*NH_3^+), 1.86 (2H, m), 1.69 (2H, m), 1.54 (1H, m), 1.28 (3H, d, J = 7.0, CH_3CH), 1.23 (5H, m).

^{31}P NMR (121 MHz, D_2O): δ 0.44 (d, J 8.1 Hz, *H*CO*P*O_3^{2-}) (Referenced to PO_4^{3-}).

Diethyl bis(hydroxymethyl)malonate 49[69, 86]

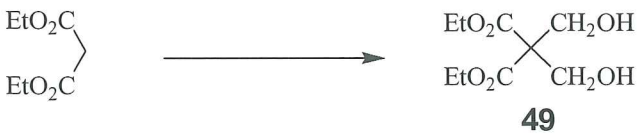

Diethyl malonate (151 mL, 1 mol) was added dropwise over 40 minutes to a solution of formalin (162 mL, 2 mol) and potassium bicarbonate (8 g, 80 mmol). The reaction mixture was stirred at room temperature for 48 hours, monitoring the pH and adding 1 M aqueous NaOH solution to ensure a pH of approximately 8. Saturated ammonium sulphate solution (250 mL) was added, followed by extraction with diethyl ether (x3). The organic extracts were dried ($MgSO_4$), and solvent removed *in vacuo* to afford the title compound as a

colourless liquid that was used immediately in the next step. TLC analysis showed loss of diethyl malonate (R_F 0.78).

R_F (1:1 EtOAc:pet ether) 0.38 (UV / $KMNO_4$).

α-(Bromomethyl)acrylic acid 50[69,87]

49 **50**

The crude solution of diethyl bis(hydroxymethyl)malonate **49** was dissolved in 47% aqueous HBr (300 mL) and distilled at 90°C for 2 hours, discarding the distillate. The condenser was altered to point vertical, and reaction mixture was refluxed for 20 hours. The solution was then evacuated for 2 hours at 70°C. The resulting colourless oil was kept at 0°C for 2 days then filtered to yield a white/orange slush. This was extracted into hot pentane (700 mL), the aqueous layer discarded, and the solvent removed *in vacuo* to provide the title compound as a white solid (8.54 g, 5.2% over two steps).

R_F (5% AcOH in ethanol) 0.85 (UV / $KMNO_4$).

^{1}H NMR (500 MHz, D_2O): δ 6.43 (1H, s, C*H*H), 6.04 (1H, s, CH*H*), 4.12 (2H, s, CH_2Br).

Dimethyl 2-(phosphonomethyl)acrylic acid 51[69,77]

50 **51**

Trimethylphosphite (1.05 mL, 10.2 mmol) was added to a solution of α(bromomethyl)acrylic acid **50** (1.60 g, 9.7 mmol) in THF (20 mL) and heated to reflux. After 40 hours, when no starting material was visible by TLC, the solvent was removed *in vacuo* to provide the title compound as a pale yellow oil (1.65 g, 87%).

R_F (5% AcOH in ethanol) 0.68 (UV / $KMNO_4$).

^{1}H NMR (500 MHz, $CDCl_3$): δ 6.37 (1H, d, J = 6 Hz, C*H*H), 5.83 (1H, d, J = 5.5 Hz, CH*H*), 3.70 (6H, d, J = 11 Hz, P(OCH_3)$_2$), 2.94 (2H, d, J = 22 Hz, CH_2).

2-(Phosphonomethyl)acrylic acid 25[69]

51 **25**

Dimethyl 2-(phosphonomethyl)acrylic acid **34** (1.65 g, 8.5 mmol) was dissolved in 100 mM formic acid (20 mL) and heated at 50°C for 72 hours. The solution was frozen with liquid nitrogen and lyophilised to provide the title compound as a white solid (1.41 g, 100%).

^{1}H NMR (500 MHz, D_2O): δ 6.25 (1H, d, J = 6 Hz, C*H*H), 5.80 (1H, d, J = 6 Hz, CH*H*), 2.80 (2H, d, J = 21.5 Hz, CH_2).

4.3 Experimental for Chapter 3

DAH7P synthase inhibition assay

To a cuvette was added, E4P (~70 μM), $MnSO_4$ (100 μM) and PEP (5-50 μM) and the volume made up to 1 mL by the addition of BTP buffer (pH 6.8). The cuvette was then placed in the UV spectrophotometer and incubated for approximately 5 minutes at 25°C. In order to initiate the reaction *E. coli* DAH7P synthase (~2.5 μg/mL) was added, the cuvette was inverted twice, and the consumption of PEP was followed (at 232 nm). The initial rate of PEP consumption (first 5-10%) was calculated and entered into the GraFit© software. This was then repeated at a range of PEP concentrations to obtain the Michalis-Menten constant (K_M).

For the determination of inhibition constants the standard assay system was used and inhibitor was included. Assays were performed using a range of 2 or 3 inhibitor concentrations.

The initial rate data obtained in this way was entered into GraFit, and the inhibition constant (K_i) was given using a non-linear regressive fit to the inhibition equation **(Equation 4.1)**.

$$v_0 = \frac{V_{max}[S_0]}{[S_0] + K_M\left(1 + \frac{[I_0]}{K_i}\right)}$$

Equation 4.1 Inhibition equation. Where v_0 is the initial rate, V_{max} is the maximum initial rate, $[S_0]$ is the PEP concentration, $[I_0]$ is the inhibitor concentration, K_M is the Michalis-Menten constant and K_i is the inhibition constant.

KDO8P synthase inhibition assay

To a cuvette was added, A5P (~80 μM) and PEP (5-50 μM) and the volume made up to 1 mL by the addition of BTP buffer (pH 6.5). The cuvette was then placed in the UV spectrophotometer and incubated for approximately 5 minutes at 25°C. In order to initiate the reaction *N. meningitidis* KDO8P synthase (~10.4 μg/mL) was added, the cuvette was inverted twice, and the consumption of PEP was followed (at 232 nm). The initial rate of PEP consumption (first 5-10%) was calculated and entered into the GraFit© software. This was then repeated at a range of PEP concentrations to obtain the Michalis-Menten constant (K_M).

For the determination of inhibition constants the standard assay system was used and inhibitor was included. Assays were performed using a range of inhibitor concentrations.

Assay systems reported at pH 5.3 were carried out in an identical manner. However, sodium acetate buffer at pH 5.3 was used instead to make up the reaction mixture to 1 mL in the cuvette.

Determination of PEP, E4P and A5P concentrations

The concentration of E4P and A5P were determined by using the appropriate standard assay method (used above). Assays were performed with an excess of PEP and the change in absorbance (at 232 nm) caused by the consumption of PEP was measured. Using Beer's law ($A = \epsilon.c.l$ where l = 1 cm and $\epsilon PEP = 2.8 \times 10^3\ M^{-1}\ cm^{-1}$) the amount of PEP consumed was calculated which directly corresponds to the amount of either the E4P or A5P

consumed in the assay. PEP concentrations were determined in the same way, however, the E4P or A5P were present in excess in these determinations.

Time-dependent enzyme inactivation

E. coli DAH7P synthase (500 μL of an approximate 1.0 mg/mL solution) was incubated (25°C) with either 1-(chloromethyl)vinyl phosphate **22** (500 μL of a 28 mM solution) or diluted with the same volume with BTP buffer (500 μL, control). An aliquot (7 μL) of either of the DAH7P synthase mixtures was then taken at different time intervals to initiate the reaction mixture of PEP (23 μM), $MnSO_4$ (100 μM) and E4P (~70 μM) in BTP buffer (pH 6.8) in a volume of 1 mL. The consumption of PEP (at 232 nm) was measured, and the initial rates were recorded.

N. meningitidis KDO8P synthase (200 μL of an approximate 1.1 mg/mL solution) was incubated (25°C) with either 1-(chloromethyl)vinyl phosphate **22** (500 μL of a 28 mM solution) or diluted with the same volume with BTP buffer (500 μL, control). An aliquot (10 μL) of either of the KDO8P synthase mixtures was then taken at different time intervals to initiate the reaction mixture of PEP (23 μM) and A5P (~80 μM) in BTP buffer (pH 6.5) in a volume of 1 mL. The consumption of PEP (at 232 nm) was measured, and the initial rates were recorded.

It is worth noting that during the initial stages of washing the enzyme samples for preparation of mass spectrometry samples, the control enzyme and the **22** incubated enzyme samples of *N. meningitidis* KDO8P synthase were accidentally mixed together. Therefore, the mass spectrum (**Figure 3.13**) represents a mixture of these enzyme samples.

Preparation of enzyme samples for ES-MS

Enzyme samples from inactivation experiments were made up to 500 μL with 5 mM ammonium bicarbonate, then concentrated to approximately 100 μL using a Vivaspin 500 (membrane: 10,000 MWCO) in a centrifuge running at 12,000 *g*. In order to desalt the solution and remove small molecules, this procedure was repeated at least five times, and on the final spin the solution was concentrated to approximately 80 μL. This solution was then used in mass spectrometer.

Mass Spectrometry

LCMS samples were analysed with a Waters 2790 HPLC system and a Waters 996 photodiode array (PDA) detector coupled in parallel to a Micromass LCT mass spectrometer equipped with an electrospray ionisation (ESI) probe with a probe voltage of 3,200 V at 150°C, a source temperature of 80°C, nebuliser gas flow of 160 L/hr and desolvation gas flow of 520 L/hr.

Protein samples were analysed with a cone voltage of typically 35 V unless otherwise stated. This system was controlled by MASSLYNX (Version 4.0) software. LC MS analysis used the following column: Phenomenex, Luna C5, 5μ, 2.00 x 150 mm; A flow rate of 200 μL/min and the following solvent profile of acetonitrile (Scharlau, Acetonitrile, Multisolvent®, HPLC grade) with water (purified using a MilliQ deionising system) with 0.5% formic acid was ultilised. A 9:1 solvent split was employed to deliver 20 μL/min solvent to the mass spectrometer and 180 μL/min solvent to the diode array detector. The gradient comprised of a 30 minute run, and consisted of the following solvent gradient timetable: a hold on 100% water for five minutes, followed by a gradient from 0% to 75% CH_3CN/H_2O (0.5% formic acid) over 20 minutes, followed by ramp in concentration to 100% CH_3CN over one minute, an isocratic hold on 100% CH_3CN for one minute and then a restoration to 0% CH_3CN over one minute. The method was finished with an isocratic hold on 0% CH_3CN over two minutes.

Testing DiphosphoPEP 23 as a substrate

The method for testing diphosphoPEP as a substrate for DAH7P synthase or KDO8P synthase was carried out in a similar manner to the studies of Benenson and co-workers.[58] A reaction mixture containing E4P (~10 mM), $MnSO_4$ (10 mM) and diphosphoPEP (~20 mM) was made up to a total volume of 0.5 mL with BTP buffer (pH 6.8). DAH7P synthase (50 μg/mL) was then added and the reaction mixture transferred to a 5 mm NMR tube with a D_2O insert. The reaction progress was then followed by obtaining ^{31}P NMR spectra every 30 minutes.

The same procedure was performed with KDO8P synthase (210 μg/mL), except A5P (~10 mM) was used instead of E4P and $MnSO_4$, and the reaction mixture was diluted with sodium acetate buffer (pH 5.3).

Computational methods

All molecular modelling experiments were conducted with the Schrödinger suite 2005. Conformational searches were carried out with MacroModel 9.0[88] to generate an ensemble of low energy conformers to establish a suitable starting conformation of each compound for the docking. The searches were conducted with the MCMM method using a GB/SA water model and the OPLS2005 force field, with 3000 steps for the conformational search and up to 5000 iterations for the minimization of each generated structure. The minimization was stopped with the default gradient convergence threshold of $\delta = 0.05$ kJ/(mol*Å). The default Polak-Ribiere Conjugate Gradient method was used for all minimizations.

The crystal structure of DAH7P synthase from *E. coli* (PDB code 1N8F) and KDO8P synthase from *E. coli* (PDB code 1GG0) were prepared using the protein preparation function of GLIDE.[89] The centre of the docking grid was defined as the ligand bound in the active site and was generated with GLIDE using default settings.

Ridged Docking

The docking of flexible ligands to the rigid DAH7P synthase or KDO8P synthase models with GLIDE[89] were performed with the following parameters: OPLS2005 force field, extra precision mode, 90000 poses per ligand for the initial docking, scoring window for keeping initial poses: 5000, keep best 1000 poses per ligand for energy minimization, energy minimization with a distance dependent dielectric constant of 2 and a maximum of 5000 conjugate gradient steps. 10 poses per ligand were saved for evaluation.

Appendices

Appendix one

Amino acid codes

A	Ala	alanine	M	Met	methionone
C	Cys	cysteine	N	Asn	asparagine
D	Asp	aspartic acid	P	Pro	proline
E	Glu	glutamic acid	Q	Gln	glutamine
F	Phe	phenylalanine	R	Arg	arginine
G	Gly	glycine	S	Ser	serine
H	His	histidine	T	Thr	threonine
I	Ile	isoleucine	V	Val	valine
K	Lys	lysine	W	Trp	tryptophan
L	Leu	leucine	Y	Tyr	tyrosine

Appendix Two

Competitive inhibition of DAH7P synthase (*E. coli*)
(GraFit© diagrams)

3-ChloroPEP **18**

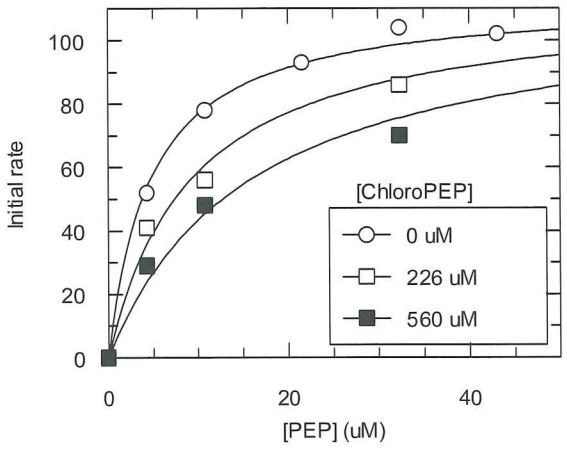

	value	error
V_{max}	110	4
K_M (μM)	4.8	0.7
K_i (μM)	240	40

Photo-isomerised 3-chloroPEP

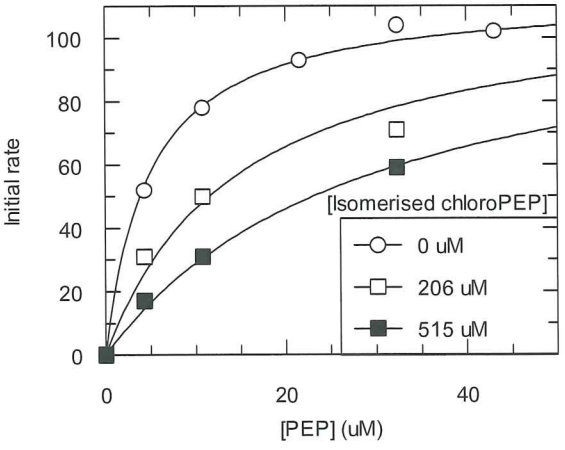

	value	error
V_{max}	110	3
K_M (μM)	4.8	0.7
K_i (μM)	100	15

3-BromoPEP **19**

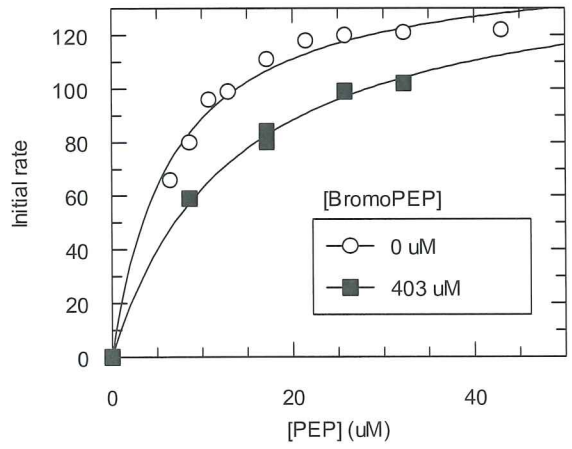

	value	error
V_{max}	150	4
K_M (μM)	6.6	0.7
K_i (μM)	390	50

Photo-isomerised 3-bromoPEP

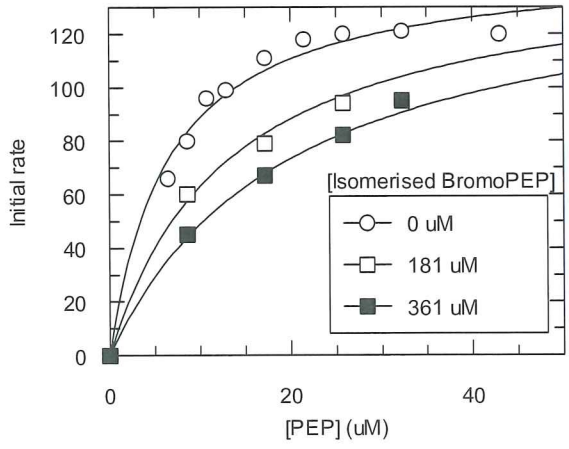

	value	error
V_{max}	150	5
K_M (μM)	6.5	0.7
K_i (μM)	180	20

3-MethylPEP **20**

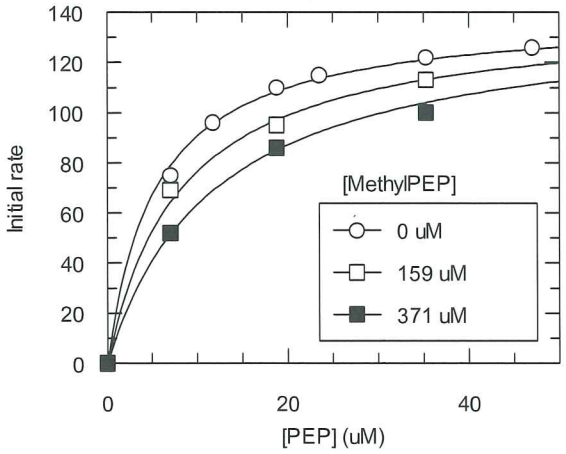

	value	error
V_{max}	140	2
K_M (μM)	5.4	0.4
K_i (μM)	300	34

Photo-isomerised 3-methylPEP

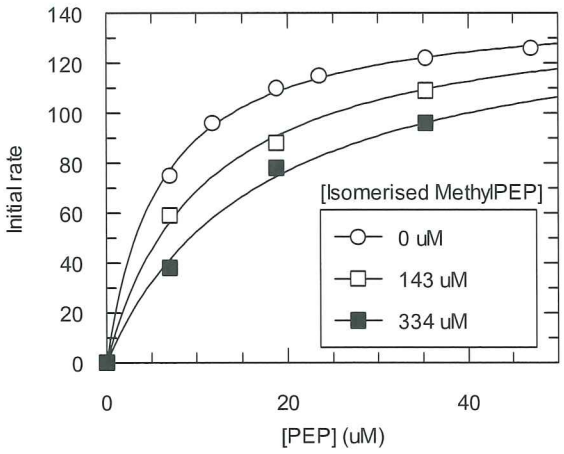

	value	error
V_{max}	140	2
K_M (μM)	6.0	0.4
K_i (μM)	180	14

1-(Chloromethyl)vinyl phosphate **22**

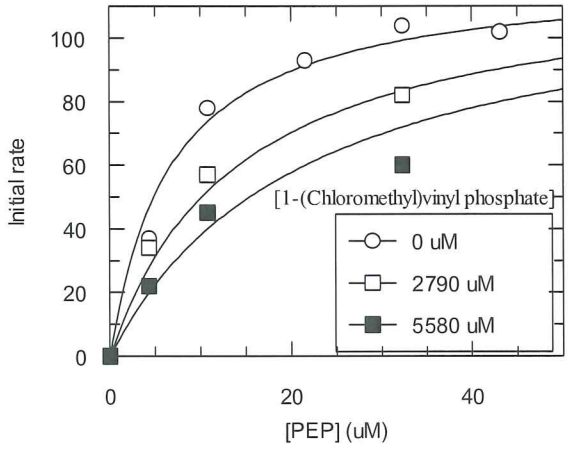

	value	error
V_{max}	120	7
K_M (μM)	6.8	1.6
K_i (μM)	2600	700

DiphosphoPEP **23**

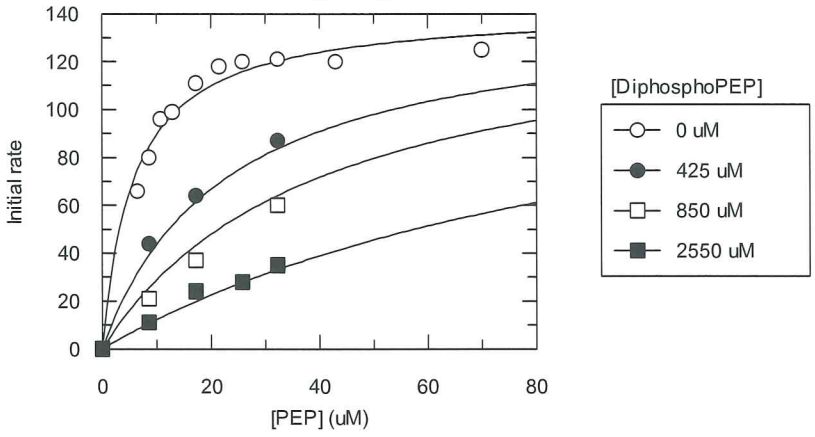

	value	error
V_{max}	140	4
K_M (μM)	5.9	0.7
K_i (μM)	140	16

(*R*)-Phospholactate **24**

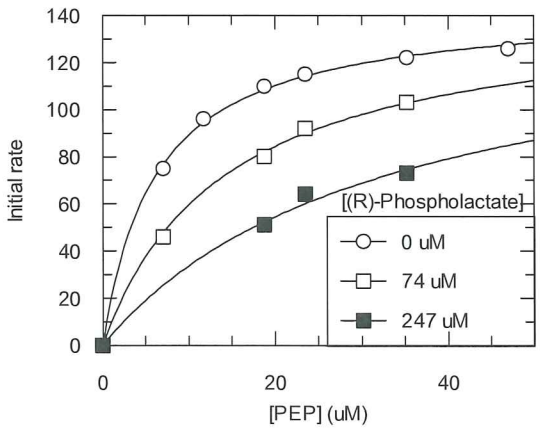

	value	error
V_{max}	140	2
K_M (μM)	6.2	0.4
K_i (μM)	57	3

(*S*)-Phospholactate **24**

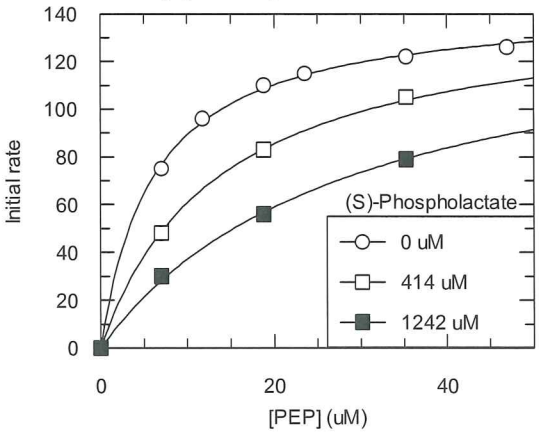

	value	error
V_{max}	140	1
K_M (μM)	6.2	0.2
K_i (μM)	340	10

PEP phosphonate **25**

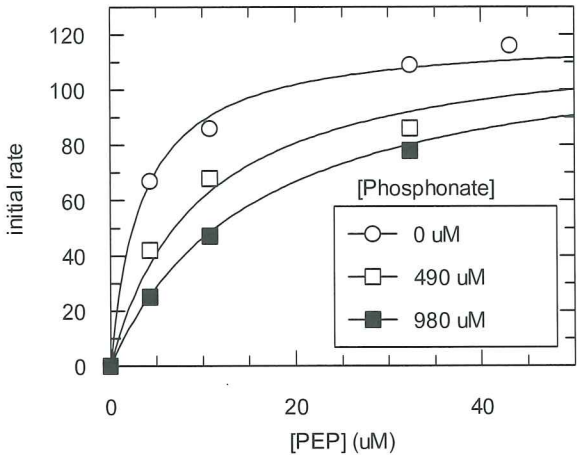

	value	error
V_{max}	120	4
K_M (μM)	3.4	0.5
K_i (μM)	270	50

Appendix three

Competitive inhibition of KDO8P synthase (*N. meningitidis*) (GraFit© diagrams)

3-ChloroPEP **18**

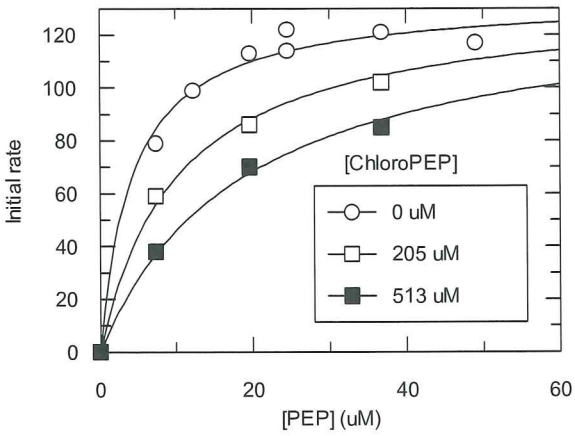

	value	error
V_{max}	130	3
K_M (μM)	4	1
K_i (μM)	150	20

Photo-isomerised 3-chloroPEP

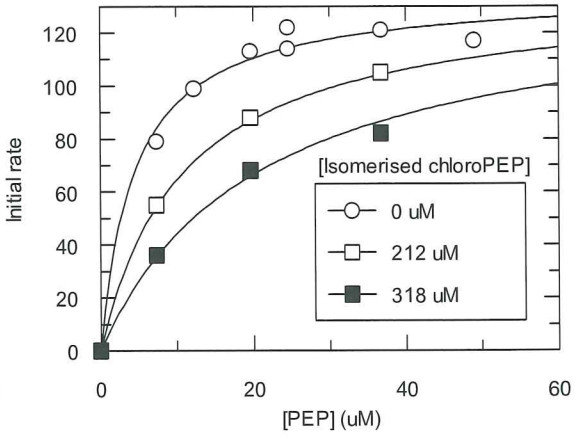

	value	error
V_{max}	140	3
K_M (μM)	5	1
K_i (μM)	140	20

3-BromoPEP **19**

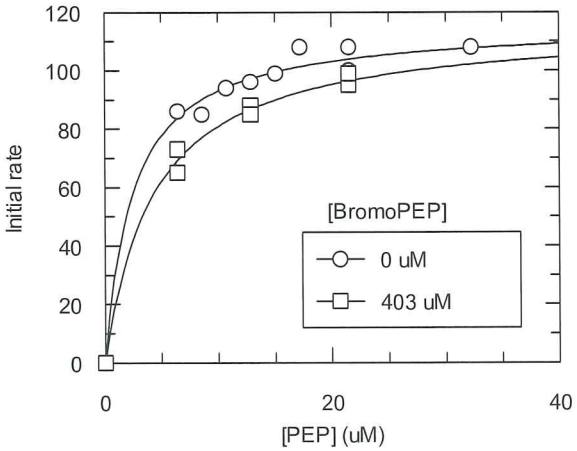

	value	error
V_{max}	120	3
K_M (μM)	2.5	0.3
K_i (μM)	530	110

Photo-isomerised 3-bromoPEP

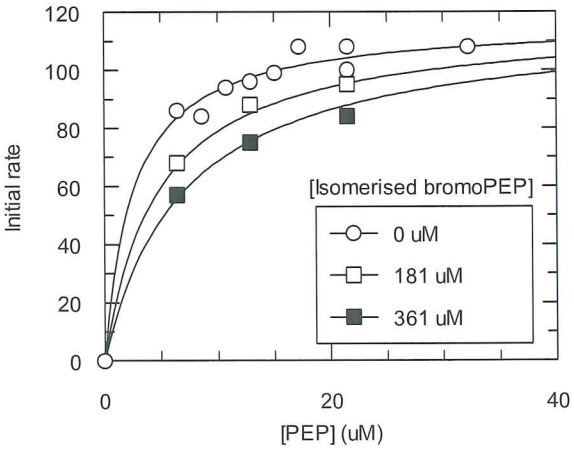

	value	error
V_{max}	120	3
K_M (μM)	2.5	0.4
K_i (μM)	210	40

3-MethylPEP **20**

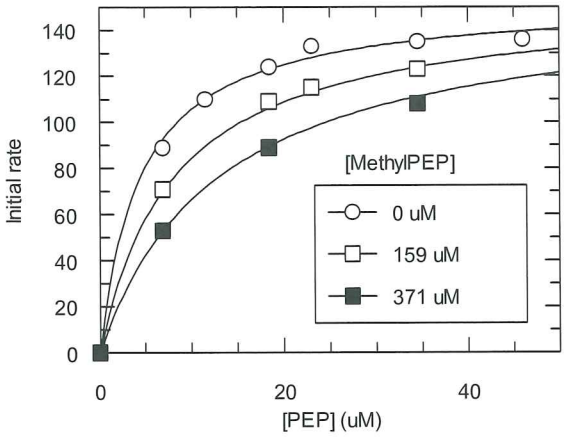

	value	error
V_{max}	150	2
K_M (μM)	4.5	0.3
K_i (μM)	200	20

Photo-isomerised 3-methylPEP

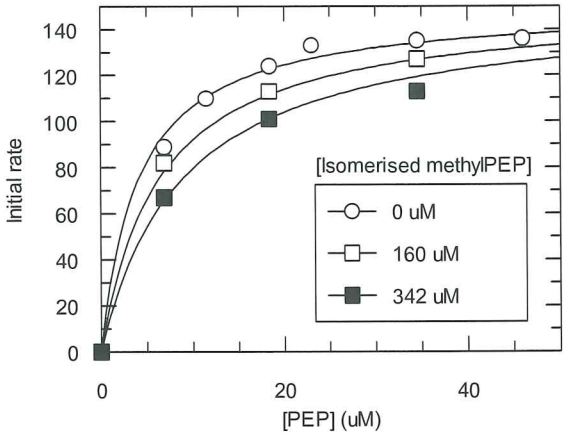

	value	error
V_{max}	150	3
K_M (μM)	4.1	0.4
K_i (μM)	300	50

1-(Chloromethyl)vinyl phosphate **22**

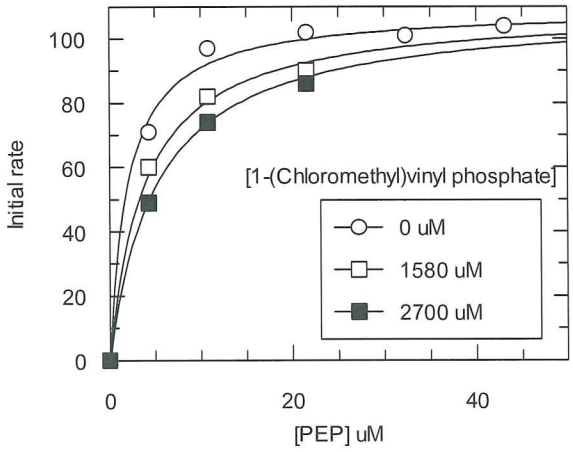

	value	error
V_{max}	110	2
K_M (μM)	2.0	0.2
K_i (μM)	1700	300

DiphosphoPEP **23**

pH 6.5

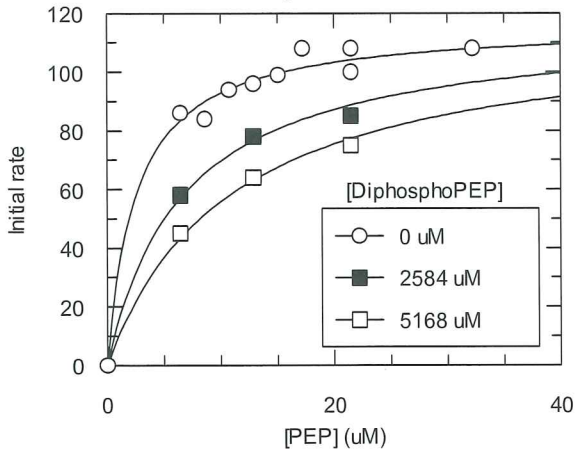

	value	error
V_{max}	116	3
K_M (μM)	2.5	0.4
K_i (μM)	1558	280

pH 5.3

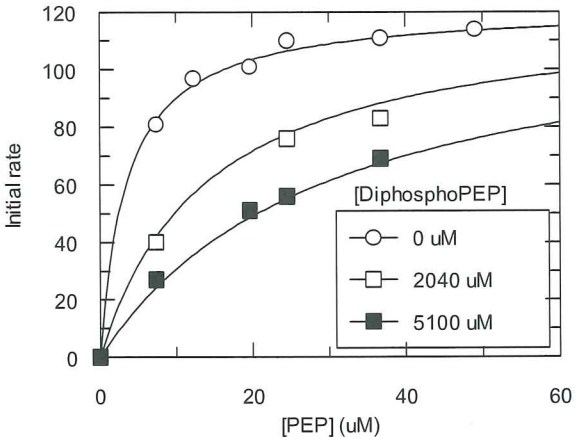

	value	error
V_{max}	122	2
K_M (μM)	3.5	0.4
K_i (μM)	689	75

2-Phospholactic acid **24**

(*R*)-isomer

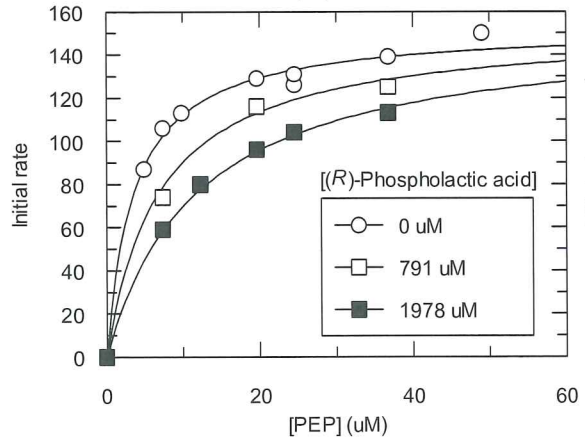

	value	error
V_{max}	150	3
K_M (μM)	3.6	0.3
K_i (μM)	870	90

(*S*)-isomer

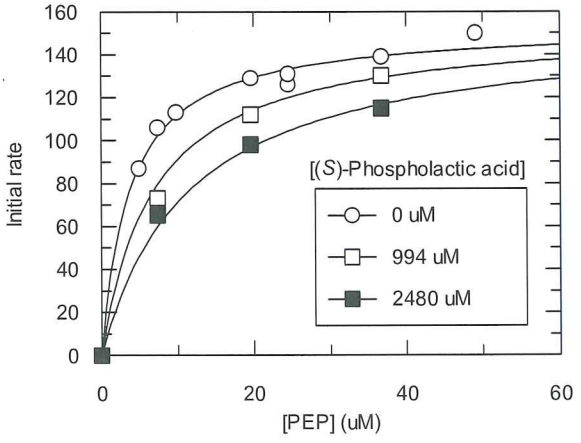

	value	error
V_{max}	150	3
K_M (μM)	3.7	0.4
K_i (μM)	1200	150

PEP phosphonate **25**

pH 6.5

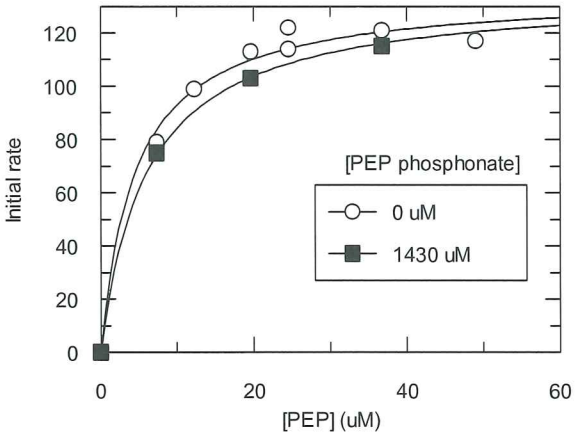

	value	error
V_{max}	140	4
K_M (μM)	4.5	0.7
K_i (μM)	4300	2000

pH 5.3

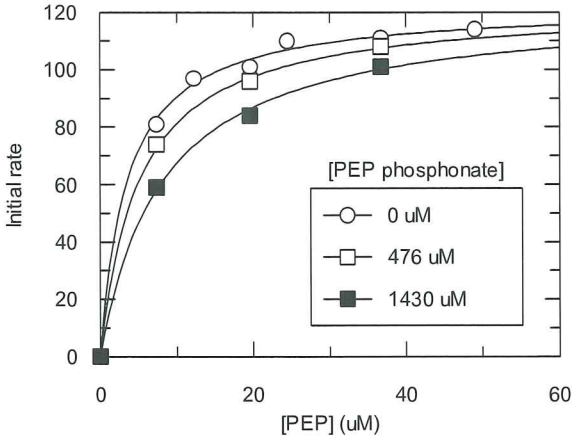

	value	error
V_{max}	120	1
K_M (μM)	3.5	0.2
K_i (μM)	1100	120

References

1. Haslam, E., *Shikimic Acid -Metabolism and Metabolites*. John Wiley and sons: Sheffield, UK, 1993.

2. Bentley, R., *Crit. Rev. Biochem. Mol. Biol.* **1990,** 25, 307-384.

3. Herrmann, K. M.; Weaver, L. M., *Annu. Rev. Plant Mol. Biol.* **1999,** 50, 473-503.

4. Steinrucken, H. C.; Amrhein, N., *Biochem. Biophys. Res. Comm.* **1980,** 94, (4), 1207-1212.

5. Srinivasan, P. R.; Sprinson, D. B., *J. Biol. Chem.* **1959,** 234, 716-722.

6. Shumilin, I. A.; Zhao, C.; Bauerle, R.; Kretsinger, R. H., *J. Mol. Biol.* **2002,** 320, 1147-1156.

7. Stephens, C. M.; Bauerle, R., *J. Biol. Chem.* **1991,** 266, (31), 20810-20817.

8. DeLeo, A. B.; Sprinson, D. B., *Biochem. Biophys. Res. Comm.* **1968,** 32, (5), 873-877.

9. Floss, H. G.; Onderka, D. K.; Carroll, M., *J. Biol. Chem.* **1972,** 247, (3), 736-744.

10. Wang, J.; Duewel, H. S.; Woodard, R. W.; Gatti, D. L., *Biochemistry* **2001,** 40, 15676-15683.

11. Wagner, T.; Kretsinger, R. H.; Bauerle, R.; Tolbert, W. D., *J. Mol. Biol.* **2000,** 301, 233-238.

12. Duewel, H. S.; Radaev, S.; Wang, J.; Woodard, R. W.; Gatti, D. L., *J. Biol. Chem.* **2001,** 276, (11), 8393-8402.

13. Li, Y.; Evans, J. N. S., *Proc. Nat. Acad. Sci. USA* **1996,** 93, 4612-4616.

14. Shumilin, I. A.; Bauerle, R.; Kretsinger, R. H., *Biochemistry* **2003,** 42, 3766-3776.

15. Shumilin, I. A.; Bauerle, R.; Wu, J.; Woodard, R. W.; Kretsinger, R. H., *J. Mol. Biol.* **2004,** 341, 455-466.

16. Konig, V.; Pfeil, A.; Braus, G. H.; Schneider, T. R., *J. Mol. Biol.* **2004,** 337, 675-690.

17. Meridith, T. C.; Aggarwal, P.; Mamat, U.; Lindner, B.; Woodard, R. W., *ACS Chem. Biol.* **2006,** 1, (1), 33-42.

18. Raetz, C. R. H.; Whitfield, C., *Annu. Rev. Biochem.* **2002,** 71, 635-700.

19. Rick, P. D.; Osborn, M. J., *Proc. Nat. Acad. Sci. USA* **1972,** 69, (12), 3756-3760.

20. Rick, P. D.; Osborn, M. J., *J. Biol. Chem.* **1977,** 252, (14), 4895-4903.

21. Levin, D. H.; Racker, E., *J. Biol. Chem.* **1959,** 234, 2532-2539.

22. Kohen, A.; Jakob, A.; Baasov, T., *Eur. J. Biochem.* **1992,** 208, 443-449.

23. Hedstrom, L.; Abeles, R., *Biochem. Biophys. Res. Comm.* **1988,** 157, (2), 816-820.

24. Dotson, G. D.; Nanjappan, P.; Reily, M. D.; Woodard, R. W., *Biochemistry* **1993,** 32, 12392-12397.

25. Ray, P. H.; Kelsey, J. E.; Bigham, E. C.; Benedict, C. D.; Miller, T. A., *ACS Symp. Ser.* **1983,** 231, 141-170.

26. Baasov, T.; Sheffer-Dee-Noor, S.; Kohen, A.; Jakob, A.; Belakhov, V., *Eur. J. Biochem.* **1993,** 217, 991-999.

27. D'Souza, F. W.; Benenson, Y.; Baasov, T., *Bioorg. Med. Chem. Lett.* **1997,** 7, (19), 2457-2462.

28. Liang, P.; Lewis, J.; Anderson, K. S.; Kohen, A.; D'Souza, F. W.; Benenson, Y.; Baasov, T., *Biochemistry* **1998,** 37, 16390-16399.

29. Radaev, S.; Dastidar, P.; Patel, M.; Woodard, R. W.; Gatti, D. L., *J. Biol. Chem.* **2000,** 275, (13), 9476-9484.

30. Du, S.; Tsipori, H.; Baasov, T., *Bioorg. Med. Chem. Lett.* **1997,** 7, (19), 2469-2472.

31. Du, S.; Faiger, H.; Belakhov, V.; Baasov, T., *Bioorg. Med. Chem. Lett.* **1999,** 7, 2671-2682.

32. Belakhov, V.; Dovgolevsky, E.; Rabkin, E.; Shulami, S.; Shoham, Y.; Baasov, T., *Carbohydr. Res.* **2004,** 339, 385-392.

33. Ahn, M.; Pietersma, A. L.; Schofield, L. R.; Parker, E. J., *Org. Biomol. Chem.* **2005,** 3, 4046-4049.

34. Ray, P. H., *J. Bacteriol.* **1980,** 141, 635.

35. Howe, D. L.; Sundaram, A. K.; Wu, J.; Gatti, D. L.; Woodard, R. W., *Biochemistry* **2003,** 42, 4843.

36. Xu, X.; Kona, F.; Wang, J.; Lu, J.; Stemmler, T.; Gatti, D. L., *Biochemistry* **2005,** 44, 12434-12444.

37. Kona, F.; Xu, X.; Martin, P.; Kuzmic, P.; Gatti, D. L., *Biochemistry* **2007,** 46, 4532-4544.

38. Li, Z.; Sau, A. K.; Shen, S.; Whitehouse, C.; Baasov, T.; Anderson, K. S., *J. Am. Chem. Soc.* **2003,** 125, 9938-9939.

39. Duewel, H. S.; Woodard, R. W., *J. Biol. Chem.* **2000,** 275, (30), 22824-22831.

40. Shulami, S.; Furdui, C.; Adir, N.; Shoham, Y.; Anderson, K. S.; Baasov, T., *J. Biol. Chem.* **2004,** 279, (43), 45110-45120.

41. Li, J.; Wu, J.; Fleischhacker, A. S.; Woodard, R. W., *J. Am. Chem. Soc.* **2004,** (126), 7448-7449.

42. Oliynyk, Z.; Briseno-Roa, L.; Janowitz, T.; Sondergeld, P.; Fersht, A. R., *J. Biol. Chem.* **2004,** 279, 45110-45120.

43. Walker, G. E.; Dunbar, B.; Hunter, I. S.; Nimmo, H. G.; Coggins, J. R., *Microbiology* **1996,** 142, 1973-1982.

44. Jensen, R. A.; Xie, G.; Calhoun, D. H.; Bonner, C. A., *J. Mol. Evo.* **2002,** 54, 416-423.

45. Subramaniam, P. S.; Xie, G.; Xia, T.; Jensen, R. A., *J. Bacteriol.* **1998,** 180, 119-127.

46. Birck, M. R.; Woodard, R. W., *J. Mol. Evol.* **2001,** 52, 205-214.

47. Webby, C. J.; Baker, H. M.; Lott, S.; Baker, E. N.; Parker, E. J., *J. Mol. Biol.* **2005,** 354, 927-939.

48. Wu, J.; Woodard, R. W., *J. Biol. Chem.* **2006,** 281, (7), 4042-4048.

49. Shumilin, I. A.; Kretsinger, R. H.; Bauerle, R., *Structure* **1999,** 7, (7), 865-875.

50. Hartmann, M.; Schneider, T. R.; Pfeil, A.; Heinrich, G.; Lipscomb, W. N.; Braus, G. H., *Proc. Nat. Acad. Sci. USA* **2003,** 100, (3), 862-867.

51. Schofield, L. R.; Anderson, B. F.; Patchett, M. L.; Norris, G. E.; Jameson, G. B.; Parker, E. J., *Biochemistry* **2005,** 44, 11950-11962.

52. Asojo, O.; Friedman, J.; Adir, N.; Belakhov, V.; Shoham, Y.; Baasov, T., *Biochemistry* **2001,** 40, 6326-6334.

53. Webby, C. Structural and functional characterisation of 3-deoxy-D-*arabino*-heptulosonate 7-phosphate synthase from *Helicobacter pylori* and *Mycobacterium tuberculosis*. Massey University, Palmerston North, 2006.

54. Hrmova, M.; Fincher, G. B., *Carbohydr. Res.* **2007,** 342, (12-13), 1613-1623.

55. Howard-Jones, A. R.; Elkins, J. M.; Clifton, I. J.; Roach, P. L.; Adlington, R. M.; Baldwin, J. E.; Rutledge, P. J., *Biochemistry* **2007,** 46, (16), 4755-4762.

56. Woods, A. E.; O'Bryan, J. M.; Mui, P. T. K.; Crowder, R. D., *Biochemistry* **1970,** 9, (11), 2334-2338.

57. Garcia-Alles, L. F.; Erni, B., *Eur. J. Biochem.* **2002,** 269, 3226-3236.

58. Benenson, Y.; Belakhov, V.; Baasov, T., *Bioorg. Med. Chem. Lett.* **1996,** 6, (23), 2901-2906.

59. Furdui, C. M.; Sau, A. K.; Yaniv, O.; Belakhov, V.; Woodard, R. W.; Baasov, T.; Anderson, K. S., *Biochemistry* **2005,** 44, (19), 7326-7335.

60. Paleta, O.; Pomeisl, K.; Kafka, S.; Klasek, A.; Kubelka, V., *Beilstein J. Org. Chem.* **2005,** 1, 1-4.

61. Li, J. J., *Name reactions*. Springer-Verlag Berlin Heidelberg: 2002; p 278.

62. Borowitz, I. J.; Yee, K. C.; Crouch, R. K., *J. Org. Chem.* **1973,** 38, (9), 1713-1718.

63. Janecki, T.; Bodalski, R., *Heteroatom Chem.* **2000,** 11, (2), 115-119.

64. Jarvis, B. B.; Marien, B. A., *J. Org. Chem.* **1976,** 41, 2182-2187.

65. Petnehazy, I.; Szakal, G.; Toke, L.; Hudson, H. R.; Powroznyk, L.; Cooksey, C. J., *Tetrahedron* **1983,** 39, 4229-4235.

66. Sekine, M.; Nakajima, M.; Hata, T., *J. Org. Chem.* **1981,** 46, (20), 4030-4034.

67. Sekine, M.; Futatsugi, T.; Yamada, K.; Hata, T., *J. Chem. Soc. Perkin Transactions I* **1982**, 2509-2513.

68. Lichtenthaler, F. W., *Chem. Rev.* **1961,** 61, (6), 607-649.

69. Parker, E. J. Mechanistic Studies on Shikimate Pathway Enzymes. University of Cambridge, 1996.

70. Bondi, A., *J. Phys. Chem.* **1964,** 68, (3), 441.

71. Stubbe, J.; Kenyon, G. L., *Biochemistry* **1971,** 10, 2669-2677.

72. Hwang, S. H.; Nowak, T., *Arch. Biochem. Biophys.* **1989,** 269, 646-663.

73. Liu, J.; Peliska, J. A.; O'Leary, M. H., *Arch. Biochem. Biophys.* **1990,** 277, (1), 143-148.

74. Bartlett, P. A.; Chouinard, P. M., *J. Org. Chem.* **1983,** 48, 3854-3855.

75. www.wikipedia.com. In.

76. Diaz, E.; O'Laughlin, J.; O'Leary, M. H., *Biochemistry* **1988,** 27, 1336-1341.

77. Stubbe, J. A.; Kenyon, G. L., *Biochemistry* **1972,** 11, (3), 338-345.

78. Glusker, J. P.; Lewis, M.; Rossi, M., *Crystal Structure Analysis for Chemists and Biologists*. John Wiley and Sons: 1994.

79. Bearne, S. L.; Kluger, R., *Bioorg. Chem.* **1992,** 20, 135-147.

80. Stubbe, J.; Abeles, R., *Biochemistry* **1980,** 19, 5505-5512.

81. Lane, R. H.; Hurst, J. K., *Biochemistry* **1974,** 13, (16), 3292-3297.

82. DeLano, W. L. *PyMOL molecular graphics system*, v0.99; DeLano Scientific LLC: 2006.

83. Leatherbarrow, R. J. *GraFit*, Version 5.0.13; Erithacus Software Limited: 1989-2006.

84. Clark, V. M.; Kirby, A. J., *Biochim. Biophys. Acta* **1963,** 78, (4), 732.

85. Cooper, D. J.; Owen, L. N., *J. Chem. Soc.* **1966**, 533-541.

86. Block, P., *Org. Synth.* **1973,** 5, 381.

87. Ramarajan, K.; Ramalingam, K.; O'Donnell, D. J.; Berlin, K. D., *Org. Synth.* **1990,** 7, 210.

88. *MacroModel*, version 9.1; Schrodinger: New York, 2005.

89. *Glide*, version 4.0; Schrodinger: New York, 2005.